

NOTICE CONCERNING COPYRIGHT RESTRICTIONS

This document may contain copyrighted materials. These materials have been made available for use in research, teaching, and private study, but may not be used for any commercial purpose. Users may not otherwise copy, reproduce, retransmit, distribute, publish, commercially exploit or otherwise transfer any material.

The copyright law of the United States (Title 17, United States Code) governs the making of photocopies or other reproductions of copyrighted material.

Under certain conditions specified in the law, libraries and archives are authorized to furnish a photocopy or other reproduction. One of these specific conditions is that the photocopy or reproduction is not to be "used for any purpose other than private study, scholarship, or research." If a user makes a request for, or later uses, a photocopy or reproduction for purposes in excess of "fair use," that user may be liable for copyright infringement.

This institution reserves the right to refuse to accept a copying order if, in its judgment, fulfillment of the order would involve violation of copyright law.

12339

VPI-SU-5103-3
Distribution Category UC-66a

EVALUATION AND TARGETING OF GEOTHERMAL ENERGY RESOURCES
IN THE SOUTHEASTERN UNITED STATES

Progress Report

John K. Costain, Lynn Glover III, and A. Krishna Sinha

Principal Investigators

November 1, 1976 - March 31, 1977

UNDER CONTRACT NO. EY-76-S-05-5103

PREPARED FOR THE
ENERGY RESEARCH AND DEVELOPMENT ADMINISTRATION
Virginia Polytechnic Institute and State University
Blacksburg, Virginia 24061

TABLE OF CONTENTS

	Page
ABSTRACT	1
RESEARCH OBJECTIVES.	2
INTRODUCTION AND REVIEW.	4
PERSONNEL OF PROGRAM	8
COMPLIANCE WITH CONTRACTUAL REQUIREMENTS	9
A. Geology.	A- 1
Operations.	A- 1
Opaque Mineralogy	A- 5
Molybdenum Mineralization in the Liberty Hill and Winnsboro Plutons	A-17
Petrography of the Liberty Hill Drill Cores	A-24
Magnetic Modeling of the Liberty Hill Pluton...	A-32
Relationship between K and U in Granitic Rocks.	A-49
The Rolesville Batholith.	A-53
Roxboro Metagranite	A-78
B. Geochemistry	B- 1
Rolesville Batholith.	B- 1
Liberty Hill Bore Holes	B- 8
C. Geophysics	C- 1
Geothermal Gradients and Heat Generation.	C- 1
Modeling of Coastal Plain Gravity Anomalies	C-23

ABSTRACT

The objective of this research is to develop and apply targeting procedures for the evaluation of low-temperature radiogenically-derived geothermal resources in the eastern United States utilizing geological, geochemical, and geophysical data. Detailed study of the Liberty Hill and Winnsboro plutons, South Carolina, is continuing in order to provide insight into the behavior of uranium and thorium in unmetamorphosed granitic plutons during periods of crystallization, deuteric alteration and weathering. The importance of the oxidation state of uranium has become apparent because the transition from U^{4+} to U^{6+} represents the division between immobile and labile uranium. Accessory uraninite has been found in the Liberty Hill pluton, and molybdenite mineralization occurs in both the Liberty Hill and Winnsboro plutons. The molybdenum mineralization is present in a number of 300 m.y. granitic plutons in the southeastern U. S.

A steep metamorphic gradient across the Roxboro, North Carolina, metagranite, which was metamorphosed during Devonian time, should provide a good opportunity to study the effect of prograde metamorphism on the distribution of uranium and thorium. Three holes have been drilled into the Roxboro metagranite for the purpose of examining the effect of metamorphism on heat generation and heat flow.

Preliminary modeling of negative gravity anomalies in the Coastal Plain supports the interpretation of a deep granitic pluton near Norfolk, Virginia, and probably at Georgetown, South Carolina.

RESEARCH OBJECTIVES

The objective of this research is to develop and apply targeting procedures for the evaluation of low-temperature radiogenically-derived geothermal resources in the eastern United States utilizing geological, geochemical, and geophysical data.

The optimum sites for geothermal development in the tectonically stable eastern United States will probably be associated with areas of relatively high heat flow derived from crustal igneous rocks containing relatively high concentrations of radiogenic heat-producing elements. The storage of commercially exploitable geothermal heat at accessible depths (1-3 km) will also require favorable reservoir conditions in rocks overlying a radiogenic heat source. In order to systematically locate these sites, a methodology employing geological, geochemical, and geophysical prospecting techniques is being developed and applied. The radiogenic distribution within the igneous rocks of various ages and magma types will be determined by a correlation between radioelement composition and the rock's bulk chemistry. Surface sampling and measurements of the radiogenic heat-producing elements are known to be unreliable as they are preferentially removed by ground water, circulation, and weathering. The correlation between the bulk chemistry of the rock (which can be measured reliably from surface samples) and radiogenic heat production is being calibrated by detailed studies at a number of locations in the eastern United States.

Initial studies will develop a methodology for locating radiogenic heat sources buried beneath the insulating sedimentary rocks of

the Coastal Plain of South Carolina, North Carolina, and Virginia.

Additional heat flow and thermal gradient measurements are being made in available deep wells.

INTRODUCTION AND REVIEW

Because even the most potassic rocks contain less than 12 wt.% potassium, relatively large concentrations of uranium and thorium must be present in a rock to raise heat production to usable levels, since heat generation in rocks is given by the equation

$$H = 0.73U + 0.20Th + 0.27K \text{ }^1.$$

The primary objective, therefore, is to find rocks with sufficiently high uranium and thorium contents, distributed over large enough volumes, to make the recovery of geothermal energy economically practicable. The project is primarily concerned with granitic rocks because they should have high uranium and thorium contents relative to other types of crystalline rocks. Our interest is directed toward understanding any geologic process that affects thorium and uranium distribution, and toward determining the concentration of these elements in granitic rocks of the southeastern United States.

Detailed study of the Liberty Hill and Winnsboro plutons is continuing in order to provide insight to the behavior of uranium and thorium in unmetamorphosed granitic plutons during periods of crystallization, deuteric alteration and weathering. This report contains work on their opaque mineralogy, deuteric alteration, descriptions of the drill holes for heat flow, additional whole rock chemistry and heat production, and preliminary isotope equilibrium studies.

The importance of the oxidation state of uranium has become apparent because the transition from U^{4+} to U^{6+} represents the division between im-

^{1/} Heat production (H) is in mass units: $\mu\text{cal/gm yr.}$, U and Th are in ppm, and K is in wt. %. Equation from F. Birch, 1954, Heat from radioactivity, in Nuclear Energy, John Wiley & Sons, Inc., p. 151, Table 5.2.

mobile and labile uranium. Speer, as noted in a report on the opaque oxides, has begun to study the oxidation conditions of the Liberty Hill and Winnsboro plutons. He finds that oxygen and sulfur fugacities increased during crystallization of the magma and that both the oxides and the sulfides reequilibrated at low temperatures. Chemical analyses of the coexisting oxides would permit a more detailed description of the evolution of the fluid phase. The calculation of approximate uranium oxide phase relations in T - f_{O_2} space from existing thermodynamic data also appears to be feasible. A combination of these two results would form a framework that would allow an understanding of the periods in the geologic history of a granite during which uranium can be transported from the system.

The study of opaque oxides, in addition, revealed the presence of accessory uraninite in the Liberty Hill pluton and of molybdenite mineralization in both the Liberty Hill and Winnsboro plutons. The identification of uraninite is the first step in locating the position of uranium in the granitic rocks of the Piedmont. Determination of the mineralogy of uranium will set severe restrictions on the behavioral history of uranium in these rocks. The molybdenum mineralization, reminiscent of molybdenum porphyry deposits, is present in a number of 300 m.y. granitic plutons in the southeastern U.S. It is associated with a late magmatic alteration, and appears to have occurred during cooling of the granite plutons. The reactions involved in the deuteritic alteration have been examined so that their effect on uranium and thorium distribution can eventually be considered.

In all studies of uranium distribution in a series of related rocks, uranium has been found to be enriched by fractional crystallization in

the rocks formed latest in the sequence. The rocks which contain relatively high amounts of uranium are also high in K_2O and SiO_2 , and low in MgO and CaO . An accompanying conclusion commonly presented is that a positive correlation exists between U and K_2O , as well as between U and SiO_2 , since all three are thought to be enriched in the residual liquid during magmatic differentiation. Speer, in a short note, maintains that these relations are found only in rocks of basic and intermediate compositions. Using the granite phase diagram and a compilation diagram of K_2O vs. SiO_2 , he demonstrates that K_2O is a poor differentiation index at the high SiO_2 contents at which potassium feldspar begins to crystallize. For this project, which is concentrating primarily on high silica rocks, K_2O is an inappropriate indicator of U and Th contents.

During the past quarter, studies were begun of metamorphosed granitic bodies which have more complex geologic histories than the Liberty Hill and Winnsboro plutons. In addition to providing the range of uranium and thorium contents of metamorphosed granitic rocks, these studies should aid in unraveling the behavior of uranium and thorium during metamorphism. The Rolesville batholith is described by Becker and Farrar as having been emplaced during a late Paleozoic metamorphic and deformational event. The first group of heat production values is available for the Rolesville rocks, but interpretation of these values is waiting on further work to increase the understanding of rock type distribution in the batholith. Glover reports on the Roxboro metagranite, which was metamorphosed during Devonian time. A steep metamorphic gradient across the granite should provide a good opportunity to study the effect of prograde metamorphism on uranium and thorium distribution.

The targeting of geothermal energy resources requires, in addition to knowledge of the uranium and thorium contents of a rock mass, a reasonable estimate of its geometry and volume. Dunbar and Speer, in their report, discuss the results of geophysical and geologic modeling of the shape of the Liberty Hill pluton. The pluton has the form of an asymmetric funnel, approximately 11 miles in diameter and 3.5 - 4.0 miles deep. Rotation of the pluton as part of a fault block is considered the best explanation of its asymmetry. Explanations for the positive and negative magnetic anomalies associated with the contact metamorphic rocks are advanced in terms of reactions producing and consuming magnetite.

As attention in the future turns toward granites insulated by coastal plain cover, geophysical modeling of a reasonably well understood body will provide a familiarity with problems likely to be encountered in the modeling of concealed rock masses. Interpretations of negative gravity anomalies near Goergetown, S.C. and Norfolk, Va. have been made and are described in this report.

PERSONNEL OF PROGRAM

(November 1, 1976 - March 31, 1977)

Geology and Petrology (South Carolina), Lynn Glover III, Principal Investigator

J. A. Speer, Research Associate
S. S. Farrar, Research Associate
S. W. Becker, Research Associate

Geochemistry, A. Krishna Sinha, Principal Investigator

B. A. Merz, Research Associate
S. Mackmull, Research Assistant
S. Hall (part-time)

Geophysics, J. K. Costain, Principal Investigator

C. S. Rohrer, Research Specialist
J. A. Dunbar (part-time)
L. D. Perry (part-time)

Structural Geology, Warm Springs Project, Northwestern Virginia

Peter A. Geiser, University of Connecticut, Storrs

Administrative Assistant, Patricia C. Sullivan

Secretary, Margie Strickler

Drillers

W. G. Coulson, Core Driller
R. G. Gravley, Driller Helper

COMPLIANCE WITH CONTRACTUAL REQUIREMENTS

Principal investigators John K. Costain, Lynn Glover III, and A. K. Sinha, in accordance with Article A-I of Appendix A to the hereinmentioned contract, have devoted one month, one month, and one-half month, respectively, of their efforts to performance under the contract. They plan to devote an equal amount of time to the contract during the next three-month report period.

All subcontract requirements have been compiled with.

John K. Costain

John K. Costain

A. K. Sinha

A. K. Sinha

Lynn Glover III

Lynn Glover III

A. Geology

Lynn Glover III, Principal Investigator

J. A. Speer, Research Associate

S. S. Farrar, Research Associate

S. W. Becker, Research Associate

Operations

Field work for the second reporting period was limited by the cold winter. Before the onset of inclement weather, 13 man-weeks were spent during the two periods from 11-3-76 to 11-15-76 and 12-2-76 to 12-12-76 conducting reconnaissance mapping of the Rolesville plutonic complex, N.C. (Figure A1). Mapping in moderate detail was continued in the Winnsboro plutonic complex, S.C. (Figure A2) during the period 11-11-76 to 11-16-76. Five drill hole sites were located, one in the Winnsboro complex, S.C. and four in the Roxboro Granite, N.C. (Fig. A1).

Curtailement of field work due to the cold weather provided time to reduce the backlog on sample characterization, to consider the results from the geochemistry and geophysics groups, and to carry on literature searches. The opaque mineralogy of the plutons and associated country rocks was examined to further the understanding of the petrogenesis of the granites, the aeromagnetic anomalies associated with these plutons, and molybdenum mineralization associated with the granites. During these studies, what appears to be primary accessory uraninite was found in the coarse-grained granite of the Liberty Hill.

Samples of the granites and associated country rocks are currently being selected and prepared for electron and ion microprobe analysis, and particle track analysis. These studies are primarily concerned with determining the location of uranium and thorium in the granites. Major element compositions of the mineral phases will also be determined to provide insight into the petrogenesis of the granitic plutons and their

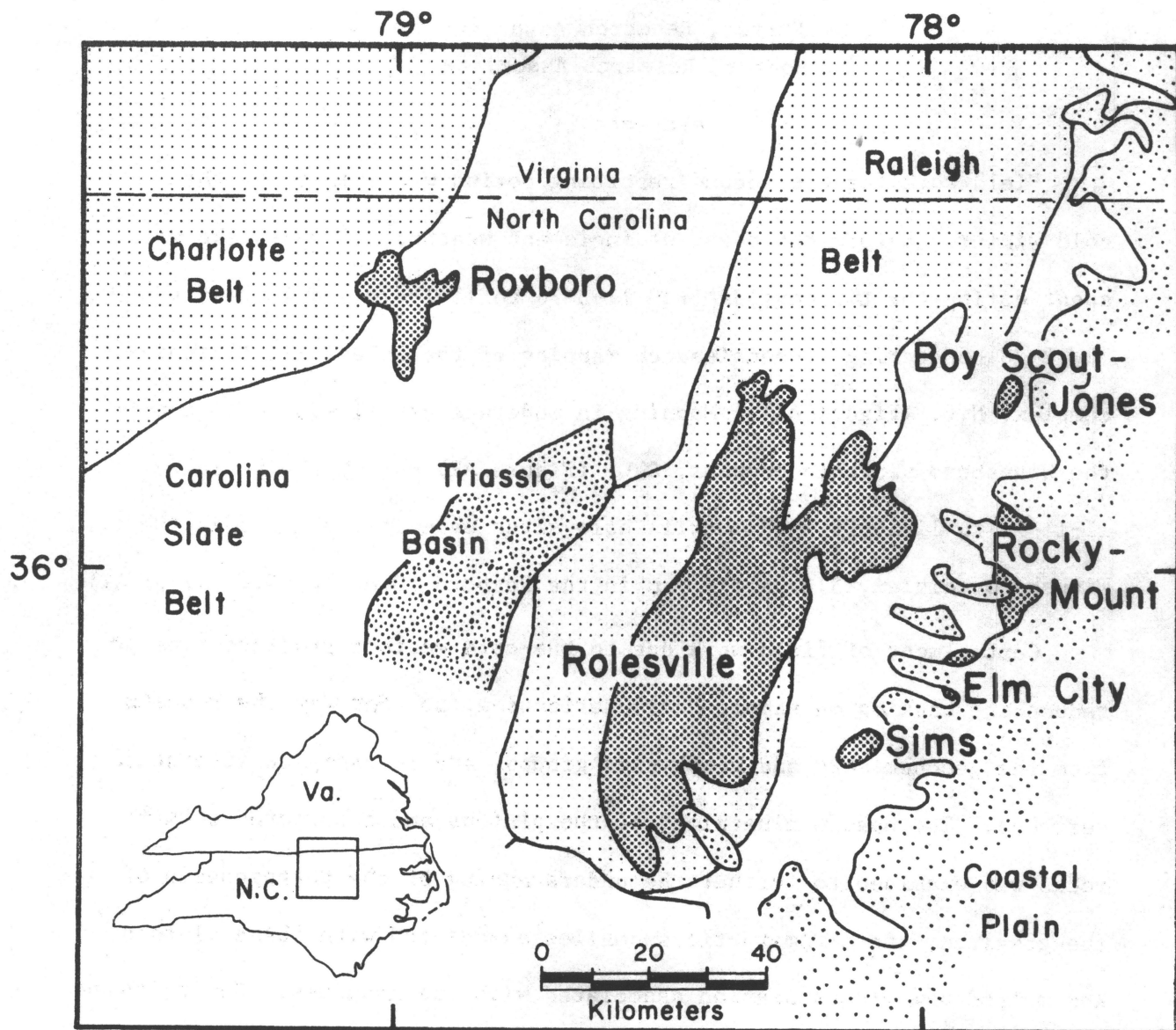


Fig. A1. Index map showing the locations of the Roanoke batholith and the Roxboro Metagranite.

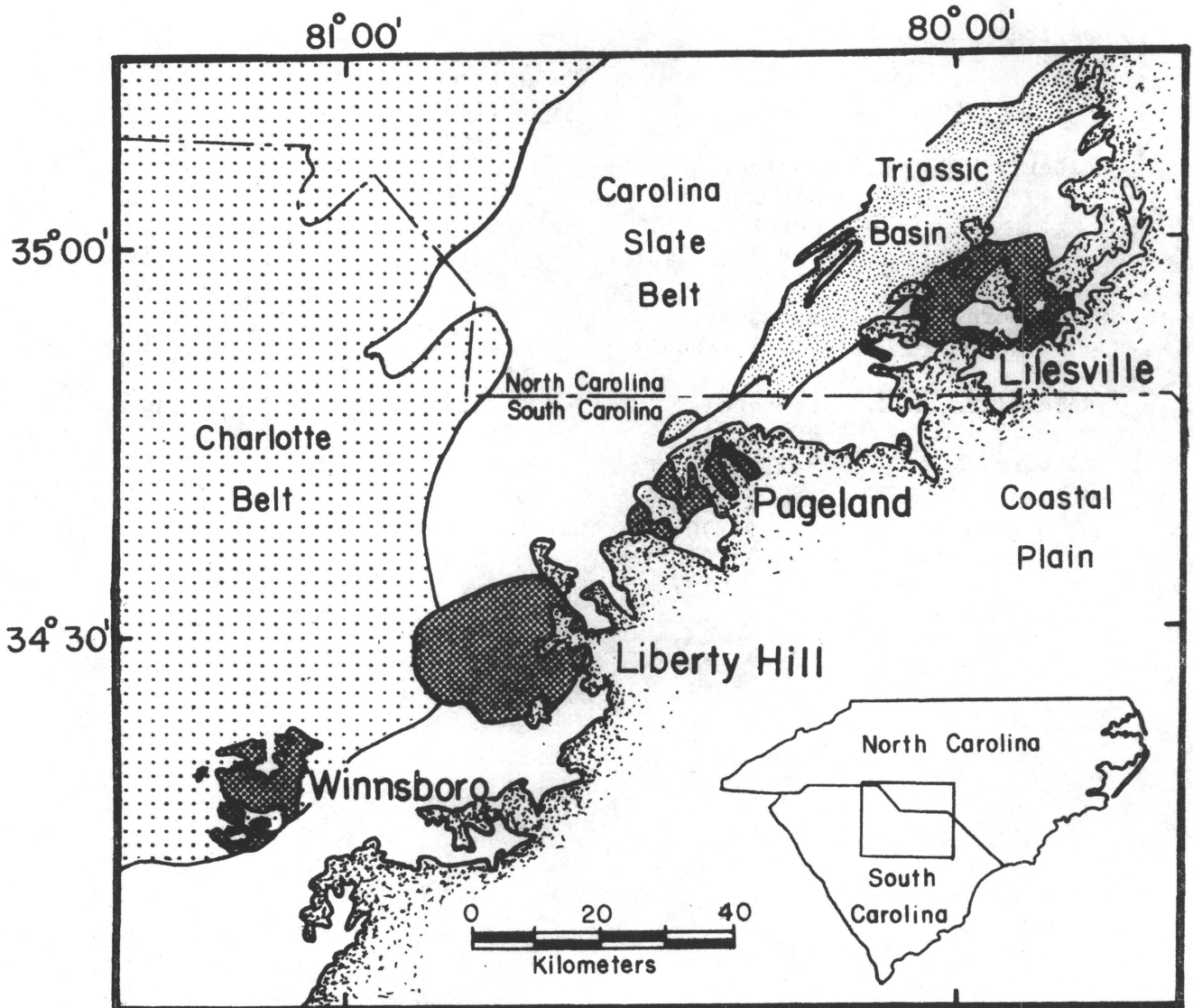


Fig. A2. Index map indicating locations of four ca. 300 m.y. postmetamorphic plutons in North and South Carolina.

contact aureoles. One granite sample (S6-65) has already been sent to the Applied Research Laboratories in Sunland, California for measurement by ion microprobe of thorium and uranium concentrations in traverses across the nine mineral phases present.

The following sampling was completed during the second reporting period:

<u>Pluton</u>		<u>Chemistry and Heat Production Samples</u>	<u>Total Samples</u>
Liberty Hill, S.C.	surface	1	17
	Ker 1 (425')	1	5
	Ker 2 (420')	5	17
	Ker 3 (1334')	13	29
Winnsboro, S.C.	surface	-	2
	Win 1 (1884')	-	17
Rolesville, N.C.	surface	27	128
Roxboro, N.C.	surface	6	6
	Rox 1 (884')		
	Rox 2 (702')		
	Rox 3 (230')		

Opaque Mineralogy

J. Alexander Speer

Granites

Mineralogic and textural data concerning the oxide and sulfide phases in the Liberty Hill and Winnsboro plutons are summarized in Table A1. Sample locations are given in Figs. A3 and A4. The rocks contain less than 2 modal percent oxide minerals and less than 0.1 modal percent sulfide minerals. In order of frequency of observation, the opaque minerals are magnetite, ilmenite, pyrite, chalcopyrite, and pyrrhotite. Hematite is common, but only as a subsolidus or weathering product. Molybdenite, sphalerite, and uraninite were also observed.

In the coarse-grained phases of the Liberty Hill and Winnsboro plutons, magnetite predominates in abundance over ilmenite. The magnetite contains octahedrally oriented, fine ilmenite lamellae as well as larger external and internal granular ilmenite. These ilmenite intergrowths are thought to represent "oxyexsolution" of a primary titanomagnetite ($\text{Usp-Mt}_{\text{ss}}$). The ilmenite intergrowths are present in the magnetite in amounts less than 10% of the grain and constitute the only ilmenite in some coarse-grained rocks. Many ilmenite grains contain networks and blebs of white-grey hematite, which contrast with the reddish grey color of the ilmenite, and indicate exsolution of the ilmenite-hematite solid solution. Only in rare instances has magnetite been oxidized to hematite in petrographically fresh rock.

In several coarse-grained rocks of the Liberty Hill and Winnsboro plutons, granular titanite mantles ilmenite and magnetite. The opaque appears to have been resorbed, suggesting that titanite has replaced

Table A1. Opaque mineralogy of the Liberty Hill and Winnsboro plutons.

sample numbers	magnetite(mt)		ilmenite(il)			hematite(hm)			chalcopyrite(cp)		pyrrhotite(po)		pyrite(py)		marcasite alter. prod.			
	plain	il intergrowths	plain	intergrowths		rims	plain	grndmass	inclusions		grndmass	inclusions		grndmass		inclusions		
				hm	mt				tit	py		po	mt			mt	silicate	mt
Winnsboro																		
F6-3	+	0	0	+	0	0	0	0	0	0	0	+	0	0	0	+	0	0
F6-3	0	+	0	0	+	0	0	0	0	0	0	+	0	0	0	+	0	0
F6-39	0	+	+	0	+	0	0	0	0	0	0	+	0	0	0	+	0	0
F6-40	+	0	+	0	0	0	+	0	+	0	0	+	0	0	0	+	0	0
F6-45	0	+	0	+	+	0	0	0	+	0	0	+	0	0	0	+	0	0
F6-52	+	0	+	0	0	0	0	0	0	0	0	0	0	0	0	0	0	0
F6-59	+	0	0	+	0	0	0	0	0	0	0	0	+	0	0	0	+	0
F6-60	+	0	0	+	0	0	0	0	0	0	0	+	+	+	0	+	+	+
F6-66	0	+	0	+	+	0	0	0	0	+	0	0	0	0	0	0	0	0
S6-18	0	+	+	0	+	0	0	0	0	0	0	+	+	0	0	+	+	0
S6-20	0	+	0	0	+	0	0	0	0	0	0	+	+	0	0	+	+	0
S6-23	0	+	0	0	+	0	0	0	0	0	0	+	0	0	0	+	0	0
S6-23-3	0	+	+	0	+	0	0	+	0	0	0	+(1)	+	+	0	+	+	0
S6-24	0	+	0	0	+	0	0	+	0	0	0	+	0	0	0	0	0	0
S6-26	+	0	+	0	0	0	0	0	0	0	0	0	0	0	0	0	0	0
S6-27	+	0	+	0	0	0	0	0	0	0	0	+	+	0	0	+	0	0
S6-34	+	0	0	+	0	0	0	0	0	0	0	+	+	+	0	+	+	0
Win 1-739	0	0	0	+	0	0	0	0	0	0	+	0	0	0	0	0	0	0
Liberty Hill - coarse-grained granite																		
F6-24	0	+	0	0	+	0	0	0	0	0	0	+	+	0	0	+	+	0
F6-25	0	+	+	0	+	0	0	0	0	0	0	+	0	0	0	+	0	0
S6-54	+	0	+	0	0	0	0	0	0	0	0	+	0	0	0	0	0	0
S6-69	0	+	0	0	+	0	0	0	0	0	0	+	+	0	0	+	0	0
S6-70	0	+	0	0	+	0	0	0	0	0	0	0	0	0	0	+	0	0
S6-87	0	+	0	+	+	0	0	0	+	+	0	+	+	0	0	0	+	0
S6-88	0	+	0	0	+	0	0	0	0	0	0	0	0	0	0	+	0	0
S6-98	0	+	0	+	+	+	+	0	+	+	0	+	0	0	0	+	+	0
S6-110(2)	0	+	0	0	+	0	0	0	0	0	0	+	0	0	0	+	0	0

(+) present
(0) absent

(1) intergrown with sphalerite
(2) also contains molybdenite

Table A1 (continued).

sample numbers	magnetite(mt)		ilmenite(il)			hematite(hm)			chalcopyrite(cp)			pyrrhotite(po)			pyrite(py)			marcasite alter. prod.
	plain	il intergrowths	plain	intergrowths		rims	plain	grndmass	inclusions		grndmass	inclusions		grndmass	inclusions			
				hm	mt				tit	py		po	mt		silicate	mt	silicate	
S6-126	+	0	+	+	0	0	0	0	0	0	0	0	0	0	0	0	0	0
S6-132	0	+	0	0	+	0	0	0	+	0	0	0	0	0	0	+	0	0
S6-135(3)	0	+	+	+	+	0	0	0	+	+	+	0	+	0	+	+	0	0
K1-323	0	+	+	+	+	0	0	+	+	+	0	+	+	0	0	0	0	0
K2-5	0	+	0	0	+	0	0	0	0	0	0	0	+	0	+	0	0	0
K2-6	0	+	0	0	+	0	0	0	+	0	0	0	+	0	+	0	0	0
K2-598	0	+	+	+	0	0	0	0	+	0	0	0	+	0	+	0	0	0
K2-118	0	+	+	+	+	0	0	0	+	0	0	0	+	0	+	0	0	0
K2-204	0	+	0	0	+	0	0	0	+	0	0	0	0	0	+	0	0	+
K3-294	+	0	0	0	0	0	0	0	+	0	0	0	+	0	+	0	0	0
K3-540	0	+	0	0	+	0	0	0	+	0	0	0	+	0	+	0	0	+
K3-794	0	+	+	+	+	0	0	0	+	+	0	0	+	0	+	0	0	+
K3-1303	0	+	+	+	+	0	0	0	+	+	+	0	+	+	+	0	0	+
Liberty Hill - fine-grained granite																		
S6-57	+	0	+	0	0	0	0	0	0	0	0	0	0	0	0	0	0	0
S6-67	+	0	+	0	0	0	0	+	0	+	+	0	+	0	0	0	0	0
S6-99	+	0	+	0	0	0	0	0	0	0	0	0	0	0	0	0	0	0
S6-100	+	0	+	0	0	0	0	0	+	+	0	0	0	0	0	0	0	0
S6-108	0	+	+	0	+	0	0	0	+	0	0	0	0	0	0	0	0	0
S6-111	+	0	+	+	0	0	0	0	0	0	0	0	0	0	0	0	0	0
K3-55(2)	0	+	0	0	+	0	0	0	0	0	0	0	+	0	0	0	0	0
K3-103	+	0	+	0	0	0	0	0	0	0	0	0	+	0	0	0	0	0

(+) present
(0) absent

(2) also contains molybdenite
(3) also contains uraninite

Table A2. Opaque mineralogy of the Liberty Hill contact metamorphic rocks.

sample number	magnetite(mt)		ilmenite(il)			hematite(hm)	pyrite(py)	pyrrhotite(po)	chalcopyrite(cp)	other
	plain	il intergrowths	plain	hm	intergrowths					
S6-52	0	0	0	0		+	0	+	0	
S6-59	0	+	0	+		0	0	0	+	marcasite after po.
S6-60	?	0	0	+		0	0	0	0	
S6-61	0	+	0	+		0	0	0	0	
S6-62	+	0	0	0		+	+	0	0	
S6-63	+	0	0	+		0	0	0	0	
S6-64	0	0	+	0		0	0	+	+	
S6-75	0	+	0	+		0	0	0	0	pentlandite in po.
S6-76	0	+	0	+		0	0	0	0	
S6-79	0	+	0	+		0	0	0	0	
S6-81	+	0	0	+		0	0	0	0	
S6-82	0	+	0	0		0	0	0	0	
S6-93	0	+	0	+		0	0	0	0	
S6-105b	0	0	+	0		0	0	+	0	
S6-127	0	0	0	+		0	0	0	0	
K3-240	+	0	0	0		0	+	+	+	
K3-472	0	0	+	0		0	+	+	+	
K3-1075	0	0	+	0		0	+	+	+	pentlandite in po. py rims po.
K3-1079	0	0	+	0		0	+	+	+	marcasite after po.

(+) present
(0) absent

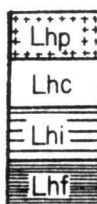
EXPLANATION

MAP UNITS

 *Tertiary and Cretaceous Coastal Plain deposits, undifferentiated.*

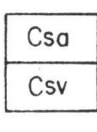
 *Diabase dikes, mostly Triassic in age. Field checked from magnetic data; dotted where concealed.*

 *Contact aureole of the Liberty Hill pluton.*

 *Liberty Hill pluton, consisting of a porphyritic border phase (Lhp), pink to white coarse-grained biotite-amphibole granite and quartz monzonite (Lhc) commonly intruded (Lhi) by dikes and small plugs of fine-grained granite (Lhf).*

 *Gabbro norite: Dutchmans Creek Gabbro of McSween (1972).*

 *Gneissic granite: Great Falls granite of Fullagar (1971) and Pleasant Hill Granite of Shiver (1974).*

 *Carolina Slate Belt: metamorphic rocks in the greenschist and amphibolite facies; originally argillites, tuffaceous argillite, and graywacke (Csa) and felsic and mafic volcaniclastic rock and volcanic flows (Csv).*

 Contact, dashed where inferred and dotted where concealed

 50 Strike and dip of foliation

 20 Strike and dip of igneous lamination

 30 Strike and dip of xenoliths

 5699 Sample locality

 Drill hole

Ker l

 Quarry

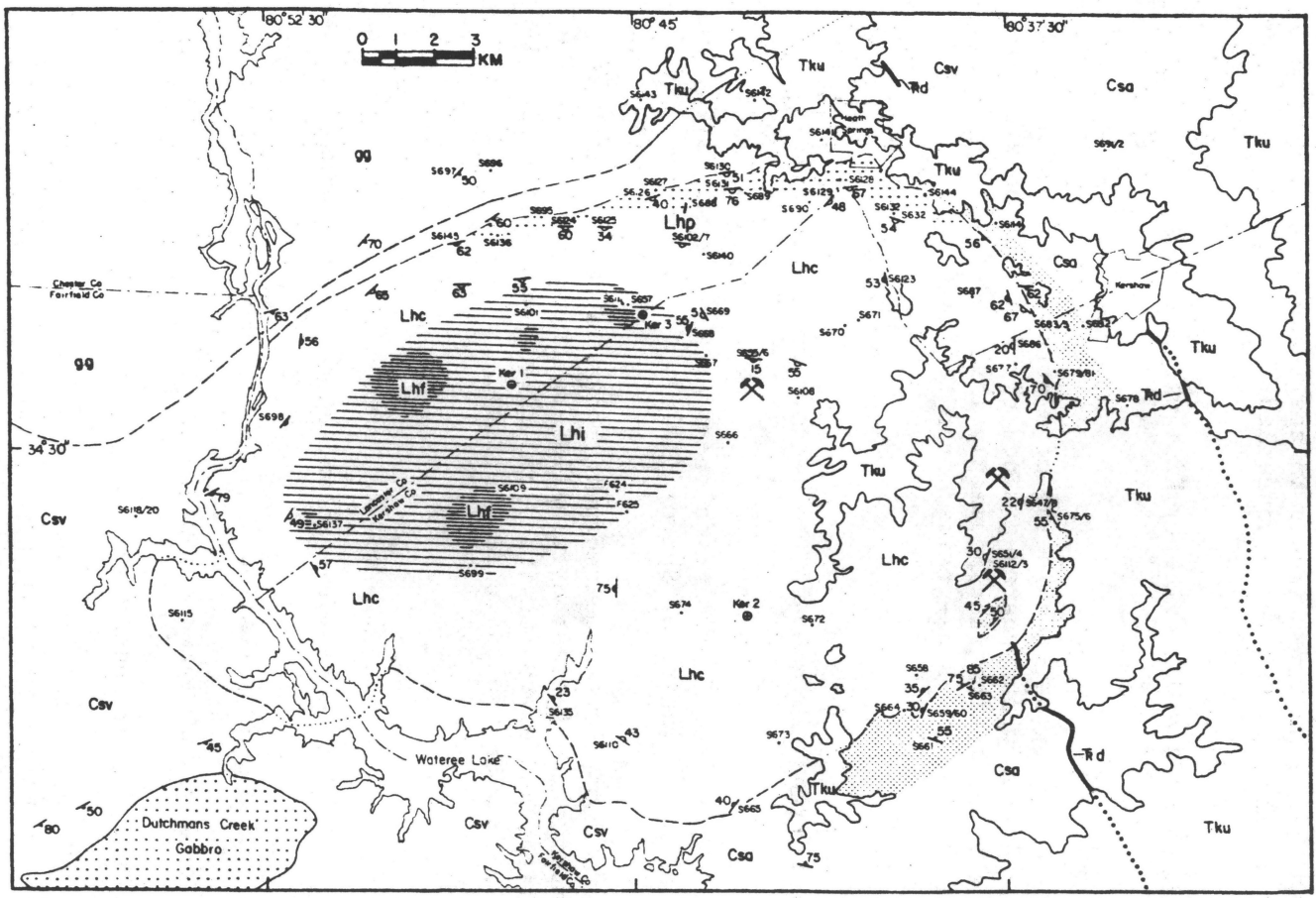


Fig. A3. Geologic map of the Liberty Hill pluton, South Carolina.

EXPLANATION

MAP UNITS

PERMIAN AND CARBONIFEROUS	RION PLUTON	rm	Medium grained biotite monzogranite
		rf	Fine-medium grained biotite monzogranite
WINNSBORO PLUTON		wg	Biotite-hornblende granite, quartz syenite, and quartz monzonite, C. I. < 10
		wgm	Biotite-hornblende monzogranite, C. I. > 10
		wgk	Biotite-hornblende syenogranite and quartz syenite, K-feldspar rich
		gb	Gabbro-norite
UPPER PRECAMBRIAN AND PALEOZOIC		Csu	Carolina slate belt undifferentiated metamorphic rocks
		Csug	Mixed granite and Csu
		Cbu	Charlotte belt undifferentiated metamorphic rocks
		Cba	Charlotte belt amphibolite
		Cbug	Mixed granite and Cbu

SYMBOLS

	Contact, dashed where inferred
	Strike and dip of foliation
	Strike and dip of igneous lamination
	Strike and dip of xenoliths
	Sample locality

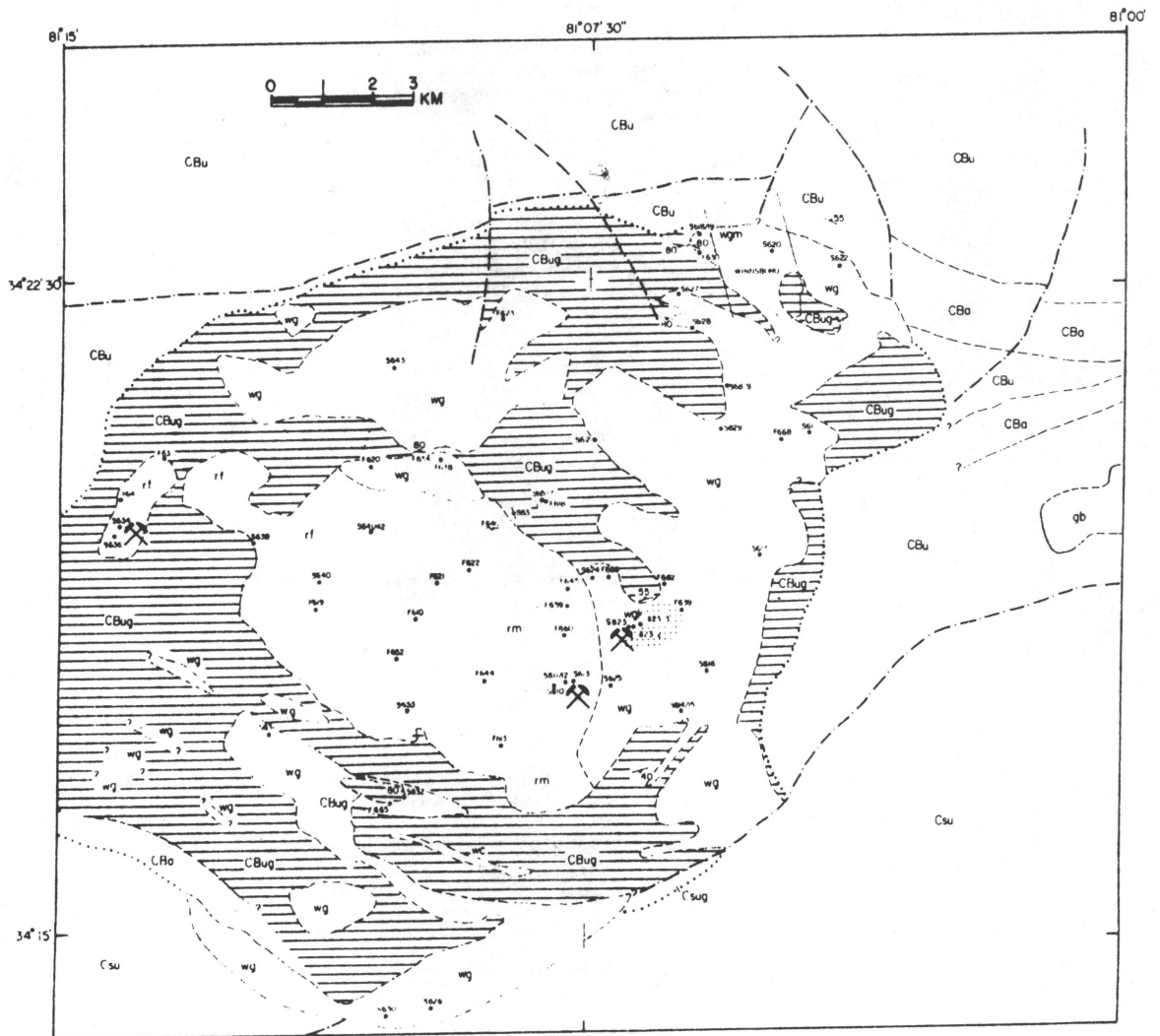
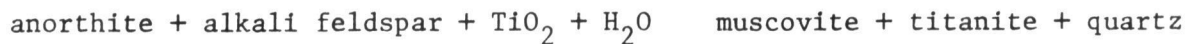


Fig. A4. Geologic map of the Winnsboro plutonic complex, South Carolina.

the oxides. The reaction probably occurred during the stage of deuteric alteration, with calcium and silica reacting with the titanium oxide component of the opaques:



The coarse-grained granites may therefore contain two generations titanite: magmatic titanite which is generally euhedral, and deuteric titanite which occurs as granular rims on opaque oxides. Hunt and Kerrick (1977) have calculated that at 4 kb, the above reaction occurs for pure rutile at a temperature of 550°C.

Two sulfide assemblages have been observed in the granitic rocks. The assemblage pyrrhotite + chalcopyrite + pyrite occurs only as inclusions, usually in magnetite and less commonly in silicates such as titanite and zircon. No sulfide inclusions have been observed in ilmenite. The intergranular assemblage, pyrite + chalcopyrite, coexists with both magnetite and ilmenite. From the contrasting occurrence of these two assemblages, it appears that pyrrhotite + chalcopyrite + pyrite is the initial sulfide assemblage that crystallized with magnetite and the early silicate minerals. Pyrite + chalcopyrite is a later sulfide assemblage that crystallized in equilibrium with both magnetite and ilmenite. Thus the activities of oxygen and sulfur appear to have increased during crystallization of the granite magma (Fig. A5).

The sulfide inclusion assemblage, pyrrhotite + chalcopyrite + pyrite, which is found in magnetite and the silicates, indicates that reequilibration occurred at low temperatures. Yund and Kullerud (1966) found that above $334^\circ \pm 10^\circ\text{C}$, pyrrhotite and chalcopyrite react to form pyrite + a cubic copper-iron solid solution + vapor. The high temperature inclusion assemblage,

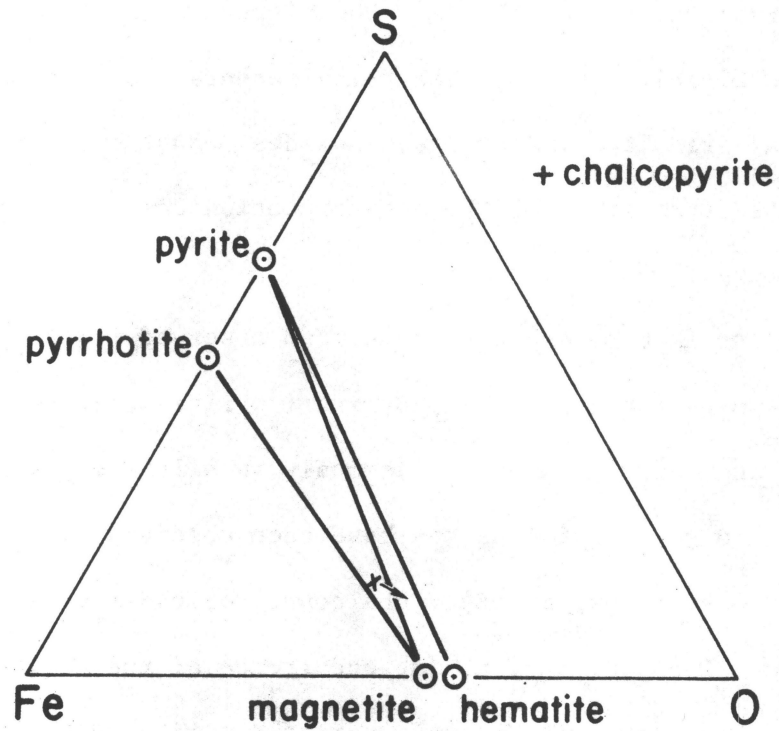


Fig. A5. Fe-O-S diagram showing the inclusion assemblage pyrite + pyrrhotite + magnetite (x), which occurs in early crystallizing phases in the granite, and the later crystallizing groundmass assemblage, magnetite + pyrite + ilmenite (represented by hematite). The transition indicates an increase in oxygen and sulfur fugacity with cooling of the magma.

therefore, was pyrrhotite + pyrite + an intermediate copper-iron solid solution + magnetite, which has a thermal stability above the granite solidus.

In the weathered granite samples, supergene alteration of the sulfides is common. Pyrite and chalcopyrite have rims of hematite and hydrous iron oxides.

Metamorphic Rocks

Mineralogic and textural data concerning the opaque mineralogy of the country rocks and hornfelses of the Liberty Hill contact aureole and xenoliths is summarized in Table A2. Locations are given in Fig. A3. As suggested by the wide variety of protoliths and metamorphic conditions represented by the metamorphic rocks, the opaque mineralogy of the country rocks is highly variable in the texture, abundance and number of phases present. Pyrrhotite and pyrite are the most common sulfides. Chalcopyrite is rare, except in calcareous rocks, where regular intergrowths with pyrrhotite make up to 5 volume percent of the rock. Such intergrowths probably represent an unmixed Cu-Fe intermediate solid solution which was the high temperature phase. Possible exsolved pentlandite from pyrrhotite was noted in two samples (S6-64, Ker 3 - 472). Sphalerite with exsolved chalcopyrite was observed in one specimen (Ker 3 - 999.3). Marcasite is a common alteration product of the pyrrhotite.

Magnetite and ilmenite are the common oxide minerals. In most metamorphic rocks they have well developed exsolution features: ilmenite from magnetite and hematite from ilmenite.

Uraninite

Uraninite, UO_{2+x} , has been identified in a coarse-grained granite of the Liberty Hill pluton (S6-135) by ore microscopy and qualitative electron

microprobe analysis. The tabular grain , 0.04x0.01mm, is included in biotite at a high angle to the biotite cleavage. It is bounded by a large radiation damage halo composed of an inner ring of yellow crypto-crystalline material and an outer ring of black isotropic biotite. This large pleochroic halo, which is several times the volume of the uraninite grain, is the most important feature that indicated the special nature of the mineral. The radiation damage halos around zircons and xenotimes are only a fraction of the size of the grains that they surround. In reflected light the uraninite is a leaden grey, in contrast to the yellow grey of magnetite and red grey of ilmenite.

A qualitative analysis by electron microprobe showed the presence of uranium, thorium, and iron. Counts were collected for no other elements. As a comparison, counts for U, Th, and Fe were also made on uraninite from a pegmatite at Spruce Pine, N.C. The Liberty Hill uraninite contains less uranium and more thorium and iron. Magmatic and pegmatitic uraninites often contain larger amounts of Th and R.E.E. than hydrothermal uraninites (Fron del, 1958). What little compositional data is available on the Liberty Hill uraninite suggests a magmatic origin for this mineral.

Molybdenum Mineralization

in the Liberty Hill and Winnsboro Plutons

J. Alexander Speer

Molybdenite occurs as widely disseminated flakes in the fine-grained phases of both the Liberty Hill and Winnsboro plutons. In the fine-grained phase of the Winnsboro, the Rion pluton, concentrations of molybdenite are also found in quartz veins with pyrite and chalcopyrite. In only one sample (S6-110) was molybdenite observed in a coarse-grained rock of the Liberty Hill pluton. The disseminated molybdenite probably represents magmatic crystallization, whereas the molybdenite-chalcopyrite-pyrite-quartz veins are similar to conventional hydrothermal veins.

Deuteric alteration is more extensive in the fine-grained granites, in which molybdenum mineralization is common, than in the coarse-grained granites. Biotite is altered to chlorite, and plagioclase is altered to albite + epidote + white mica + calcite + quartz. Alkali feldspar is locally, but not invariably, altered to a red-brown, fine-grained material, but the reaction is probably caused by weathering rather than by deuteric alteration. The present alkali feldspar is apparently in equilibrium with the products of deuteric alteration. The deuteric mineral assemblage is the same as that found in the molybdenite-chalcopyrite-pyrite-quartz veins, suggesting that the reaction of the late magmatic fluids with the previously consolidated granite occurred under the same conditions and perhaps simultaneously with the molybdenite vein mineralization.

Recent experimental work in the $\text{CaO-K}_2\text{O-Al}_2\text{O}_3\text{-SiO}_2\text{-CO}_2\text{-H}_2\text{O}$ system (Johannes and Orville, 1974) allows an understanding of the

reactions and conditions of the deuteric alteration associated with the molybdenum mineralization. Fig. A6 illustrates several reactions in $T-X_{CO_2}$ space. The proposed path of $T-X_{CO_2}$ conditions in Fig. A6 is suggested by the presence of the deuteric assemblages epidote and epidote + calcite and the absence of calcite alone in the Liberty Hill and Winnsboro plutons. The residual fluid of a granite magma would approach the invariant point from the water-rich side. Conditions remain those of the invariant point until either the fluid or one of the feldspars is consumed, and the rock is completely solidified. Because both feldspars remain in the rocks, the fluid must have been the first reactant to disappear.

The deuteric alteration, and probably the molybdenum mineralization, occurred at conditions along these reaction curves and at the invariant point. The intensity of alteration depends on the initial ratio of fluid to rock. Low fluid contents produce minimal alteration, as in the coarse-grained Liberty Hill and Winnsboro rocks, whereas higher fluid contents cause more extensive alteration as in the fine-grained Rion and Liberty Hill.

Fig. A6 is drawn for a total pressure of 4 kb, which is an estimate of the Liberty Hill emplacement pressure based on the mineralogy of the contact aureole. At 4 kb, the invariant point is at $475^{\circ}C$ and $X_{CO_2} = 0.03$. This is an estimate of the maximum temperature and carbon dioxide content. The reduction of fluid pressure below total pressure or the addition of sodium to the system would lower the temperature and the X_{CO_2} of the invariant point along the line shown in Fig. A6, inset. The effect of sodium is evident in both the Liberty Hill and Winnsboro plutons in the restriction of

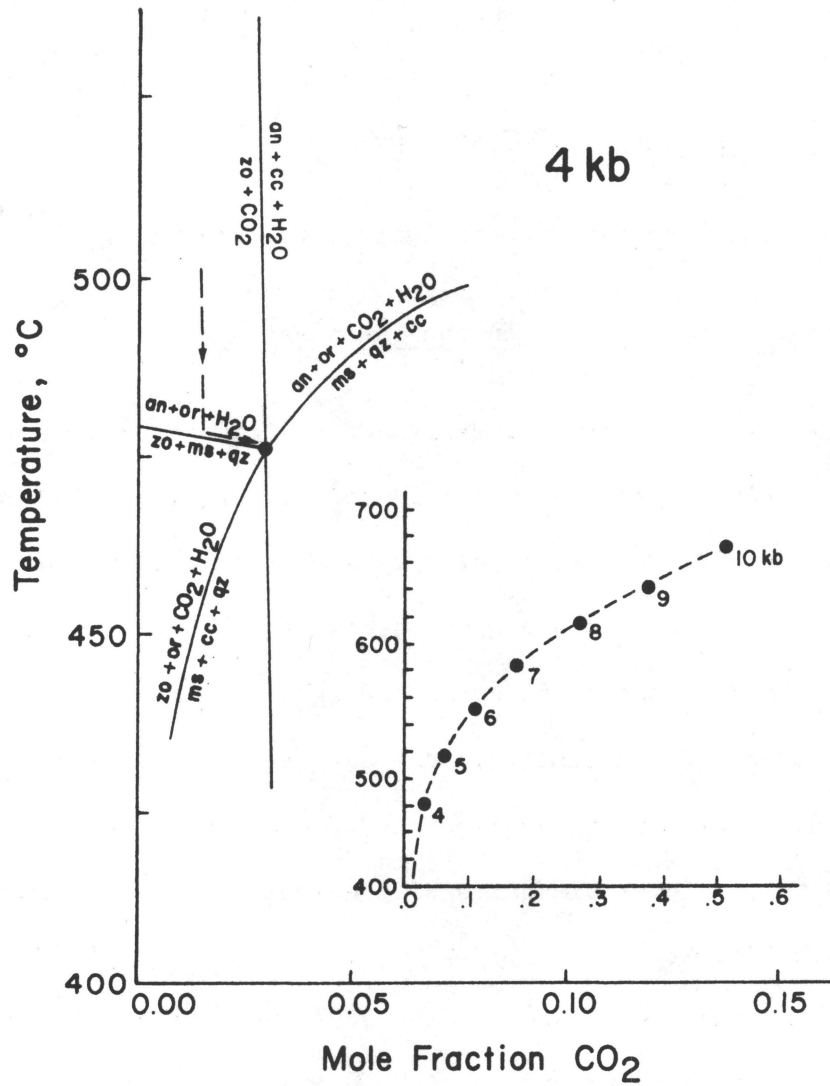
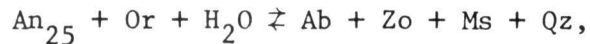


Fig. A6. Phase relations in the water-rich portion of the system $K_2O-CaO-Al_2O_3-SiO_2-H_2O$ from Johannes and Orville (1974). Dashed line shows probable path of descent of deuteritic conditions in the Liberty Hill and Winnsboro plutons. Inset shows variation of the invariant point with pressure.

saussuritization of plagioclase to the cores of zoned crystals with an anorthite content greater than 25 mole percent. The reaction



would thus be changed to



which accounts for the reverse zoning observed in altered plagioclase.

Molybdenum mineralization in the Southeast

The molybdenum mineralization of the Liberty Hill and Winnsboro plutons falls within the criteria used by Lowell and Guilbert (1970) and Clark (1972) to define porphyry copper-molybdenum and molybdenum deposits. Compared to ore grade deposits, the southeastern molybdenum occurrences differ only in scale and intensity rather than in nature. Any differences, especially in the alteration, can be accounted for by the high pressure of emplacement of the South Carolina plutons, as opposed to the lower pressures of the shallow Mesozoic deposits of the western United States.

Molybdenum occurrences in the southeastern United States are summarized in Table A3 and located in Fig. A7. All appear to be vein or disseminated copper-molybdenum mineralizations associated with granitic intrusive rocks with varying types of alteration. The plutons are post-metamorphic, 300 m.y. in age, except for the Newell prospect, which is probably older. Mineralization is a late magmatic feature in both the Liberty Hill and Winnsboro plutons as discussed above. Andersen and Fullagar (1977) dated altered material at the Boy Scout-Jones

Table A3. Molybdenite occurrences
in the southeastern United States.

pluton or prospect	location	mineralization ¹	alteration	age	references
Boy Scout - Jones Moss - Richardson unnamed granite stock	Halifax Co., NC	mo-cp-py	prophyllitic + argillic	307 ± 6 m.y. Rb-Sr	Robertson <i>et al.</i> , 1947 Harvey, 1974 Andersen & Fullagar ² , 1977 Schrader <i>et al.</i> , 1977
Sims (Connor) biotite granite	Wilson & Nash, Co., NC	mo-cp-py-sph-ga	yes	post-metamorphic	Council, 1954 Cook, 1972
Newell or Dixie Queen mine Boger's Chapel quartz monzonite	Cabarrus Co., NC	mo-cp-py vein-disseminated	prophyllitic	syn-metamorphic 388 ± 12 m.y. K-Ar 417 ± 15 m.y. K-Ar	Bates & Bell, 1965 Worthington & Lutz ² , 1975
Woodleaf granite	Rowan Co., NC	mo-cp-py vein	prophyllitic w/ zeolites & fluorite	post-metamorphic	Privett, 1973
Catawaba granite	York Co., SC	mo-cp-py-bn vein-disseminated	potassic	325 ± 50 m.y. Rb-Sr	Fullagar ² , 1971 Beg and Larson, 1975
Liberty Hill pluton	Kershaw, Lancaster & Fairfield Co., SC	mo-cp-py disseminated	potassic/ prophyllitic	299 ± 8 m.y. Rb-Sr	Fullagar ² , 1971 this report
Winnsboro pluton	Fairfield Co., SC	mo-cp-py vein-disseminated	potassic/ prophyllitic	301 ± 4 m.y. Rb-Sr	Fullagar ² , 1971 this report
Wilton pluton	Granville Co., NC	mo	unknown	(~300 m.y.) Rb-Sr	Anderson & Fullagar ² , 1977 Carpenter, 1970

¹sulfide abbreviations: mo, molybdenite; cp, chalcopryrite; py, pyrite; sph, sphalerite; ga, galena; bn, bornite.

²reference for age of pluton.

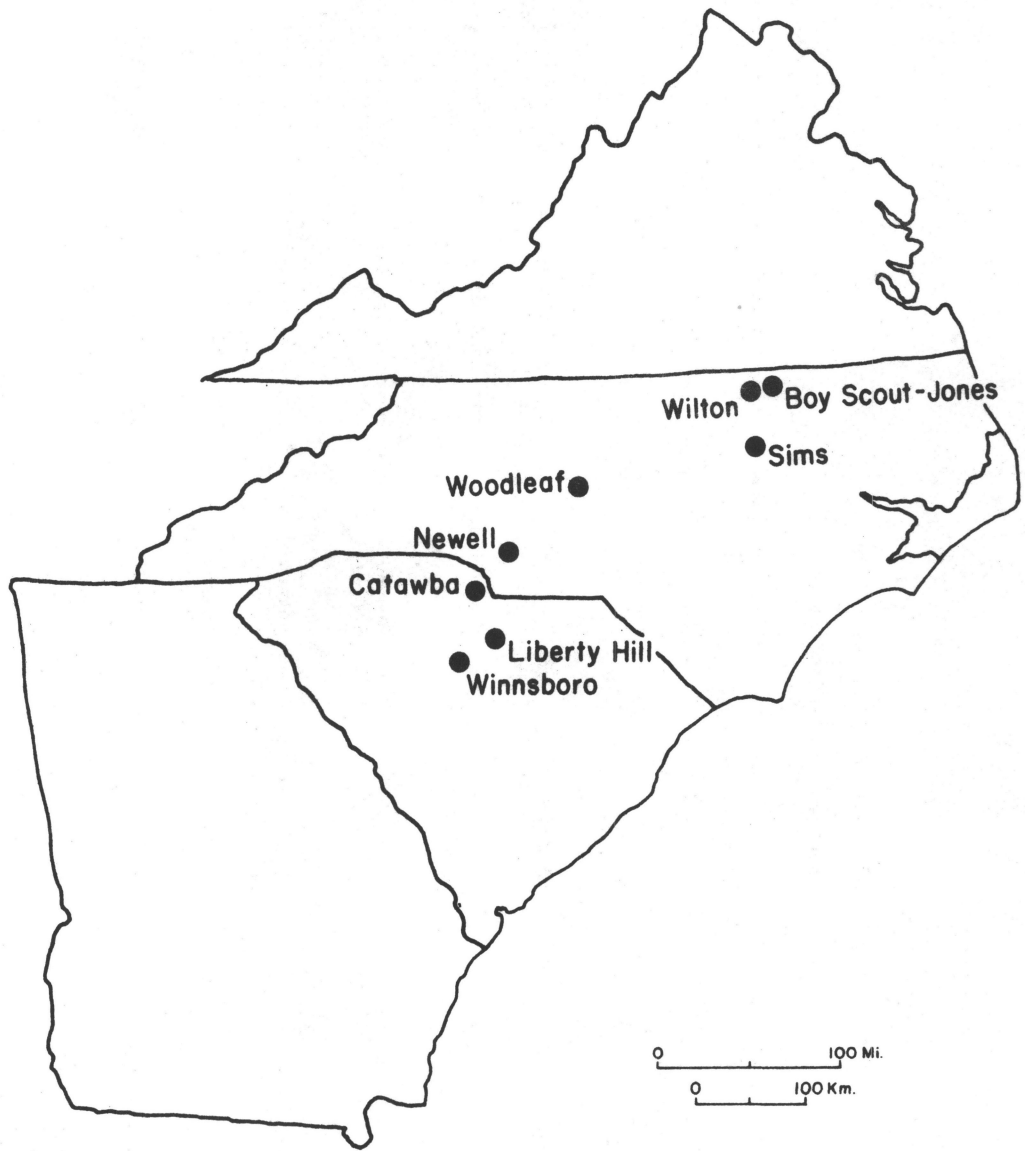


Fig. A7. Index map showing known localities of molybdenum mineralization associated with the ca. 300 m.y. plutons.

prospect at 288 ± 7 m.y. and determined an age of 279 ± 6 m.y. from a sericite mineral isochron. With an age of 307 ± 6 m.y. on the fresh granite, they concluded that the mineralization was a late consolidation feature of the granite. The sparse molybdenum-copper mineralization may be a general feature of the 300 m.y. old plutons, as suggested by Andersen and Fullagar (1977). As of this time, no deposit appears to be of economic value.

Uranium-molybdenum relations

Lowell and Guilbert (1970) suggest that the differentiation index of an intrusive rock may dictate whether copper or molybdenum predominates in a deposit, molybdenum tending to be associated with more silicic rocks. Uzkut (1974) demonstrates that molybdenum increases with increasing silica and alkali contents, with alkaline rocks exhibiting the highest molybdenum contents. If, as is commonly suggested, uranium is also enriched in more silicic and alkali-rich rocks, a sympathetic relation may exist between molybdenum and uranium. For the Liberty Hill and Winnsboro plutons, the fine-grained granites, which are more closely associated with the molybdenum mineralization, have the highest uranium contents. Uraninite-molybdenite deposits constitute one of the several types of uranium deposits that have been recognized (Dybek, 1962). Associated with granitic rocks, they have been found as veins (Stevenson, 1951) and as massive deposits near country rock contacts (Harshman and Bell, 1970).

Petrography of the Liberty Hill Drill Cores

J. Alexander Speer

Three holes have been drilled in the Liberty Hill pluton; locations are shown in Fig. A3. Core samples from these holes are petrographically similar in most respects to the surface samples and can be characterized by rock descriptions included in the first report.

Lithologic logs for drill holes Ker 2 and Ker 3 are illustrated in Figs. A8 and A9. Two types of granite are encountered in the drill cores: coarse-grained granite cut by large dikes of a fine-grained granitic phase, a maximum of 130 feet in vertical height. Xenoliths and xenocrysts from the coarse-grained granite occur within the margins of these fine-grained dikes. Small (1-5 cm) mafic clots, consisting largely of biotite and amphibole, are found in the coarse-grained granite. Amphiboles with pyroxene cores, which are otherwise rarely seen, usually occur in these clots. Several large hornfels xenoliths, up to 45 ft. in vertical height, were encountered. Thin dikes of aplite and muscovite-quartz-alkali feldspar are ubiquitous.

Modes of samples selected for chemical analysis and measurement of heat production are listed in Table A4. On the quartz-alkali feldspar - plagioclase diagram (Fig. A10), the modes fall within the field defined by the surface samples. The drill hole specimens, however, are notably different from the surface samples in that they have a uniformly higher color index (Fig. A11). This phenomenon may be a result of the more rapid weathering of the more mafic granite. Surface sampling therefore probably results in a disproportionate number of more felsic samples. The difference in composition between the surface and subsurface samples indicates that the granite is more mafic in composition than would have been postulated from the surface samples alone.

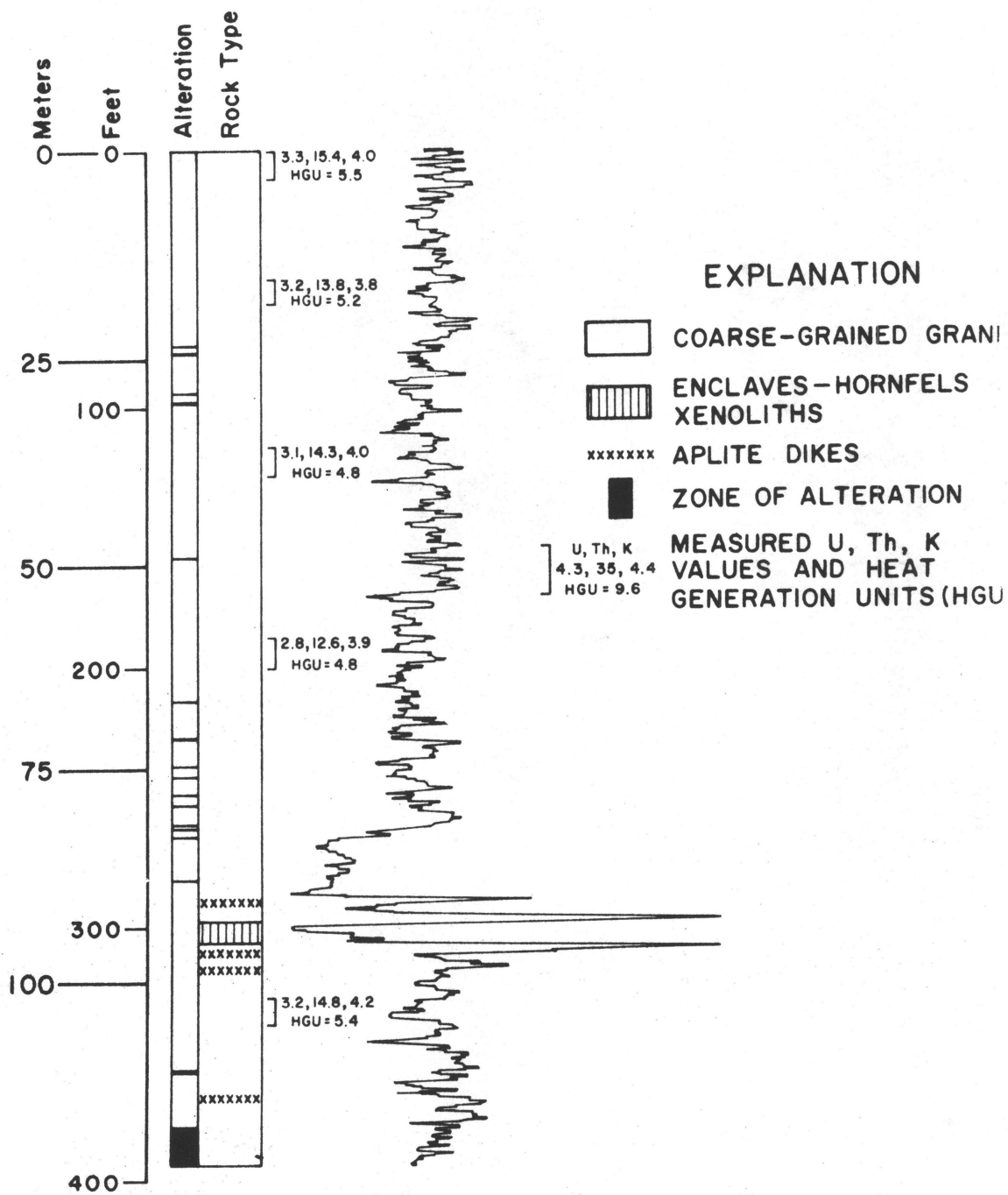


Fig. A8. Lithologic log of drill hole Ker 2, with corresponding alteration and gamma ray spectrometer log. Radioactivity measurements increase to the right.

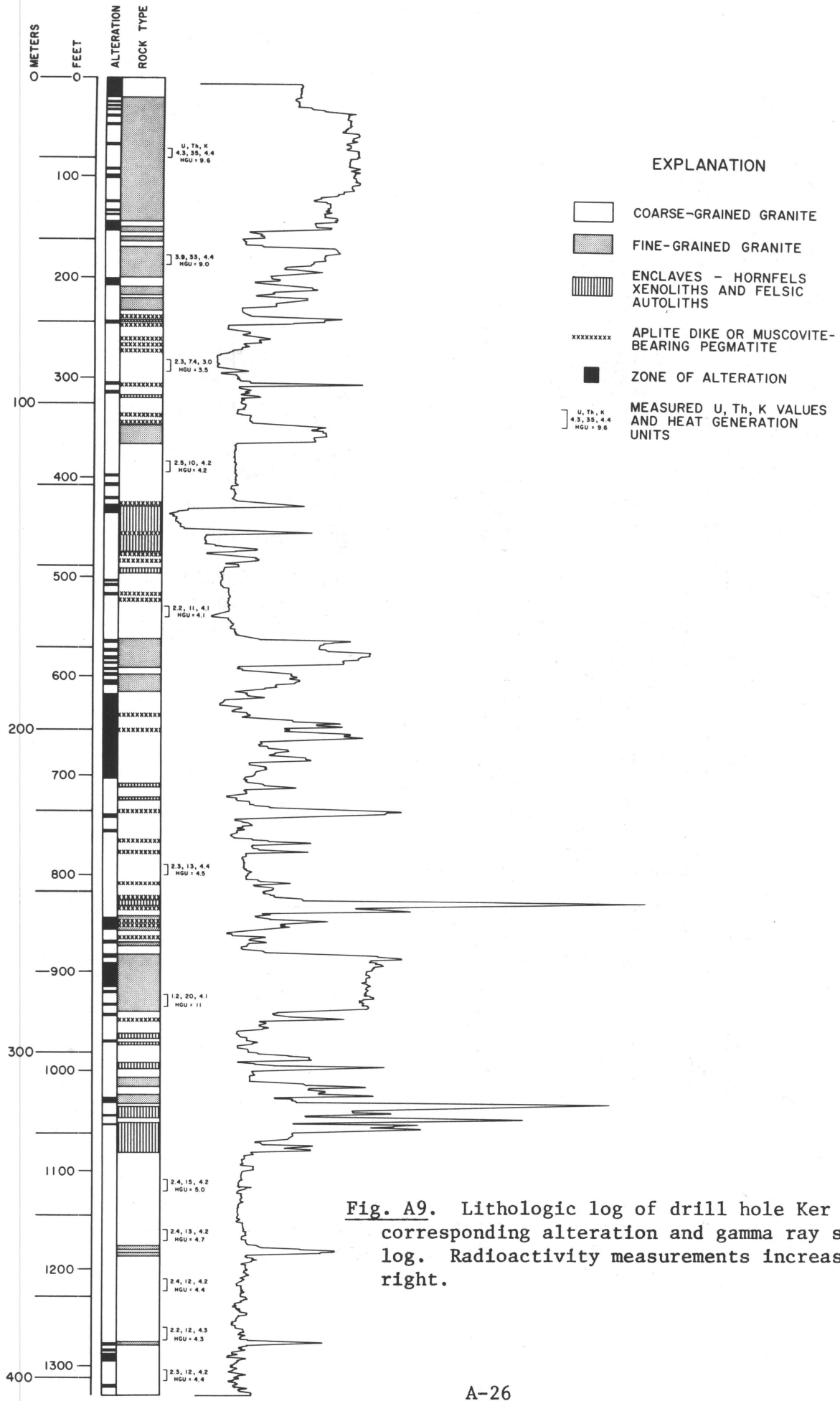


Fig. A9. Lithologic log of drill hole Ker 3, with corresponding alteration and gamma ray spectrometer log. Radioactivity measurements increase to the right.

Table A4. Modal Data for Drill Holes in the Liberty Hill Pluton.

Drill Hole	Depth	Quartz	K-feldspar	Plagioclase	Color Index
Ker 1	135/145	28.3	43.3	21.6	6.8
Ker 2	1.5/11	19.2	42.1	29.1	9.7
	53.5/59.7	16.6	37.4	36.2	9.8
	118.1/128.5	16.9	39.5	34.3	9.3
	194/204	17.2	36.1	35.3	11.4
	334/344	15.4	36.7	36.9	11.0
Ker 3	284/294	21.9	36.9	26.7	16.1
	384/394	14.5	40.1	37.1	8.7
	530/540	12.9	36.1	32.9	17.9
	784/794	23.3	40.1	29.1	7.4
	1110/1120	18.6	37.7	35.0	8.7
	1140.2/1150.7	14.4	37.1	37.6	11.0
	1160/1170	17.2	41.2	32.5	9.1
	1210/1220	19.5	39.7	30.0	10.7
	1260/1270	16.0	39.5	32.8	11.7
	1304/1314	11.0	39.0	37.8	12.1

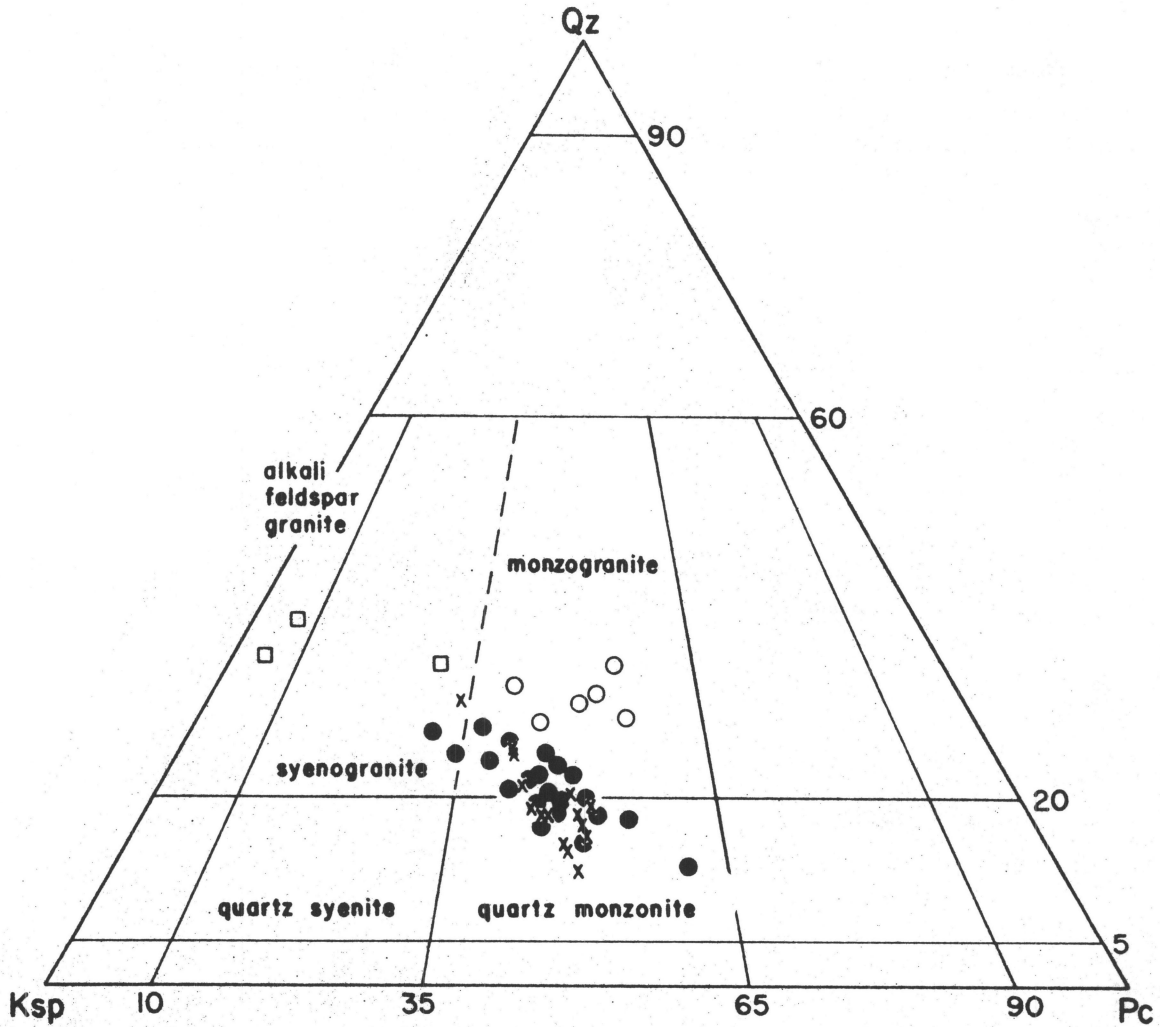


Fig. A10. Triangular diagram of modal volume percent of alkali feldspar (Ksp), plagioclase (Pc), and quartz (Qz) for samples from the Liberty Hill drill cores (Ker-1,-2,-3) (x), and surface samples (□, ○, and ●).

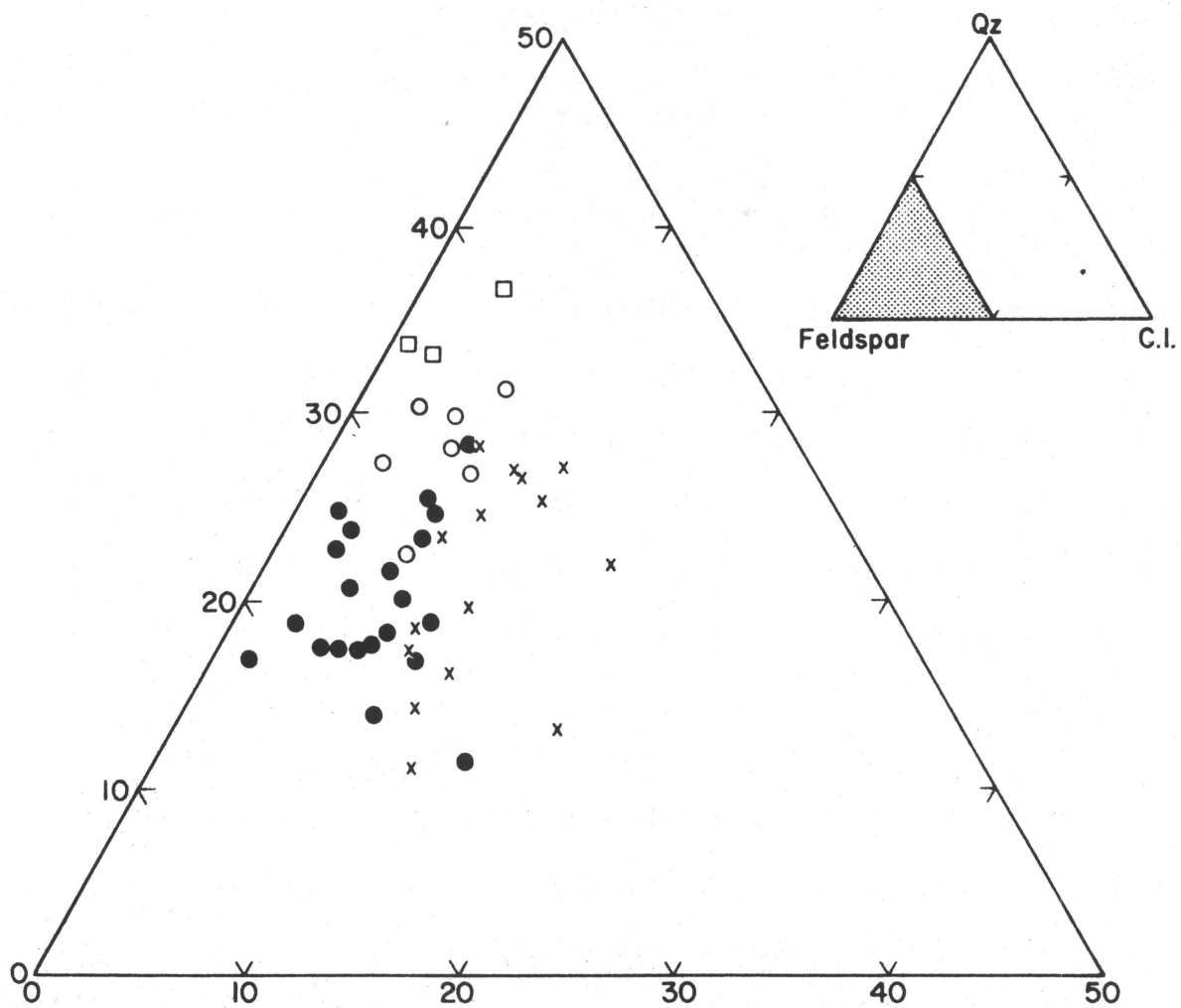


Fig. A11. Modal data for the Liberty Hill drill cores (x) and surface samples (□, ○, and ●) plotted on triangular diagram showing volume percent total feldspar, color index (C.I.), and quartz (Qz).

The mineralogy of the hornfels xenoliths is similar to that of the surface hornfels samples. Mineral assemblages indicate metamorphic conditions of the amphibole and pyroxene hornfels facies. Two new mineral assemblages of the pyroxene hornfels facies were found:

- * Ker 3 - 1074.2 Orthopyroxene-garnet-cordierite-biotite-K-feldspar-plagioclase-quartz

- Ker 3 - 472
 and Orthopyroxene-clinopyroxene-plagioclase-quartz-garnet
- Ker 3 - 465

These are the first observed occurrences of orthopyroxene with garnet + cordierite or clinopyroxene in the xenoliths. Its presence confirms the conclusion, derived from other assemblages (see previous report), that the granite was emplaced at an unusually high temperature. Compositions of the coexisting orthopyroxene + clinopyroxene and garnet + cordierite coexisting with orthopyroxene can be used to determine their temperature and pressure of formation.

Some xenoliths are cut by a number of muscovite-bearing granitic dikes, 1-2 cm wide. The adjacent hornfels also contains muscovite, indicating a locally fluid-rich environment. These granitic dikes may represent either partial melts of the xenoliths, or invading fluid-rich residual melts derived from the enclosing granite.

Natural gamma-ray logs were made of drill holes Ker 2 (Fig. A8) and Ker 3 (Fig. A9). Gamma rays measured are emitted principally from K^{40} and from U and Th and their daughter products. The daughter products may not be in equilibrium with their parent isotopes so that the gamma-ray readings may not represent U and Th contents along the length of the log. However, heat production determinations for powdered core samples (Figures A8 and A9) do show a good correlation with the gamma-ray log. The coarse-grained granite, which has an average heat production of 5.01 H.G.U.

/* Samples are labeled by drill hole number and depth or depth interval (feet).

(30 samples), gives lower gamma log readings than the fine-grained granitic dikes, which have an average heat production of 9.33 H.G.U. (8 samples). The aplite dikes and muscovite-bearing pegmatites have gamma ray spikes with magnitudes similar to or greater than those of the fine-grained granite. One heat production value determined for an aplite is 10.5 H.G.U.

Radiation levels within the xenoliths, as recorded by the gamma ray spectrometer, are variable. For xenoliths Ker 2- 302/315 and Ker 3- 430/476, the readings are lower than for the coarse-grained granite. The xenolith from Ker 3- 1038/1083 produces a highly erratic response. This xenolith is cut by a number of thin granitic dikes which probably cause the high spikes of Figure A9.

Nearly all spikes on the two gamma ray logs are associated with fine-grained granitic dikes, aplites, or pegmatites. The peak at Ker 3 - 302 is not associated with any of the above rock types, but occurs at an interface between hornfels and coarse granite. A thin section of this contact shows a number of small grains of xenotime (YPO_4). Large radiation damage halos surround the grains, suggesting that the mineral is more radioactive than any other phase present except uraninite. The concentration of xenotime along the top of the xenolith probably causes the observed spike.

Magnetic Modeling of the Liberty Hill Pluton and its Contact Aureole with Comments on the Mineralogy of Magnetic Phases

John Dunbar and J. Alexander Speer

Introduction

The Liberty Hill pluton and its contact aureole have a readily recognizable expression on the aeromagnetic map of the Camden-Kershaw area (U.S.G.S., 1970, reproduced in part in Fig. A12b). The pluton is associated with a uniform magnetic high, 300 gammas greater than the approximately 700 gamma regional magnetic field of the Carolina slate belt. This high falls off sharply at the northern and eastern edges of the pluton, but decreases more gradually over the southern margin. The contact aureole shows a 400 gamma magnetic high 2 km wide on the eastern rim of the pluton, where the aureole is developed in the Carolina slate belt argillites.

The north-northwest trending magnetic linears are expressions of diabase dikes, and a magnetic high, which appears in the southwest corner of Fig. A12b, is caused by the Dutchman's Creek gabbro.

Magnetic Modeling

A model for the shape of the Liberty Hill pluton was derived from the magnetic data of Fig. A12b. The procedure used, based on Talwani's method of computing profiles over bodies of infinite length (Talwani and Heirtzler, 1964), is not especially well-suited to bodies with circular outcrop patterns, but should provide a first-order approximation of the pluton's shape. Magnetic profiles were computed from starting models based only on geologic information. The computed profiles were then compared to the observed magnetic profiles (Fig. A12b), and the pluton model was modified to improve the agreement between the computed and observed profiles.

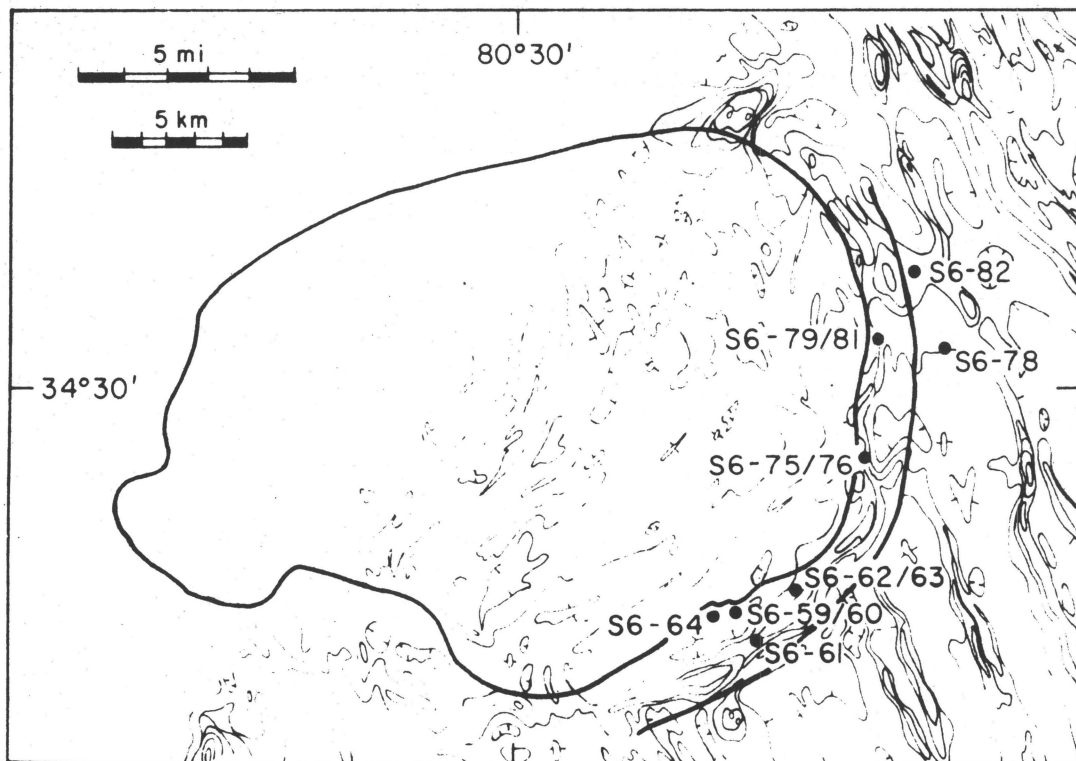
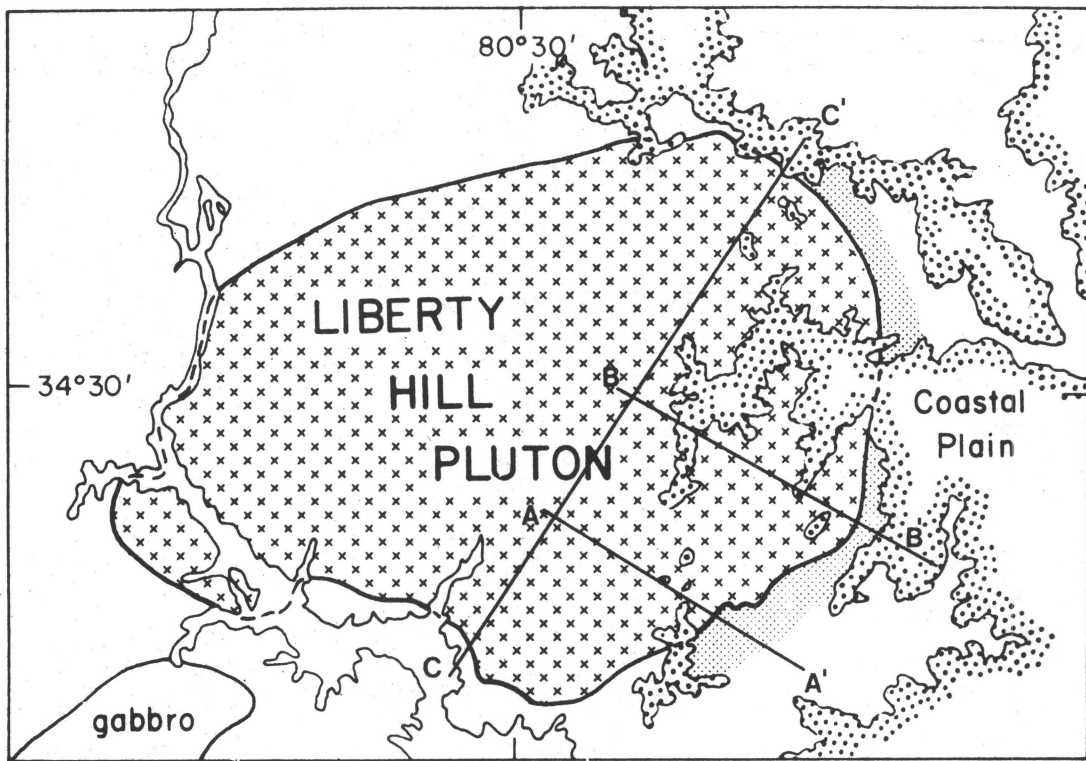


Fig. A12. (a) Geologic map of the Liberty Hill pluton, showing section lines used for magnetic modeling. (b) Aeromagnetic map of the eastern half of the Liberty Hill pluton and contact aureole with locations of hornfels samples. From aeromagnetic map of the Kershaw-Camden area, S. C. (USGS, 1970).

Magnetic susceptibility measurements of the two major granite types of the pluton are shown in Table A5. For modeling purposes, it was assumed that the pluton is a homogeneous body with a susceptibility of 0.001cgs. The hornfels of the metamorphic aureole was found to have highly variable susceptibilities; the values used are shown in the profiles (Figs. A11, A12, A13). The volcanoclastic units in contact with the pluton on the north and south appear to have uniformly low susceptibility. Susceptibilities, measured by Waskom (1970), of various units of the country rock surrounding the Lilesville pluton, similar to rocks bordering the Liberty Hill pluton, are shown in Table A5.

In this model, the metamorphic aureole is represented by thin shells of material of different susceptibilities, running within the argillite parallel to the surface of the pluton. The shells extend laterally along the face of the pluton and end at the contact with the volcanoclastic units, in which the aureole is not developed. The depth to which the shells extend was arbitrarily chosen. The volcanoclastic rocks and the parent material of the aureole, the argillites, were assumed to have no susceptibility.

Results

The models shown in Figs. A13, A14 and A15 correspond to section lines in Fig. A12a. Along lines A-A' and B-B', the dip of the granite/country rock interface is shallow, so that near the margin of the pluton the shapes of the computed profiles are well constrained, and are not affected by the depth to which the granite extends.

The behavior of the southern part of section C-C' is similar to the behavior of A-A' and B-B'. In the northern part, however, the granite dips steeply, so that the dip is not well constrained, and the shape of

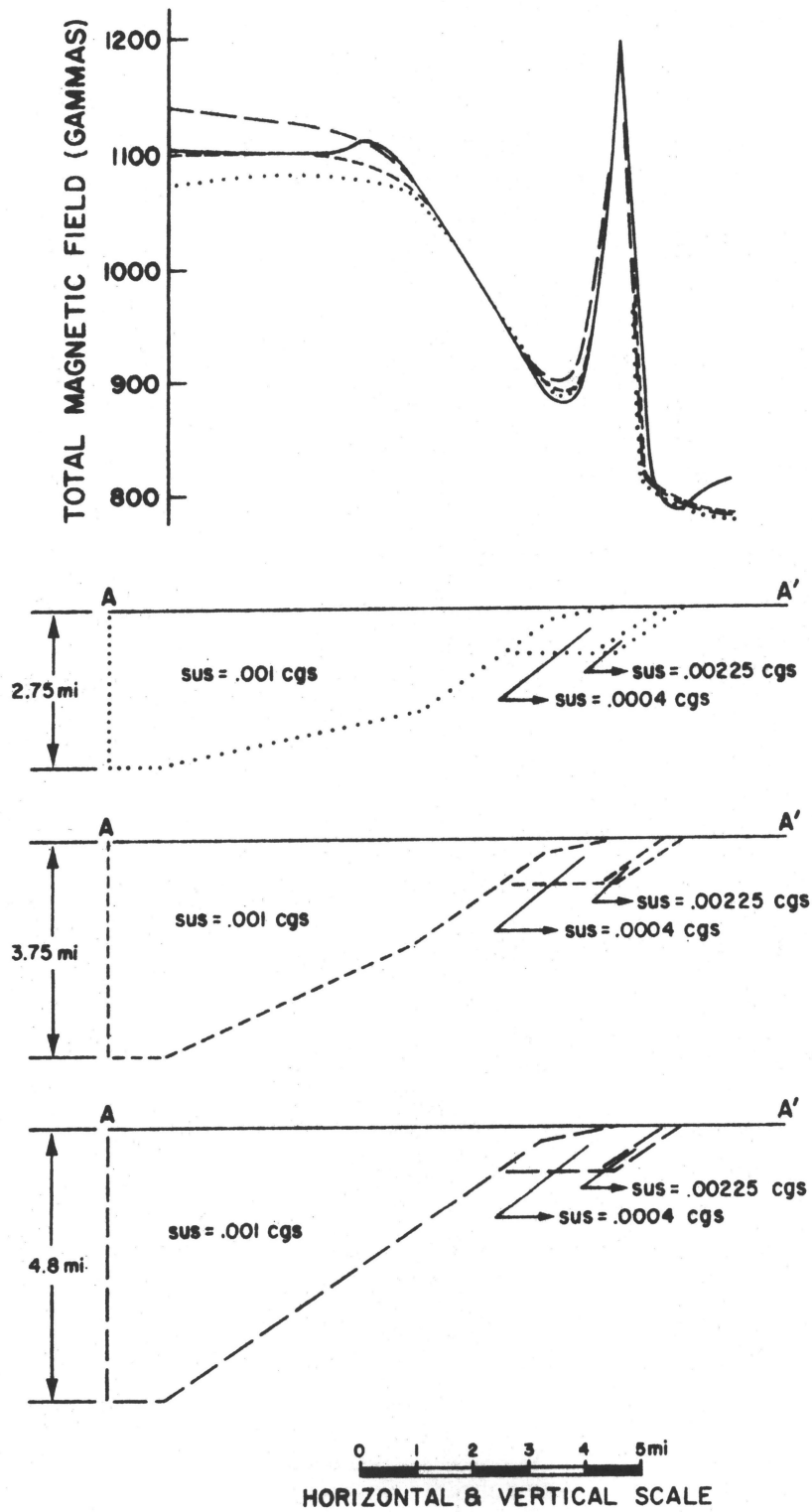


Fig. A13. Three models of the Liberty Hill pluton along the section A-A' and their calculated magnetic profiles compared to the observed magnetic profile (solid line). The strike of the A-A' section is N42W (N137E). Each model is extended to the northwest (left) 10 miles.

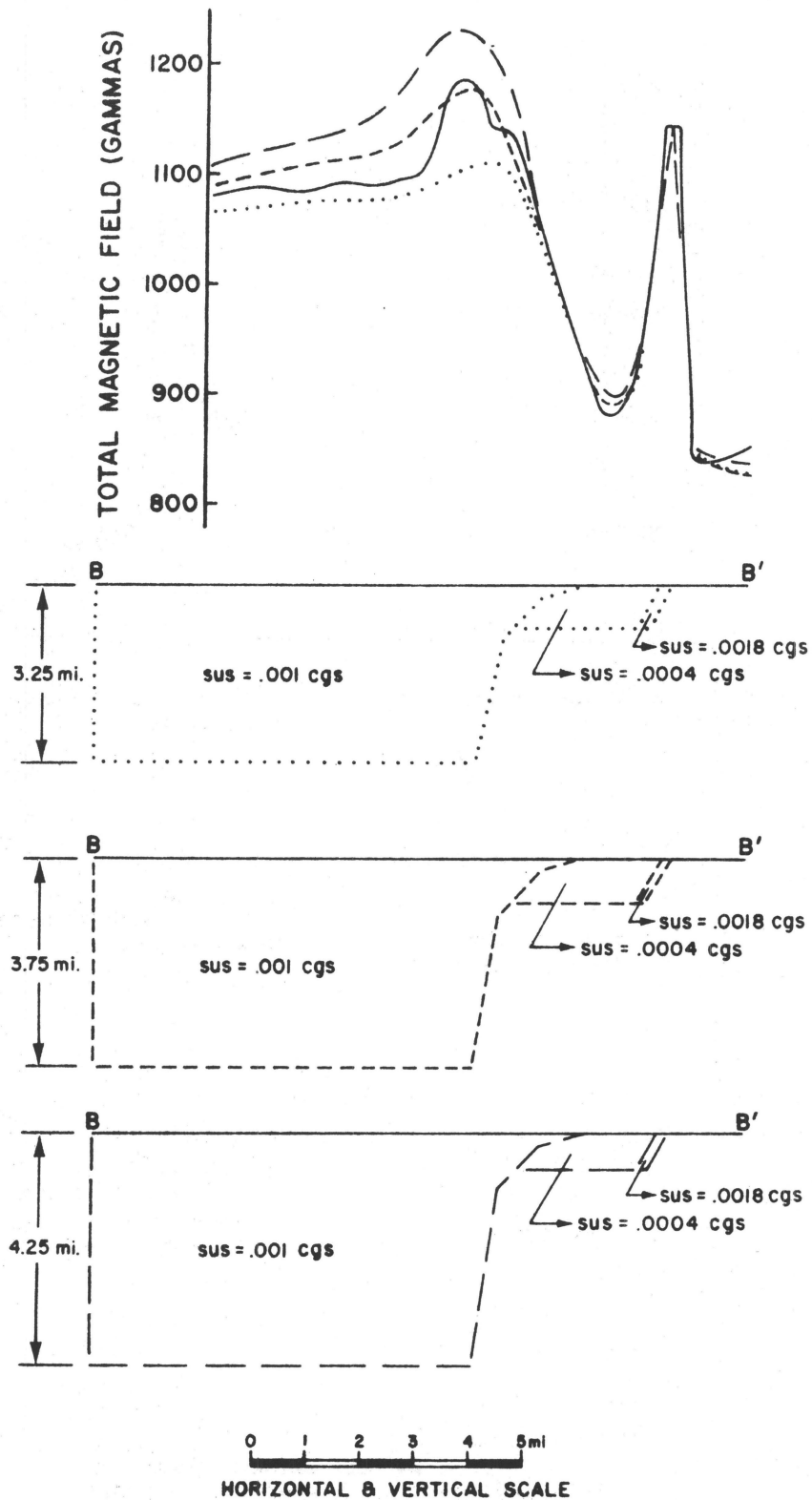


Fig. A14. Three models of the Liberty Hill pluton along the section B-B' and their calculated magnetic profiles compared to the observed magnetic profile (solid line). The strike of the B-B' section is N52W (N125E). Each model is extended to the northwest (left) 10 miles.

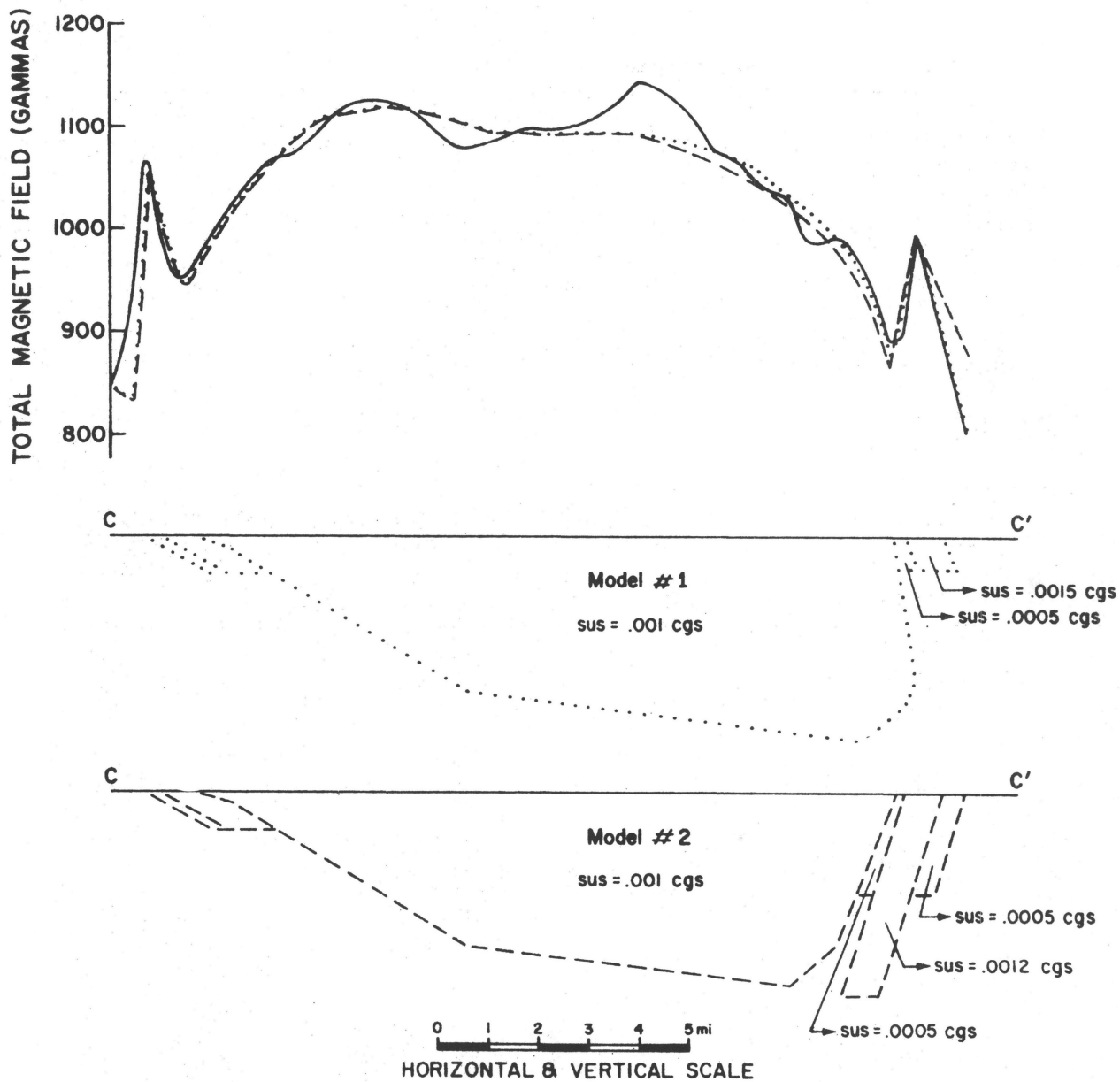


Fig. A15. Two models of the Liberty Hill pluton along the section C-C' and their calculated magnetic profiles compared to the observed magnetic profile (solid line). The strike of the C-C' section is N33E. Model #2 incorporates a diabase dike of susceptibility = 0.0012 cgs.

Table A5. Susceptibilities of Rocks of the Liberty Hill Pluton and the Carolina Slate Belt.

Rock Type	No. Samples	Mean Susceptibility (10^{-4} cgs)	Range of Susceptibility (10^{-4} cgs)
Coarse-grained granite (Lhc)	10	10.7	
Fine-grained granite (Lhf)	10	9.75	
Values from Waskom (1970, Table 3).			
Granite	30	5.6	0-12.7
Argillite	6	2.3	0- 2.5
Mica gneiss	4	7.0	1.4- 9.1
Mica schist	4	1.3	0- 3.3
Felsic volcanic	3	0.3	0- 0.9

the profile is strongly dependent on the depth to which the granite extends. In addition, a diabase dike runs tangential to the pluton in this area. Because the thickness of the granite, the dip of the granite/country rock interface, and the nature of the diabase dike all influence one area of the profile, there is little control over any of these parameters. A wide range of granite depths and dips could be made to agree with the observed field by varying the shape and susceptibility of the dike. For reasonable dike models, however, the range of the dip of the granite contact varies between 70° inward and 80° outward.

Conclusion

The general shape of the eastern half of the Liberty Hill pluton, as defined by the models discussed above, is shown in Fig. A16. The pluton appears to be asymmetrical: in the south and southeast, the granite-country rock interface dips inward at 20° to 40°; in the north, the interface is nearly vertical to a depth of about 21,000 feet. From this point, a relatively flat bottom slopes gently upward toward the south.

Comparison of the Magnetic Model to Gravity and Geologic Data

The model derived from the magnetic data for the shape of the Liberty Hill pluton agrees well with a model based on gravity studies, derived by Bell and Popenoe (1976). In their model (Fig. A17), also, the pluton is asymmetric, dipping steeply inward on the north and west, and sloping more gently inward on the south and east. In addition, they suggest that the pluton is bounded on the northwest by a normal fault that is an extension of the faults bounding the Triassic Wadesboro basin (Bell and Popenoe, 1976, Fig. 3).

Geologic data supports the two mathematical models. In the granite,

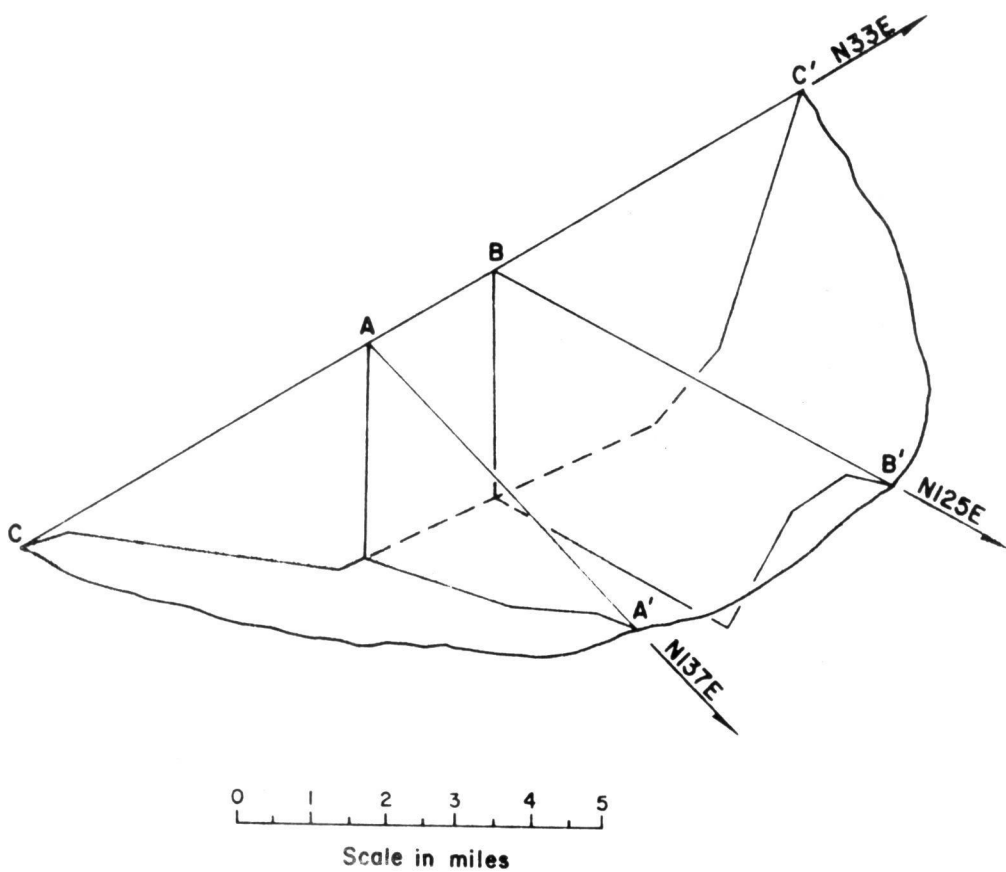


Fig. A16. Model for the shape of the eastern half of the Liberty Hill pluton, derived from profiles illustrated in Fig. 13, 14 and 15.

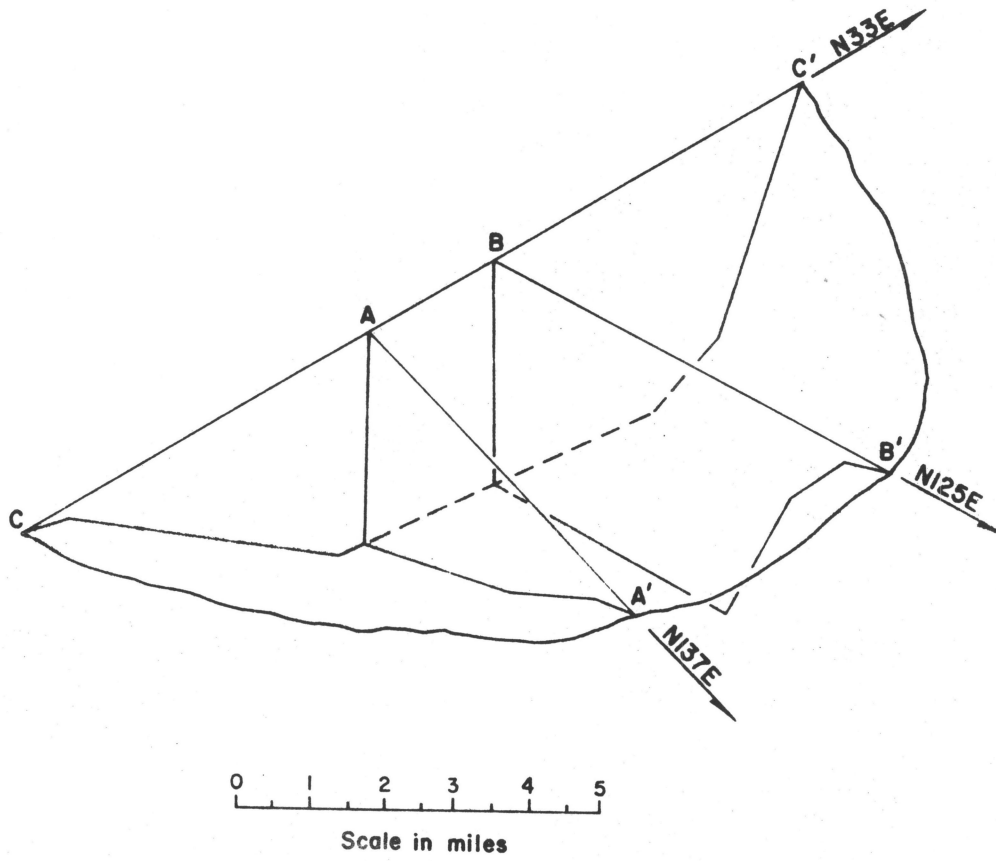


Fig. A16. Model for the shape of the eastern half of the Liberty Hill pluton, derived from profiles illustrated in Fig. 13, 14 and 15.

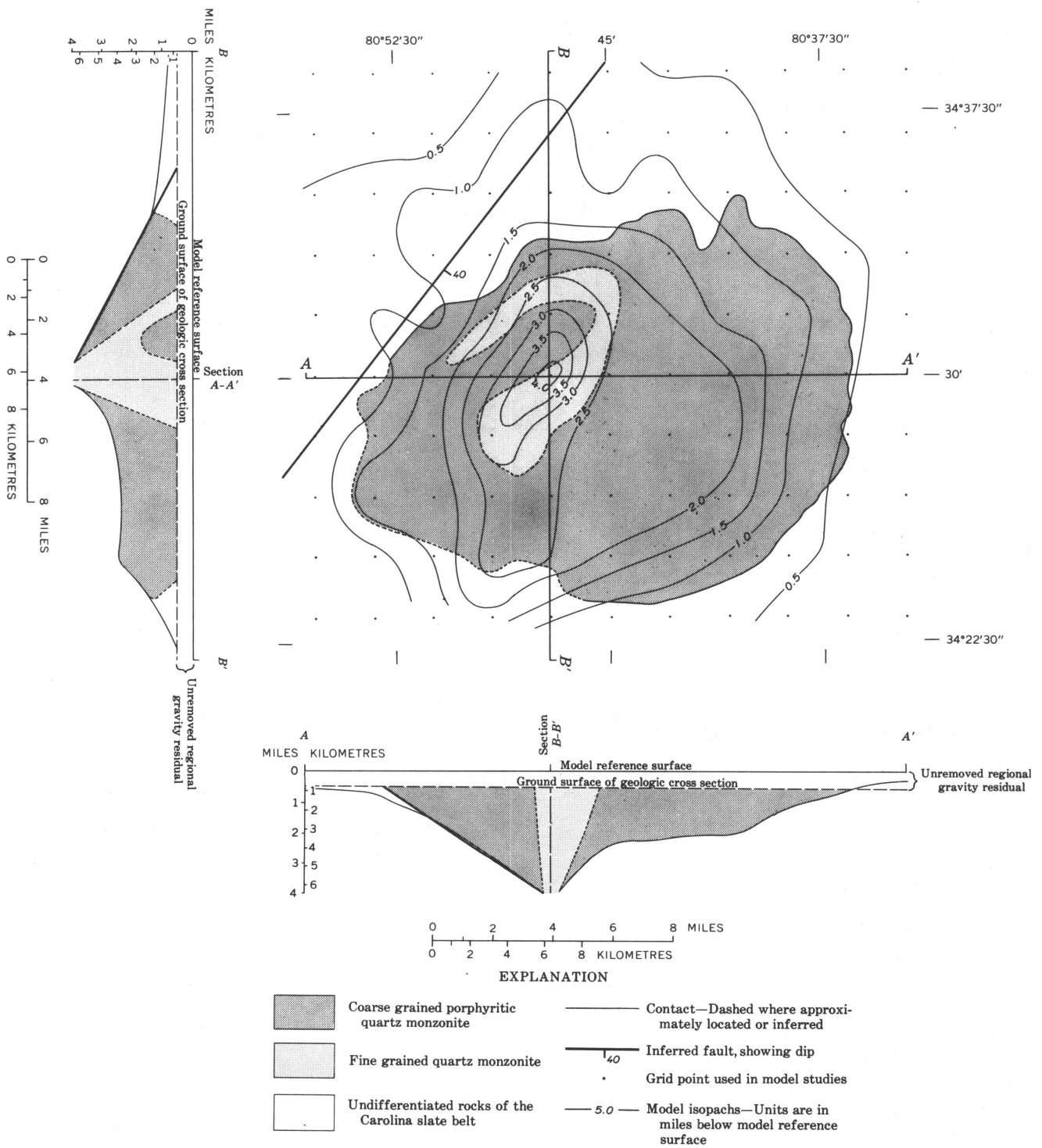


Fig. A17. Model of the shape of the Liberty Hill pluton derived from gravity data by Bell and Popenoe (1976).

tabular enclaves and potassium feldspar crystals are aligned parallel to the outer contact of the pluton and dip inward, defining an asymmetric funnel shape (Fig. A3).

Magnetic Mineralogy of the Granite and Country Rocks

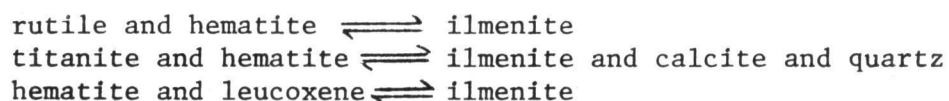
An aeromagnetic map shows the relative magnetic susceptibilities of the lithologic units in an area and the magnetic susceptibility of a rock is primarily a function of the volume percentage of magnetite.

In the Liberty Hill pluton, the coarse-grained phase contains up to 2 modal volume percent magnetite and ilmenite. Sulfides are generally rare. The fine-grained phase, which has little exposure in the area covered by the magnetic map, contains magnetite and equal or greater amounts of ilmenite in modal volume amounts less than 1%. The differences in the percentage and mineralogy of the opaque phases between the coarse and the fine-grained rocks should create contrasting magnetic susceptibilities. This may account in part for the magnetic anomalies of ± 40 gammas within the pluton (Fig. A12b).

The opaque mineralogy of the granites causes high magnetic susceptibilities in these rocks relative to the Carolina slate belt rocks, in which the only oxides observed are hematite and limonite. Magnetite and ilmenite have been identified by x-ray from other Carolina slate belt argillites (Sundelius, 1970; Randazzo, 1972), but if present in the rocks surrounding the Liberty Hill pluton, they are minor in amount.

The contact metamorphic aureole of the Liberty Hill pluton exhibits strong magnetic anomaly (Fig. A12b). Bell et al. (1974) attribute this high magnetic anomaly to large amounts of magnetite in the hornfels. Study of the opaque mineralogy shows that ilmenite is also an important oxide mineral. Opaques in the hornfels are coarser grained than those in the argillite,

because of metamorphic recrystallization, but the increase in magnetic susceptibility from the argillite to the hornfels requires an increase in the amount of magnetic minerals in the hornfels. Magnetite can be produced by the reduction of less magnetic hematite and limonite with increasing metamorphic grade (increasing T, decreasing f_{O_2}). The formation of additional ilmenite is hampered by the lack of any identified titanium-bearing phase other than ilmenite in the argillites. However, very fine-grained detrital titanite, rutile, or their cryptocrystalline alteration products (leucoxene), as yet undetected, could be involved in the following reactions:



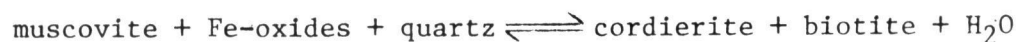
Additional iron and titanium oxides could be produced by reactions of iron silicates in the low grade, regionally metamorphosed argillites in response to increasing metamorphic grade in the aureole. The white micas of the argillites, for example, may be phengites, which with increasing metamorphic grade react to produce a purer muscovite, iron oxides, and alkali feldspar. Other possibilities include decomposition of the iron-rich chlorite and epidote.

The above reactions that produce magnetite and ilmenite coincide with the beginning of the muscovite hornfels facies. Opaque minerals are generally rare in the country rocks except for samples in this facies (Table A2). The magnetic anomaly is largely associated with the muscovite hornfels facies and disappears with the beginning of the amphibole hornfels facies of the inner aureole.

The disappearance of the oxides and the magnetic anomaly close to the pluton is thus a result of continuous metamorphic reactions that occur with increasing metamorphic grade. The appearance of cordierite at the beginning of the muscovite hornfels facies is probably a result of the idealized reaction:



When the reaction has gone to completion by exhausting the supply of chlorite (Figure A18), the production of cordierite and biotite can continue with the consumption of iron oxides. This takes place by a reaction of the type:



which probably begins to take place at the axis of the magnetic high. This reaction will continue until one of the reactants is exhausted or until muscovite + quartz becomes unstable, producing Al_2SiO_5 + K-feldspar. The persistence of small amounts of oxides (mostly ilmenite) in the high grade rocks, and the scarcity of aluminosilicates, suggest that it is the disappearance of muscovite that halts the reaction.

The lower magnetic field of the inner aureole is most easily seen in the southeast quadrant (Figure A12b), where the zones of both the magnetic high and inner magnetic low are wide. To the north the anomalies become narrower and are closer to the granite. This geometry is a result of the increase in dip of the contact between the granite and country rock from south to north, as discussed above (p.A-39).

Hornfels xenoliths in the Liberty Hill pluton have very little magnetic susceptibility, as suggested by qualitative measurements of magnetic susceptibility and the rarity of magnetic minerals noted in polished sections. The silicate mineral assemblages indicate that the xenoliths are in the amphibole and pyroxene hornfels facies. At these high grades,

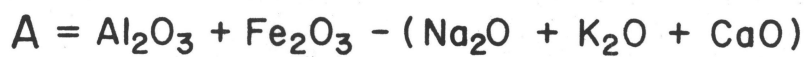
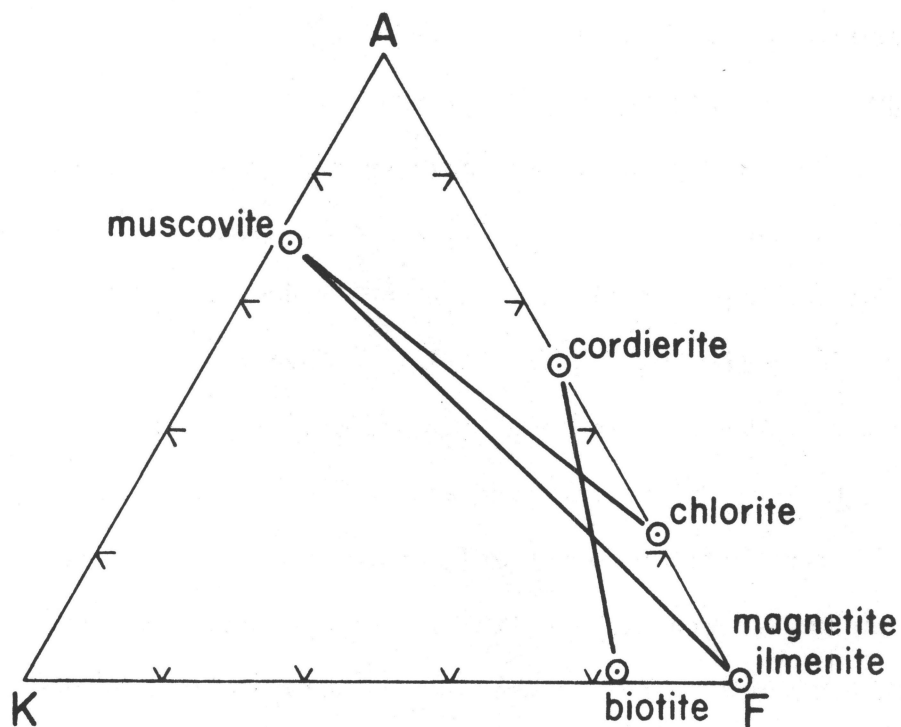


Fig. A18. AFM diagram showing the topology of reactions that occur with increasing metamorphic grade in the Liberty Hill contact aureole: $ms + chl + qtz = bt + cd + \text{H}_2\text{O}$, and $ms + \text{Fe-oxide} + qtz = cd + bt + \text{H}_2\text{O}$.

the reactions consuming Fe-oxides would have occurred, as in the inner aureole, depleting the xenoliths of magnetic minerals. An effect of the magnetic low of the xenoliths is apparent on the aeromagnetic map, where a low magnetic anomaly is centered over a large mapped xenolith in the southeast quadrant of the pluton (Fig. A12b). These non-magnetic xenoliths probably account in large part for the concentric magnetic anomalies within the pluton.

Shape and Orientation of the Pluton

Geologic, magnetic and gravity models of the Liberty Hill pluton indicate that its shape is similar to an asymmetric funnel. On the north, the pluton dips steeply inward at 60° - 90° , whereas it dips inward at only 30° on the south (Fig. A19a). Several explanations could account for the asymmetric nature of the pluton.

The rocks along the northern margin of the pluton may have acted as a resistant barrier to outward flow as the magma was enlarging its chamber during emplacement (Fig. A19b). On the north, the two units in contact with the granite are the Great Falls metagranite and the Carolina slate belt metavolcanics. Although the Great Falls metagranite could have acted as a resistant unit, it is unlikely that the metavolcanics would have acted similarly, because equivalent rock types crop out along the southern contact, where the dip of the granite contact is shallow and no "damming" action occurred.

Bell and Popenoe (1976) suggest that a Triassic reverse fault, dipping 40° to the southeast, bounds the northwest margin of the pluton (Fig. A19c), causing the steep dip of the contact between the granite and the country rock. The presence of the fault does not explain the steep contact along the northeast side of the pluton, and, more importantly, it fails to account for the steep dip of the igneous layering in the northern part of the pluton.

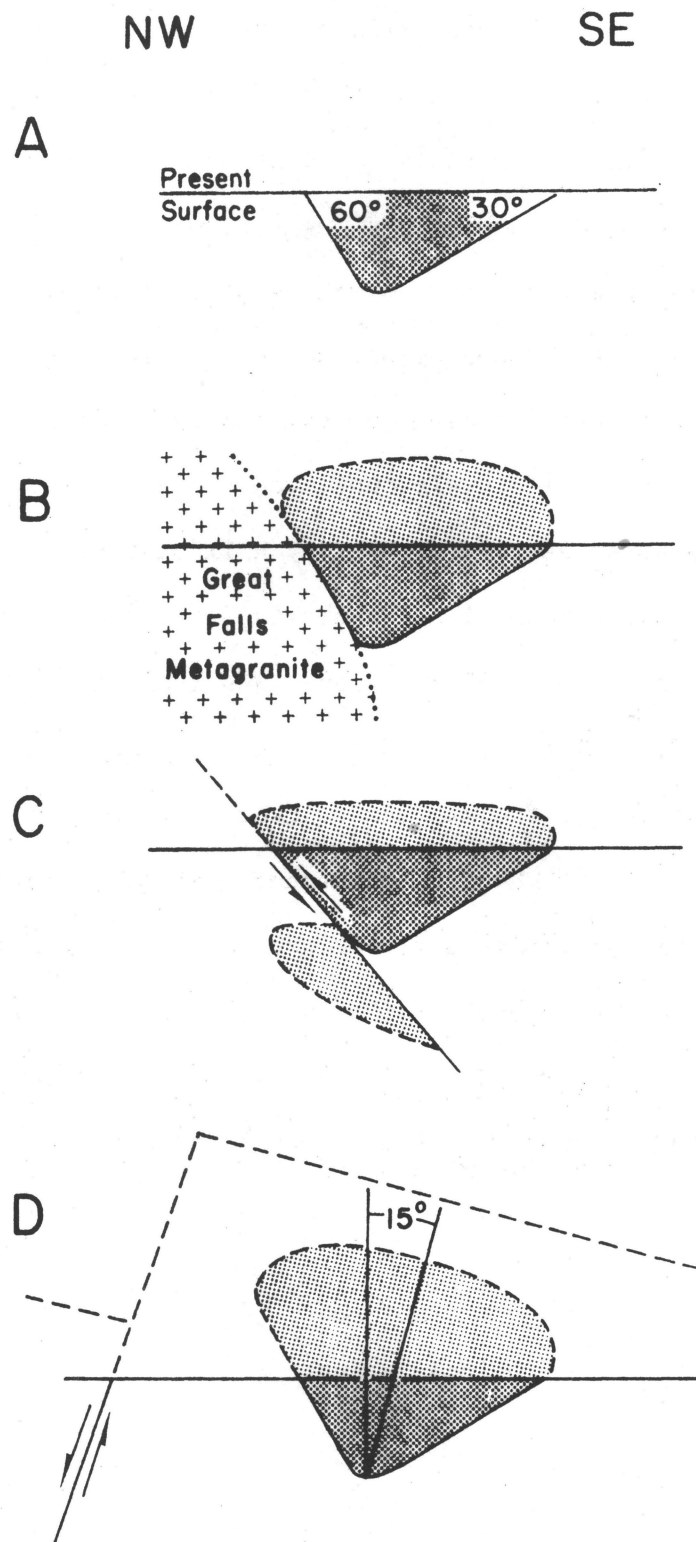


Fig. A19. Models for derivation of the shape of the Liberty Hill pluton: (a) observed asymmetrical shape; (b) resistant rock units limited northward expansion, causing steep dip on that side; (c) faulting along northwest margin truncated the pluton; (d) the pluton was rotated by Triassic normal faulting.

The asymmetry of the Liberty Hill pluton could also be caused by rotation. A 15° rotation about a southwest-northeast axis through its center would bring the pluton to its present orientation. This movement could be achieved by block faulting along a normal fault to the northwest (Fig. A19d). The presence of a normal fault is likely, because the southeastern borders of the nearby Wadesboro and Deep River Triassic Basins are high angle, northeast trending, normal faults which dip to the northwest (Randazzo and Copeland, 1976). If continued along strike, these faults would pass to the northwest of the Liberty Hill pluton.

The amount of displacement along the faults bounding the basins appears to be adequate to produce a 15° rotation. The minimum thickness of the Wadesboro Basin, determined in a gravity study by Mann and Zablocki (1961), is 3800 ft. Estimates of the maximum thickness of sediments in the Triassic basins are as great as 10,000 ft. (Reinemund, 1955). Displacements near this order of magnitude would be sufficient for a 15° rotation.

The rotation of the Liberty Hill pluton by normal faulting associated with the formation of nearby Triassic basins appears to be the most reasonable explanation for the asymmetry of the shape of the pluton.

Relationship between K and U in Granitic Rocks

J. Alexander Speer

Several previous workers (Dostal et al., 1976; Heier and Rogers, 1963; Heier et al., 1965, Larsen and Phair, 1954, and Tilling et al., 1970) have concluded that the potassium and uranium contents of a rock are positively correlated with magmatic fractionation indices, and that potassium content should therefore be related to uranium content, or heat production. Examination of phase diagrams for the granite system and of whole rock analyses presented in the literature shows, however, that a correlation between uranium and potassium exists only for rocks of basic and intermediate compositions.

During fractional crystallization of a basic magma, potassium and uranium remain in the melt because they do not easily fit into the structures of minerals comprising mafic rocks. With continued crystallization, and removal of solids containing little potassium or uranium, these two elements become progressively enriched in the liquid.

When the melt reaches a granitic composition, potassium-bearing phases begin to crystallize, and the melt is then increasingly depleted in potassium. Potassium depletion in a granitic melt can be illustrated by the synthetic granite system An-Ab-Or-Qz (Fig. A20). The initial melt composition lies at L1, above the two-feldspar surface (HGEF) and on the feldspar side of the quartz-feldspar surface (XWHG). On cooling, plagioclase of composition P1 appears. As the temperature falls, the plagioclase reacts with the liquid to become more sodic and the liquid changes composition along the curved path L1 - L2. When the liquid composition reaches the two-feldspar surface, plagioclase (composition P2) is joined by an alkali feldspar A2. The liquid composition path changes radically in direction, moving along the two-feldspar surface toward the

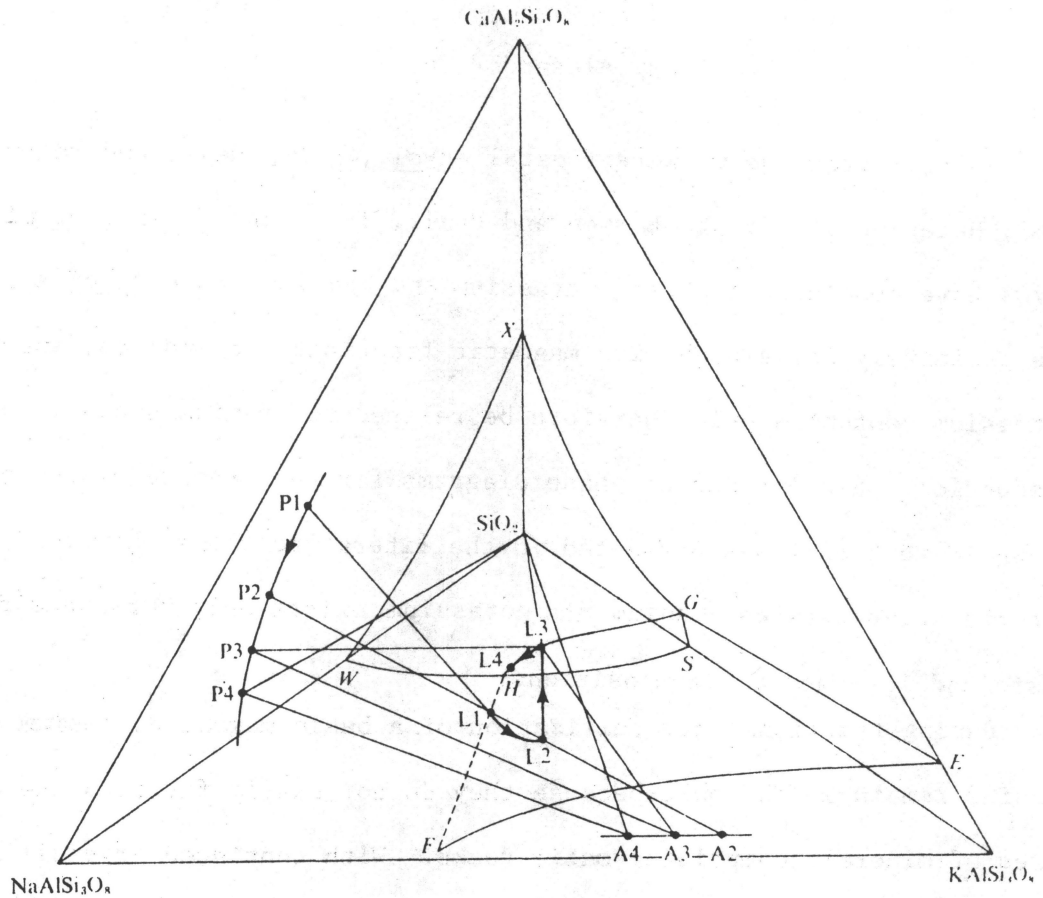


Fig. A20. Phase diagram showing path of crystallization (L1-L4) for a two-feldspar granite in the system $\text{SiO}_2\text{-KAlSi}_3\text{O}_8\text{-NaAlSi}_3\text{O}_8\text{-CaAl}_2\text{Si}_2\text{O}_8$, from Carmichael *et al.* (1973, p. 234).

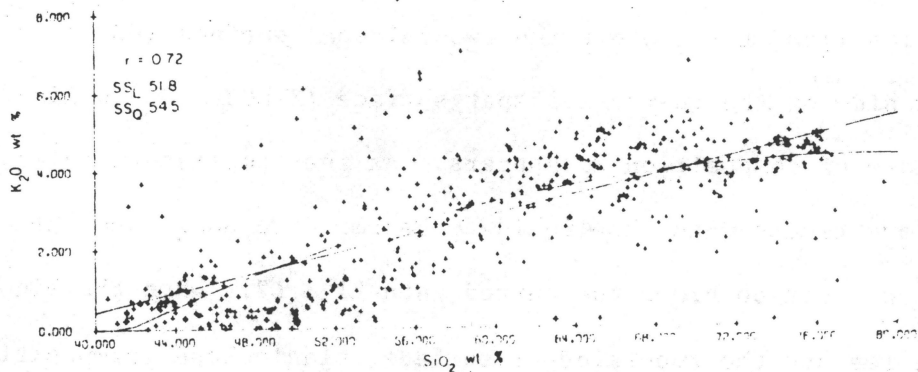


Fig. A21. Harker diagram compiled by Whitten (1975), demonstrating the leveling off of K_2O contents at high silica concentrations.

quartz-feldspar surface, L2 - L3. The plagioclase and alkali feldspar crystals become more sodic by continuous reaction with the melt, P2 - P3, A2 - A3. When the liquid has the composition of L3, quartz begins to crystallize in equilibrium with plagioclase of composition P3 and alkali feldspar of composition A3. Further cooling of the liquid changes its composition from L3 to L4, with crystallization of quartz, plagioclase, and sanidine. At L4, the liquid is used up, because L4-P4-A4-quartz are coplanar. Along the described crystallization path, the melt is continuously enriched in potassium prior to the appearance of alkali feldspar. When alkali feldspar does begin to crystallize, at L2 the melt becomes progressively depleted in potassium. Silica is concentrated in the melt until the last stage of crystallization, along path L3 - L4.

For mafic and intermediate rocks, then, potassium contents should increase with increasing differentiation indices at relatively low SiO₂ values. With increasing SiO₂ contents found in granitic rocks, concentrations of potassium should level off and eventually decrease. These relationships are illustrated in a Harker diagram for 505 rock analyses compiled by Whitten (1975) (Fig. A21). K₂O increases with increasing SiO₂ to approximately 65% SiO₂, the lower limit for silica in granites. At higher silica contents, K₂O concentrations no longer increase, but level off. Similar trends are reported by Bateman *et al.* (1963) and Dostal (1975).

Uranium, unlike potassium, appears to be continuously enriched in the liquid phase of a magma with increasing crystallization. Under magmatic conditions, uranium primarily occurs as U⁴⁺ (~1.0Å atomic radius) and is associated with the rare earth elements (0.9 - 1.2Å) and Th⁴⁺ (~1.0Å). Its large size and high charge prevent its entry into the principal rock-

forming minerals. In the final stages of solidification it is partitioned into the residual liquid.

Uranium is progressively concentrated in the liquid phase of a crystallizing magma of any composition, whereas the melt is enriched in potassium only until alkali feldspar begins to crystallize. For magmas of granitic composition from which alkali feldspar is crystallizing, potassium cannot be directly correlated with uranium as it can be for basic and intermediate rocks. For the purpose of targeting high heat production, the association of potassium and uranium appears to be inappropriate for granitic rocks because of the complex behavior of potassium during crystallization.

The Rolesville Batholith

Susan W. Becker and Stewart S. Farrar

Geologic Setting

The Rolesville batholith covers an area of 1710 sq. km. (Butler and Ragland, 1969) east of Raleigh in the eastern Piedmont of north-central North Carolina (Fig. A1). Medium- to coarse-grained, foliated granitic rocks comprise the majority of the batholith; on the northeast side of the batholith, unfoliated, coarse-grained quartz monzonite constitutes a nearly separate lobe, called the Castalia pluton (Fig. A22).

The exposed eastern Piedmont of northern North Carolina is bordered on the west by the Triassic Durham Basin and on the east by Coastal Plain deposits. Small pods of ultramafic rocks crop out 15 km. west of the batholith, north of Raleigh. Surrounding the Rolesville batholith are metasedimentary and metavolcanic rocks comprised predominantly of granitic gneisses, muscovite and muscovite-biotite schists, and lesser amounts of amphibolite, chlorite schists and metaquartzites.

North and northwest trending dikes of Jurassic(?) age (de Boer, 1967) cut the metamorphic country rocks and the batholith.

Age of Rocks

The age of the main Rolesville batholith is not known. Julian (1972) reported a Rb-Sr whole rock age, determined by Fullagar, of 316 ± 6 m.y. for the Castalia pluton. The age of the eastern Piedmont rocks bordering the batholith is also uncertain. Kulp and Eckelmann (1961) determined K-Ar ages for biotite in gneisses west of Raleigh at 238 m.y.

EXPLANATION

R

Triassic sedimentary rocks of the Durham basin.

Rmp

Rolesville main phase. Moderately to well foliated, medium-grained biotite granite, locally porphyritic.

Lp

Louisburg pluton. Fine-to medium-grained, well foliated, grey biotite granite.

Cp

Castalia pluton. Poorly foliated, medium- to coarse-grained biotite granite.

App

Archer's Lodge porphyritic phase. Poorly foliated, medium-grained, porphyritic biotite granite containing potassium feldspar phenocrysts 1-4 cm long.

Mu

Undifferentiated metamorphic rocks, including granitic gneisses; muscovite, biotite, and chlorite schists; amphibolites, quartzites, greenstones, and metamorphosed ultramafic rocks.



Inferred geologic contact.

• S6-240

Locality of sample collected for thin section.

• F6-208

Locality of sample collected for chemical analysis and heat production measurement.

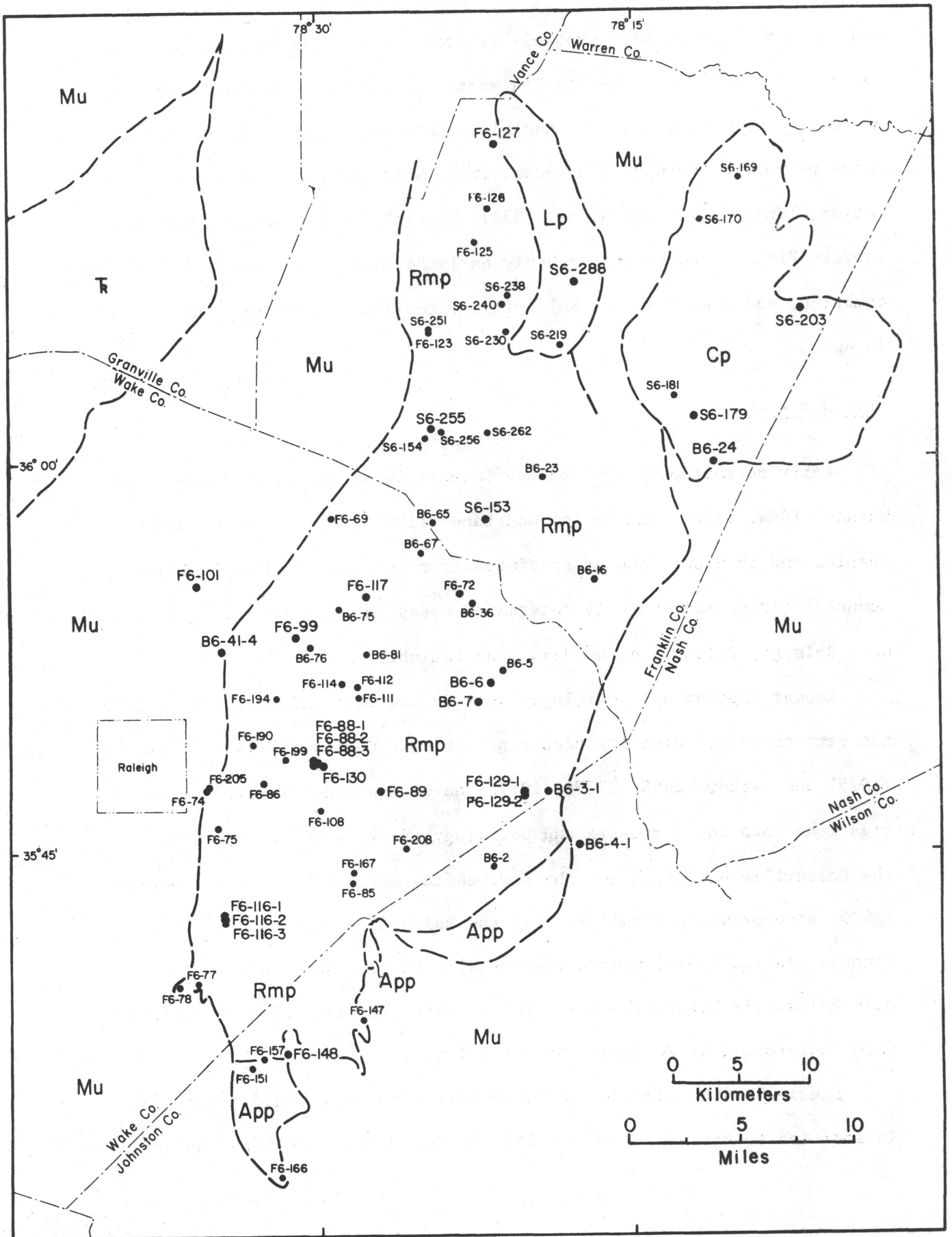


Fig. A22. Geologic map of the Rolesville batholith, North Carolina, showing sample locations.

and 259 m.y., dates which probably represent a cooling age. Rocks in the Carolina Slate Belt 100 km. to the west are similar in lithology to rocks of the eastern Piedmont Belt, and yield Late Precambrian and Early Cambrian dates by various methods (St. Jean, 1964; White et al., 1963; Hills and Butler, 1969; Glover and Sinha, 1973). Parker (1968) suggests that the eastern Piedmont rocks are probably early Paleozoic, but possibly late Precambrian, and that the main Rolesville batholith is probably early Paleozoic in age.

Previous Work

Early petrographic work on the Rolesville batholith includes Watson (1904, 1910), and Watson and Laney (1906), who describe hand samples and thin sections of specimens from quarries in Wake County. Councill (1954) subsequently determined modes for samples from quarries near Raleigh, Rolesville, Wendell, and Louisburg.

Recent mapping and petrologic work on the main Rolesville batholith has been concerned with its occurrence in Wake County. Wilson et al. (1975) and Parker (1968, 1977a, 1977b) have conducted extensive investigations into the structure and petrology of the southern half of the Rolesville batholith and the surrounding metamorphic rocks. Bowman (1970) also presents modal data for the Rolesville batholith in Wake County. Julian (1972) mapped the Castalia pluton, northeast of the main Rolesville batholith, and reports modal analyses and a whole rock date, determined by Fullagar, of 316 ± 6 m.y.

Studies of the country rock surrounding the Rolesville batholith, in addition to those by Parker (1968, 1977a, 1977b) have been conducted

by Farquhar (1952), Fortson (1958), and Dickey (1963), who described rocks west and north of Raleigh.

A gravity study of the Rolesville batholith was made by Glover (1963), who determined that the deepest part of the intrusion, near Wendell, is probably 5.3 km. Aeromagnetic surveys of the area covered by the batholith have been made by the U.S. Geological Survey (U.S.G.S., 1973a, 1973b, 1973c, 1974, 1976).

Metamorphic Rocks

Exposure in the vicinity of the Rolesville batholith is extremely poor, and most of the outcrop is highly weathered. The country rocks that were examined are probably only the more resistant units, which may not be representative of the majority of rock types present.

Quartzo-feldspathic rocks. Quartzo-feldspathic rocks, common in the area surrounding the Rolesville batholith, consist of granitic gneisses, metavolcanic rocks, and lineated gneisses. The granitic gneisses, which border the batholith on the west and crop out near Zebulon on the eastern boundary, are interlayered with the granite in a zone reaching a kilometer in width. The two rock types are similar in mineralogy and texture, and are commonly difficult to distinguish.

In hand specimen, the gneisses are light grey with C.I. \approx 10. The moderate to strong foliation is defined by the parallel alignment of biotite flakes and elongate quartz and feldspar grains or by bands of light and dark minerals. More mafic bands in the gneisses contain amphibole in addition to biotite.

The major constituents, examined in thin section, are quartz with undulatory extinction, microcline microperthite, unzoned plagioclase

(An₁₉₋₂₀) with albite rims, and biotite, pleochroic dark brown to light tan. Accessory minerals are iron oxides, zircon, apatite, and highly altered allanite. Chlorite, hematite, and a white mica are alteration products. More mafic bands contain titanite and amphibole that is optically (-), with $2V \approx 70$, X = pale yellow-brown, Y = dark yellow-green, and Z = blue-green.

Metavolcanic rocks, which crop out south of the batholith, contain deformed relict phenocrysts of plagioclase and rarely, potassium feldspar. Other phases present include quartz, muscovite, epidote, chlorite and iron oxide + biotite, garnet, titanite, and pyrite. Lineated gneisses crop out near Falls, west of the batholith (F6-101, Fig. A22), and in Franklin County on the Tar River, 1.5 km. from the Granville County line. At Falls, the lineation is defined by clumps of biotite, allanite, titanite, and opaques in a groundmass of quartz, plagioclase, and microcline. Apatite is an accessory phase; chlorite is present as an alteration product of biotite. The gneiss in Franklin County contains lineations defined by zircon, titanite, opaques, and scarce biotite in a matrix of quartz, plagioclase (?), and potassium feldspar; chlorite is a secondary mineral.

Quartzites. Well-foliated rocks consisting predominantly of quartz and muscovite occur locally east, south, and west of the batholith. Other phases present in small amounts in some samples include plagioclase, potassium feldspar, biotite, garnet, chlorite, calcite, epidote, opaques, and zircon.

Pelitic rocks. Muscovite and muscovite-biotite schists crop out along much of the southern and eastern edges of the batholith, and

to the west of the gneisses bordering the western margin. Mineral assemblages vary, but generally include quartz and muscovite \pm biotite, chlorite, oxides, garnet, tourmaline, and zoisite. The rocks are fine- to medium-grained, well foliated, and commonly crenulated.

Mafic rocks. Chlorite schists, amphibolites, and metagabbros comprise the mafic country rocks. Highly weathered chlorite schists crop out locally along the southern and southeastern margins of the batholith.

Amphibolites, concentrated along the western border in a zone 1-5 km wide, approximately 4 km from the edge of the batholith, also occur to the south. Sample S6-170 (Fig. A22), which may represent a topographic high on the floor of the intrusion, was collected within the Castalia Pluton. All specimens examined contain quartz, plagioclase (calcic oligoclase to sodic andesine), and amphibole (optically negative, $2V = 70-75^\circ$, $X = \text{tan}$, $Y = \text{yellow-green}$, and $Z = \text{blue-green}$). Iron oxides, epidote, and biotite are present in some samples. Accessory phases, which vary among samples, include titanite, apatite, and zircon. Chlorite and hematite appear as secondary minerals, and a carbonate and white mica as products, with the epidote, of saussuritization. One sample, collected 3 km northwest of Raleigh, has a relict gabbroic texture with plagioclase grains enclosing a relict ophitic pattern of opaque inclusions, small plagioclase grains, and scarce remnants of plagioclase laths.

Metamorphic Grade

Previous workers (Fortson, 1958; Broadhurst and Parker, 1959; Parker, 1968) suggest that the country rocks west of Raleigh increase

in metamorphic grade from the chlorite zone eastward through biotite, garnet, kyanite, and staurolite zones. Parker (1968) also proposes that the rocks surrounding the Rolesville batholith can be divided into "high" and "low" grade: "low" grade rocks contain chlorite, biotite, and epidote, whereas almandine and higher temperature minerals occur in the higher grade rocks.

Preliminary work in the country rocks suggests that variations in mineral assemblages now present may be due to differences in rock compositions, rather than to disparate metamorphic conditions. All assemblages observed can occur in the lower amphibolite facies, and plot on a projection of an AFCM diagram with one set of tie lines (Fig. A23). The formation of garnet does not require a higher metamorphic grade, but may instead provide evidence of a more iron-rich composition.

The boundary between the "high" grade and "low" grade zones of Parker (1968) may separate high grade metamorphic rocks that have been retrograded to the lower amphibolite facies from rocks of a prograde amphibolite facies. Evidence for retrogression can be found in the "high" grade zone west and south of the batholith in schists, currently at lower amphibolite grade, that contain a relict, refolded metamorphic layering. Other rocks, completely recrystallized, contain what appear to be relict potassium feldspar porphyroblasts. These textures, which have not been observed in the "low" grade zone, suggest that the rocks may have previously been metamorphosed at P-T conditions higher than lower amphibolite grade.

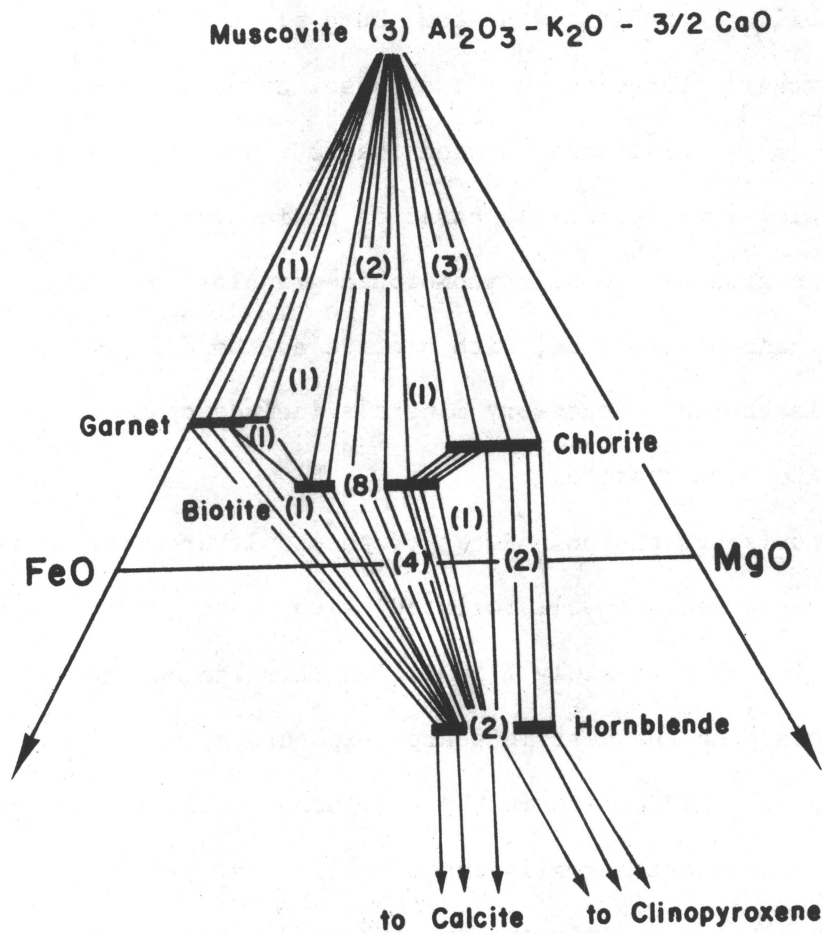


Fig. A23. Mineral assemblages of metamorphic rocks surrounding the Rolesville batholith, plotted on AFCM projection (Griffin and Styles, 1976). The number of samples containing each assemblage is indicated.

Rocks of the Rolesville Batholith

Four distinct petrologic units have been recognized within the Rolesville batholith: the Louisburg pluton, the Castalia pluton, the Archer's Lodge porphyritic phase, and the Rolesville main phase (Fig. A22). Divisions between the four phases, which are similar in mineralogy, are primarily based on grain size. All rocks are hypidiomorphic granular to allotriomorphic granular and contain quartz, microcline, and plagioclase, with biotite as the only mafic phase. Myrmekite is common. Accessory minerals include opaques, zircon, allanite, titanite, and apatite.

Louisburg pluton. Rocks of the Louisburg pluton are fine- to medium-grained and well foliated, with quartz and feldspar grains averaging approximately 1 mm in length. The contact with the Rolesville main phase on the west is sharp; exposure along the eastern contact is very poor. Microcline in the Louisburg pluton is microperthite; plagioclase grains are normally zoned An_{23} to An_{17} , with albite rims. Accessories present are zircon, apatite, and opaques; hematite, chlorite, and muscovite occur as secondary minerals.

Castalia pluton. The Castalia pluton, studied in detail by Julian (1972), is poorly foliated and contains quartz and feldspar grains averaging approximately 5 mm in length, and biotite grains 2-4 mm long. The potassium feldspar is microcline microperthite. Plagioclase is unzoned, approximately An_{25} in composition, and extensively saussuritized to a carbonate, white mica, and epidote. Accessory minerals are opaque, titanite, zircon, allanite, and apatite. Biotite has been extensively altered to chlorite; epidote and garnet are also secondary.

Rolesville main phase. Rocks within the main Rolesville phase appear to be fairly uniform. Most specimens are moderately- to well-foliated and non-porphyrific, with quartz and feldspar averaging 3 to 4 mm in length. Potassium feldspar grains reaching 2 cm in length have been observed at the Rockton Quarry east of Wendell (F6-129) and at the Garner Quarry (F6-116), and have been reported by Parker (1977a) in the Lassiter Quarry near Rolesville.

All samples examined in thin section contain plagioclase with slight normal zoning, $An_{22}-An_{18}$, that is commonly mantled by thin albite rims. Perthites in the microcline are small or absent. Biotite is partially altered in many samples to chlorite. Allanite, a common accessory phase, is usually zoned and highly altered. Several allanite grains examined were twinned on (100). Opaques, zircon, apatite, and scarce titanite comprise the remaining primary minerals. Secondary minerals are chlorite, hematite, and muscovite, which commonly occur as large flakes associated with biotite. Plagioclase is lightly to highly altered; saussuritization products consist of epidote, white mica, and a carbonate in varying combinations and proportions.

Archer's Lodge porphyritic phase. The Archer's Lodge porphyritic phase, which constitutes much of the southern margin of the batholith, contains microcline macroperthite phenocrysts 1-4 cm in length. Quartz, biotite, plagioclase, and potassium feldspar averaging 4-5 mm in length comprise the groundmass. Accessory and secondary minerals are similar to those in the Rolesville main phase.

Classification of Rocks of the Rolesville Batholith

Modal analyses (Table A6) were determined from rock slabs and thin sections. A minimum of 700 points was counted; for three-fourths of the samples, more than 1000 points were counted. Rocks from all four phases of the Rolesville batholith plot in the monzogranite field (Fig. A24); one sample (S6-255) falls in the granodiorite field. In the triangle quartz-feldspar-C.I. (Fig. A25), most samples cluster at C.I. < 7.

Pegmatites

Pegmatite veins, common throughout the Rolesville batholith, contain quartz, potassium feldspar, plagioclase, biotite, and muscovite ± garnet. They are especially large and abundant in the Castalia pluton, where one vein, just west of sample S6-170, reaches 50 m in width and contains euhedral potassium feldspar crystals 0.3 m long, graphic intergrowths of quartz and potassium feldspar, and fine-grained aggregates of granular garnet up to 0.2 m in width. The size and density of pegmatites appear to decrease with distance from the Castalia pluton.

Table A6. Modal analyses of the rocks
of the Rolesville Batholith.

Sample	quartz	plagioclase	K-feldspar	color index	biotite	chlorite *	muscovite *	opaques	zircon	apatite	fluorite	allanite	carbonate *	hematite *
S6-154	29.39	40.14	25.39	-	3.84	0.61	0.31	0.10	0.20	tr	tr			
S6-230	28.07	34.77	32.22	-	3.62	0.11	0.53	0.65	tr	tr	tr	tr		
S6-255	21.44	49.34	18.64	-	7.26	0.91	1.94	0.40	<0.01	0.05		<0.01	tr	tr
S6-288	29.91	34.88	29.47	-	4.59	0.05	0.64	0.21	0.16	0.05				tr
B6-24	29.40	40.72	22.69	7.19										
F6-117	21.75	39.65	34.62	3.98										
F6-78	23.6	33.2	37.7	5.5										
F6-86	21.3	42.5	31.4	4.7										
F6-89	24.3	38.7	31.1	5.9										
F6-108	18.7	26.2	46.9	8.1										
F6-111	24.8	38.8	34.0	2.4										
F6-112	23.4	30.5	45.2	1.0										
F6-130	23.3	33.4	41.4	1.8										
F6-147	35.5	25.5	37.3	1.8										
F6-148	25.5	40.8	27.9	5.8										
F6-157	23.9	42.3	27.4	6.3										
F6-190	26.2	28.9	40.3	4.6										
F6-194	26.3	35.5	32.9	5.2										
F6-199	24.1	45.1	27.9	2.9										
F6-208	24.3	37.9	32.4	5.5										

* Secondary

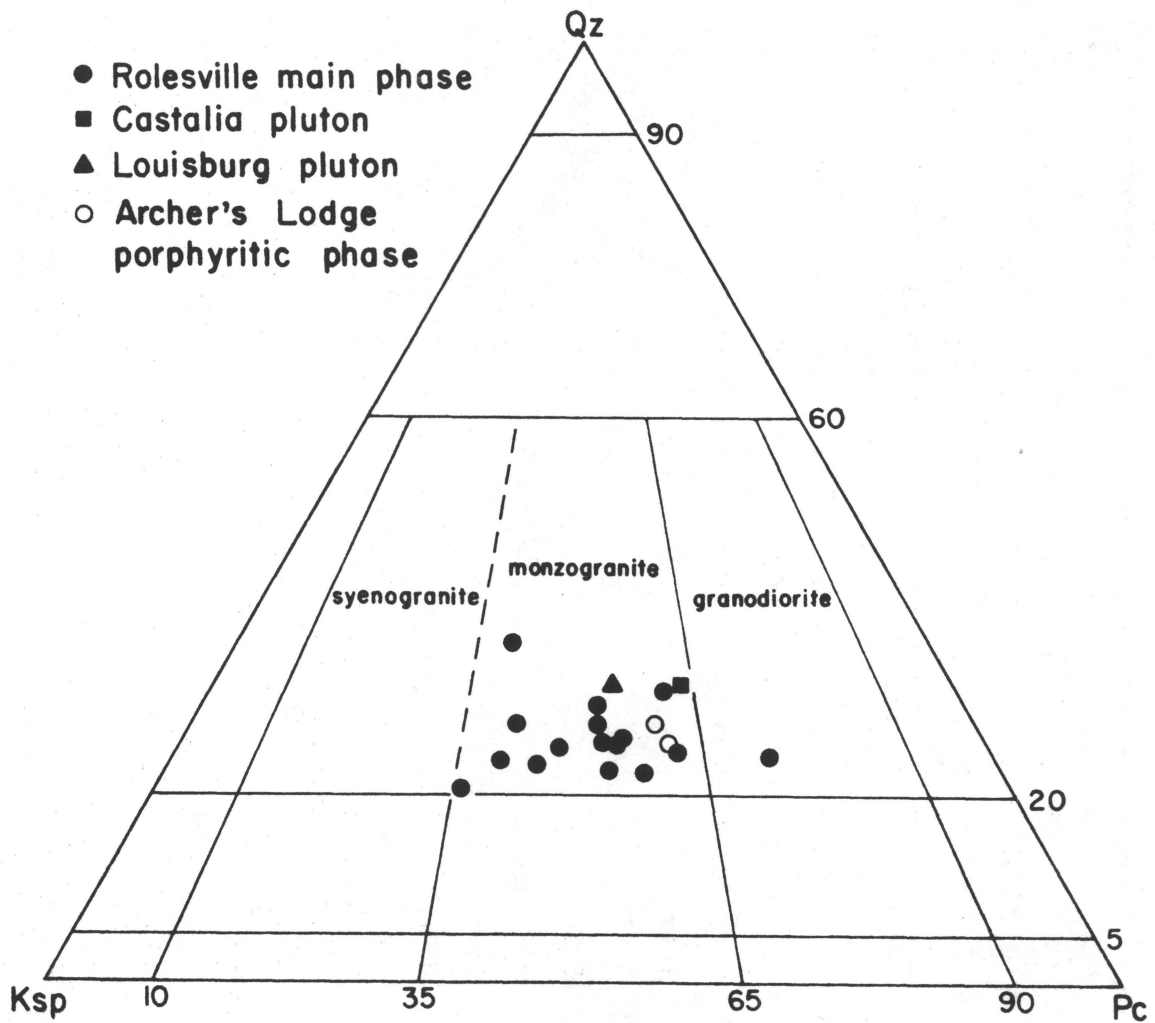


Fig. A24. Triangular diagram for samples from the Rolesville batholith, showing modal volume percent alkali feldspar (Ksp), plagioclase (Pc), and quartz (Qz).

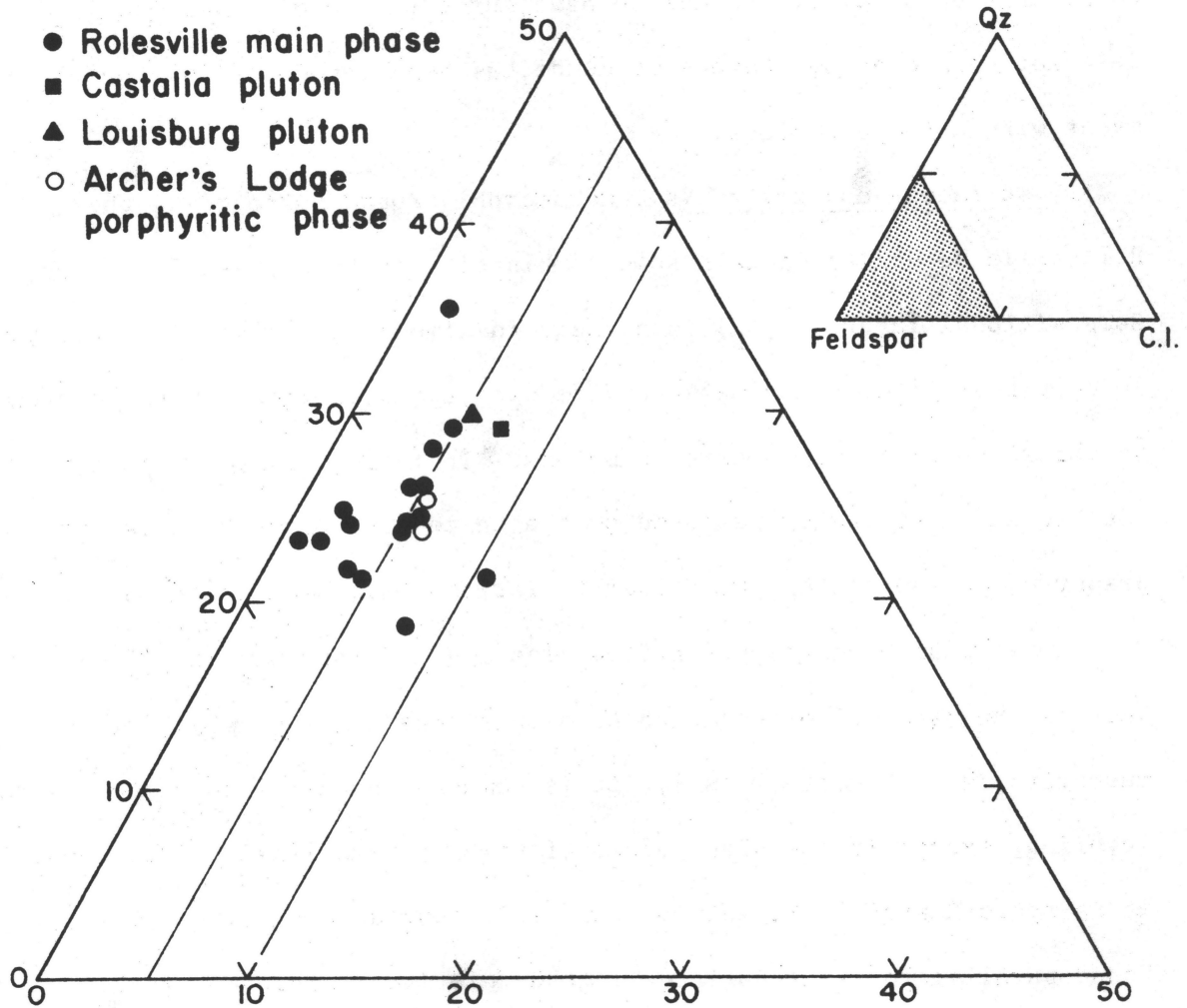


Fig. A25. Triangular diagram of modal data for the Rolesville batholith, showing volume percent total feldspar, color index (C.I.), and quartz (Qz).

Structure

The Rolesville batholith forms the core of the Wake-Warren anticlinorium as described by Parker (1968). The metamorphic rocks which surround the Rolesville batholith have suffered a minimum of two deformational events, whereas evidence has been found for only one event within the batholith.

S-surfaces--country rocks. Metamorphic rocks surrounding the Rolesville batholith contain some combination of three S-surfaces (Fig. A26). Compositional layering (S_0) is present in almost all metamorphic rocks. It occurs as alternating mafic and felsic or quartz-rich layers ranging in thickness from millimeters to meters. It is generally the most visible and most easily measured of the three foliations. It is often preserved in saprolite after other foliations have been destroyed.

Axial plane foliation (or flow cleavage) (S_1 and S_2) is defined here as the parallel orientation of planar minerals--usually biotite, muscovite, and chlorite. As S_1 , it is commonly parallel to compositional layering, except in the hinge areas of tight to isoclinal folds, where it is approximately parallel to their axial surfaces. As S_2 , it is found parallel to axial surfaces in the relatively mica-poor rocks.

Crenulation foliation (or crenulation cleavage) (S_2) is the set of surfaces defined by the axial planes of crenulations in mica and chlorite-rich rocks. In the rocks surrounding the Rolesville batholith, it has been found in quartz-muscovite schists and epidote-chlorite-muscovite phyllite.

S_2 axial plane foliation and crenulation foliation developed during the same deformational event, with crenulation foliation

EXPLANATION



Strike and dip of compositional layering of the country rocks (S_0+S_1).



Strike and dip of compositional layering of the granite (S_0').



Strike and dip of biotite and muscovite foliation (S_2).



Trend and plunge of lineation.



Inferred geologic contact.

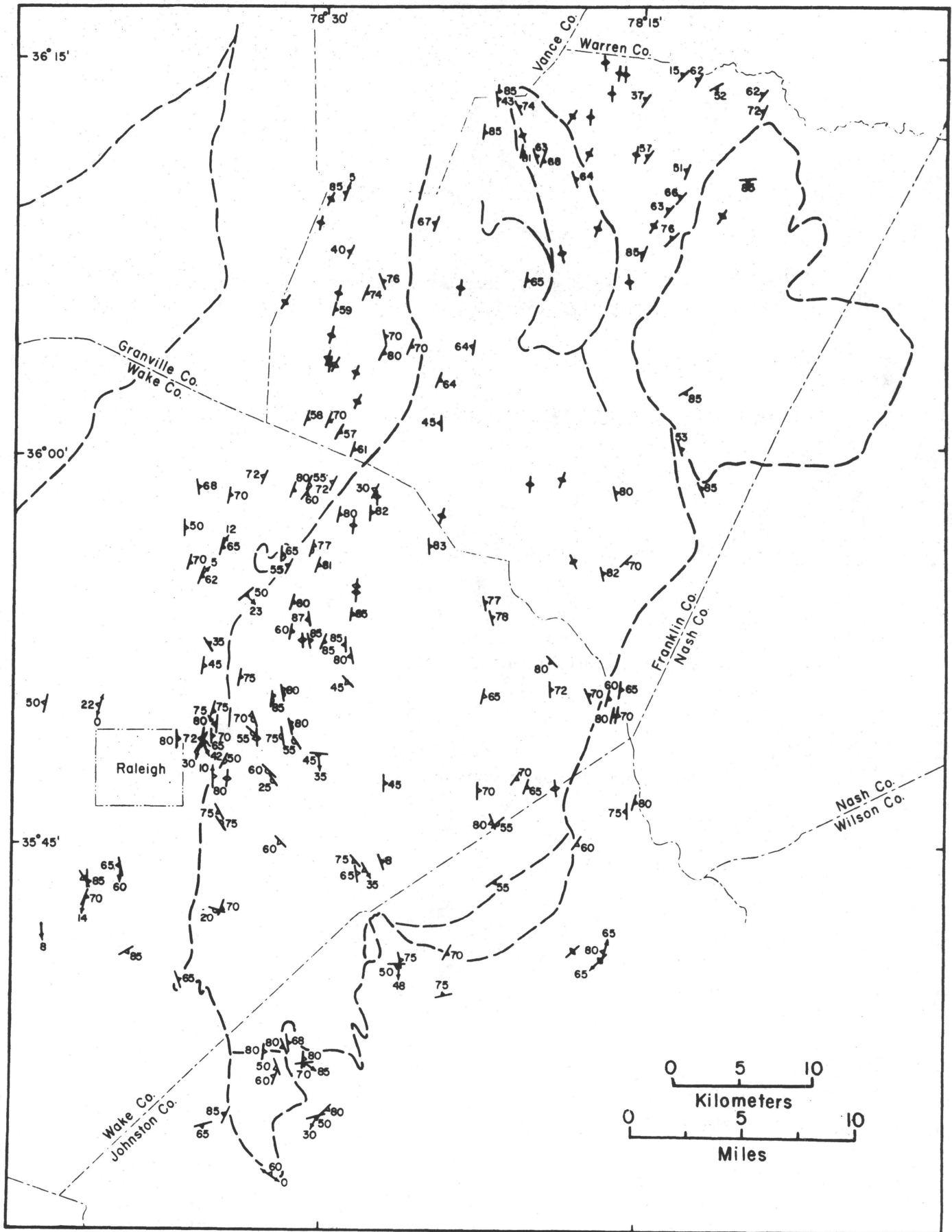


Fig. A26. Map showing structural features of the Rolesville batholith and surrounding rocks. Geologic units are given in Fig. A22.

forming in the micaceous rocks and axial plane foliation in rocks of other compositions.

S-surfaces--batholith. The rocks of the Rolesville batholith have only two S-surfaces. Compositional layering (S_0') is probably of igneous origin. At the Garner quarry (F6-116, Fig. A22), it is visible as changes in color index and grain size in layers from about 10 cm to 10 m thick. In some other areas of the batholith, large pavements have no apparent layering. Near the contact, especially along the western edge of the batholith, a distinct compositional layering has developed which may be metamorphic in origin. In this area it is also difficult to distinguish between the batholith and granitic gneisses of the country rock.

An axial plane foliation (S_2), defined by the planar orientation of biotite and minor muscovite, occurs through most of the Rolesville batholith. There is little small-scale deformation associated with this foliation except where it parallels compositional layering along the western margin of the batholith.

Folding. Isoclinal (F_1) folds occur in the country rock surrounding the Rolesville batholith. They are commonly very attenuated, and have an axial plane foliation (S_1). Considering the isoclinal nature of these folds, no attempt was made in this reconnaissance survey to separate S_0 and S_1 . They are plotted together in the following diagrams.

A second deformational event produced tight to open F_2 folds which commonly refold the isoclinal F_1 folds. These F_2 folds generally have

an axial plane or crenulation foliation (S_2). Along the east and west sides of the Rolesville batholith, S_2 has a strike approximately parallel to S_1 , and they are very difficult to distinguish, particularly in the western pencil gneisses (F6-101, Fig. A22), where we may be seeing only their intersection which forms the pencil structure. S_1 and S_2 foliations are most readily distinguished at the southern end of the Rolesville batholith, where S_1 is folded around the granite, while S_2 passes through it (Fig. A26). The only F_1 folds found within the Rolesville batholith are found in rocks which are apparently large xenoliths, the best example of which is at the Wake Stone Quarry (F6-116), Fig. A22). No evidence has been found for F_1 deformation of the granite. F_2 deformation of the granite is illustrated by the muscovite-biotite foliation which is present almost everywhere, but F_2 folding is seen only at map scale.

Structural interpretation. For the purposes of this discussion, the Rolesville batholith and surrounding rocks have been divided into two subareas, with the dividing line running east-west approximately 5 km north of Raleigh.

It was observed in the field that, in some cases, biotite is aligned parallel to compositional layering, and in some cases, cuts across it. Therefore, there is some mixing of foliations in the following plots, since all biotite-muscovite foliations are plotted as S_2 , while some are probably S_1 and S_0 .

Fig. A27 is a stereographic projection of S_0' and S_2 in the southern part of the Rolesville batholith. It illustrates that S_0' has been folded with an axis of approximately 30,S15E. Fig. A28 is

a stereographic projection of $S_0 + S_1$, and S_2 for the country rocks surrounding the southern Rolesville batholith. In this plot, poles to $S_0 + S_1$ define the fold axis 60, S15E. Both plots have concentrations of poles to biotite-muscovite foliation (S_2) near the western perimeter, approximately defining the S_2 plane N05°E, 70-80°E.

Mineral lineations and minor fold hinge lines are concentrated in the vicinity of the fold axes, and distributed approximately along the S_2 plane. At this point, they cannot be interpreted in detail, and they include both F_1 and F_2 linear features.

In the northern part of the Rolesville area, outcrop is more sparse and measurements on layering of the granite are lacking. Fig. A29 is a stereographic projection of all data for the northern Rolesville area. It includes both country rock and granite and is essentially a plot of S_2 in the granite, and $S_0 + S_1$, and S_2 in the country rock.

Deformation of the country rock has produced folds with nearly horizontal axes (F_1 folds?) which have axial surfaces approximately parallel to S_2 . These folds produce the $S_0 + S_1$ variation in the stereographic projection shown as Fig. A29. The lack of measurements on compositional layering crossing the axial surface of the anticlinorium in this area precludes an in-depth discussion. However, it is clear from Fig. A26 that foliations have been warped around the Castalia pluton. This suggests that the Castalia pluton was intruded later than the rest of the Rolesville batholith. This late intrusion caused some of the variability of attitudes seen in Fig. A29.

This brief examination suggests that, as Parker (1968) previously described, the Rolesville batholith forms the core of a major antiform

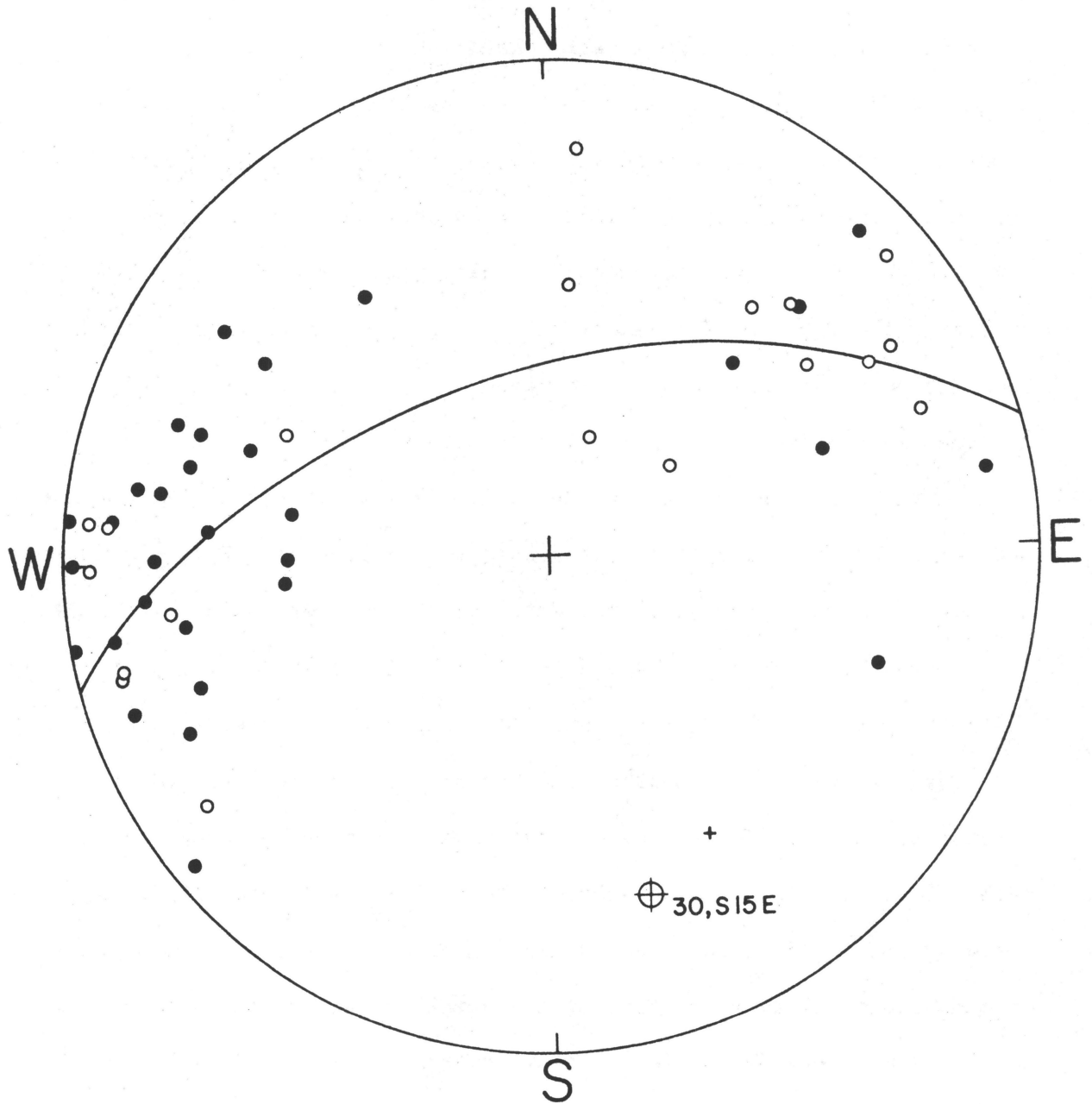


Fig. A27. Equal area projection of poles to S_0' (O) and S_2 (●), and lineations (+) in the southern half of the Rolesville batholith. The interpreted F_2 fold axis (⊕) is 30° , S15°E.

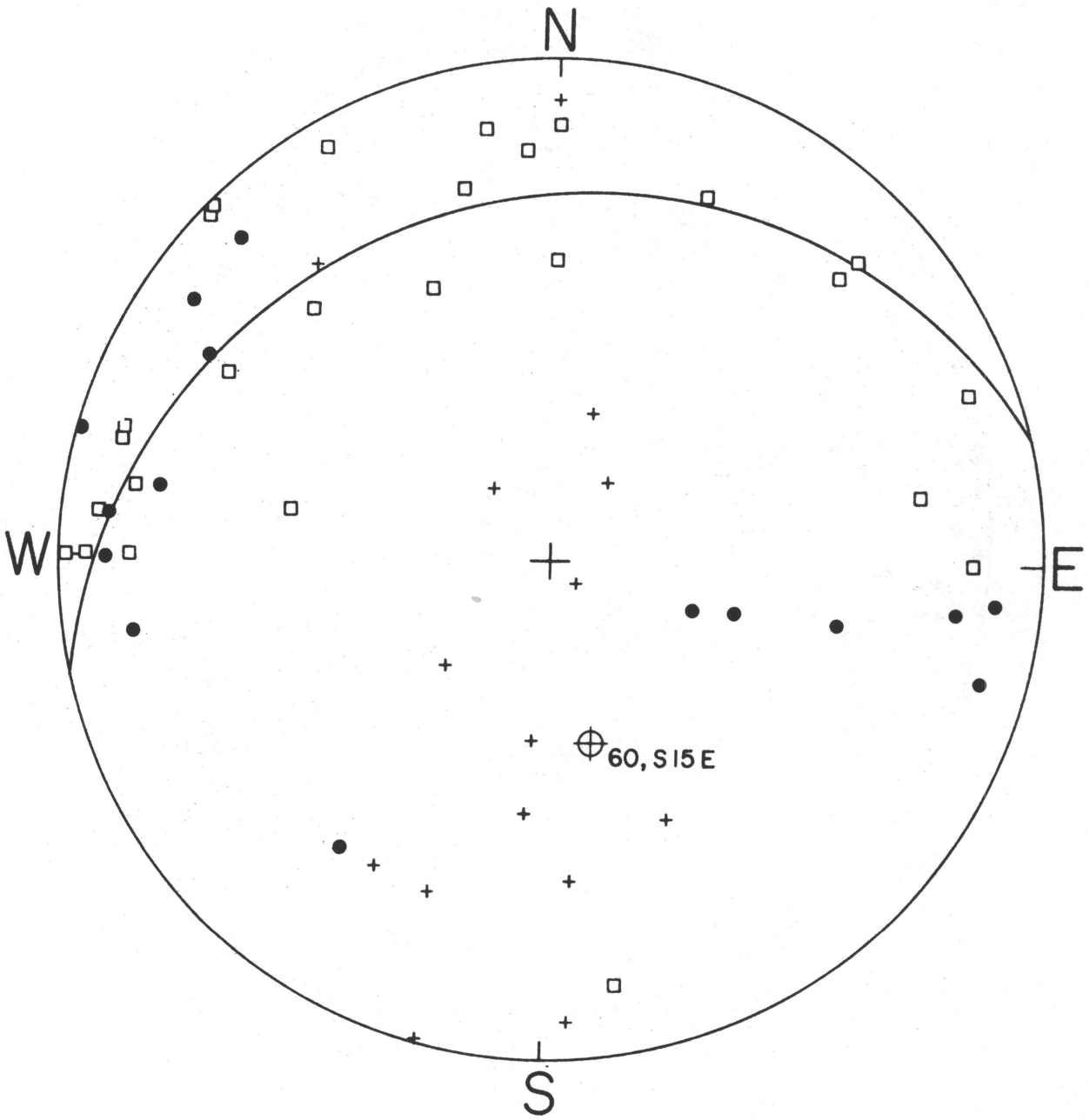


Fig. A28. Equal area projection of poles to $S_0 + S_1$ (□) and S_2 (●), and lineations (+) in country rocks surrounding the southern half of the Rolesville batholith. The interpreted F_2 fold axis (⊕) is 60° , $S15^\circ E$.

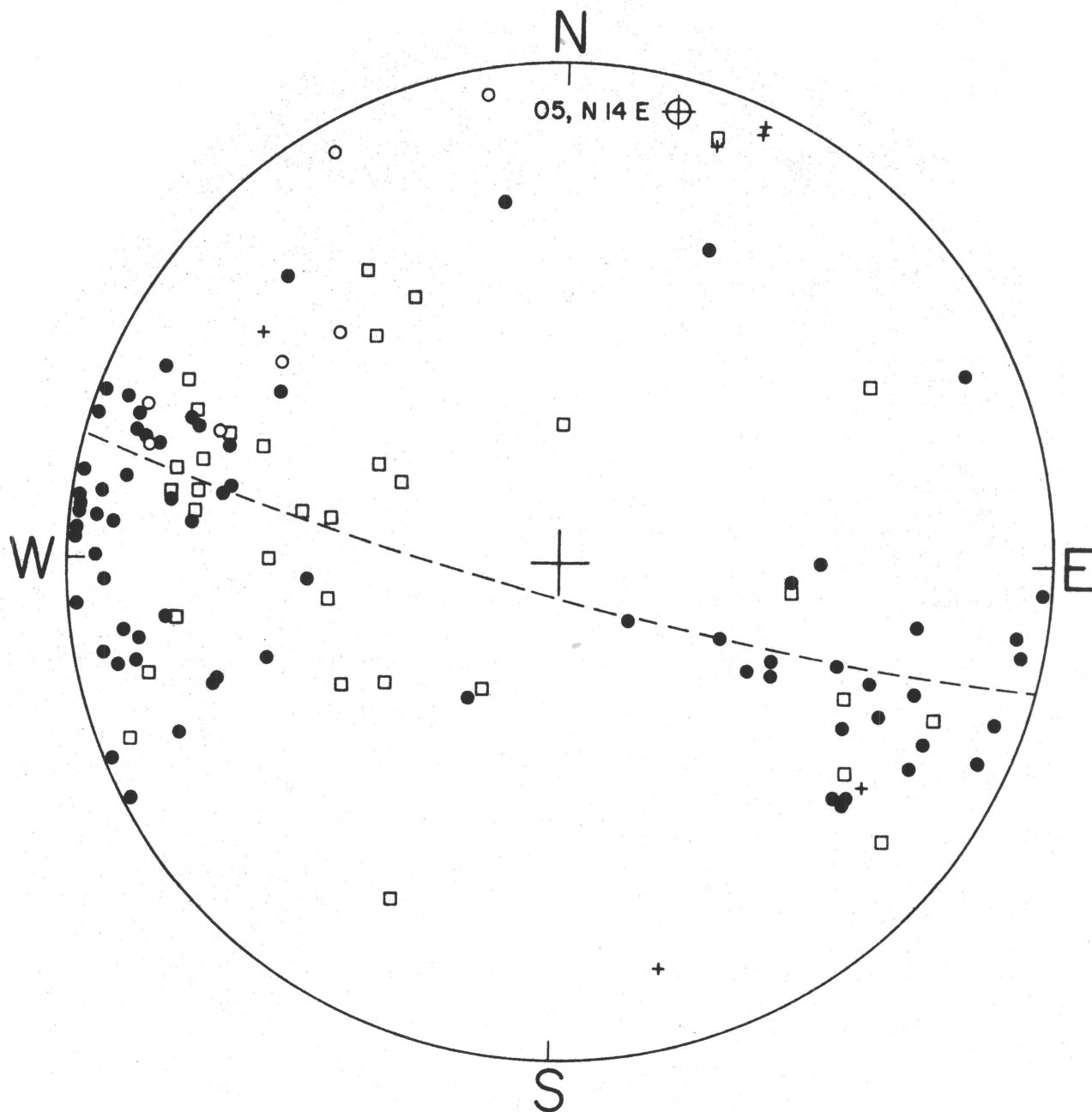


Fig. A29. Equal area projection of structural data from the northern half of the Rolesville area, including poles to S_0' (○) and S_2 (●) in the granite and S_0+S_1 (□) and S_2 (●) in the country rock. Also plotted are lineations (+) and a poorly-defined F_2 fold axis (⊕).

(Parker's Wake-Warren anticlinorium) which has the axial plane N05°E, 70° - 80°E. Three previously existing surfaces ($S_0 + S_1$ of the country rock and S_0' of the granite) have been folded to give the axis 30°, S15°E for the granite and 60°, S15°E for the country rock. The limbs of the anticlinorium can be traced beyond the northern extent of the Rolesville batholith, but the nose is clearly defined only in the southern half of the mapped area.

Roxboro Metagranite

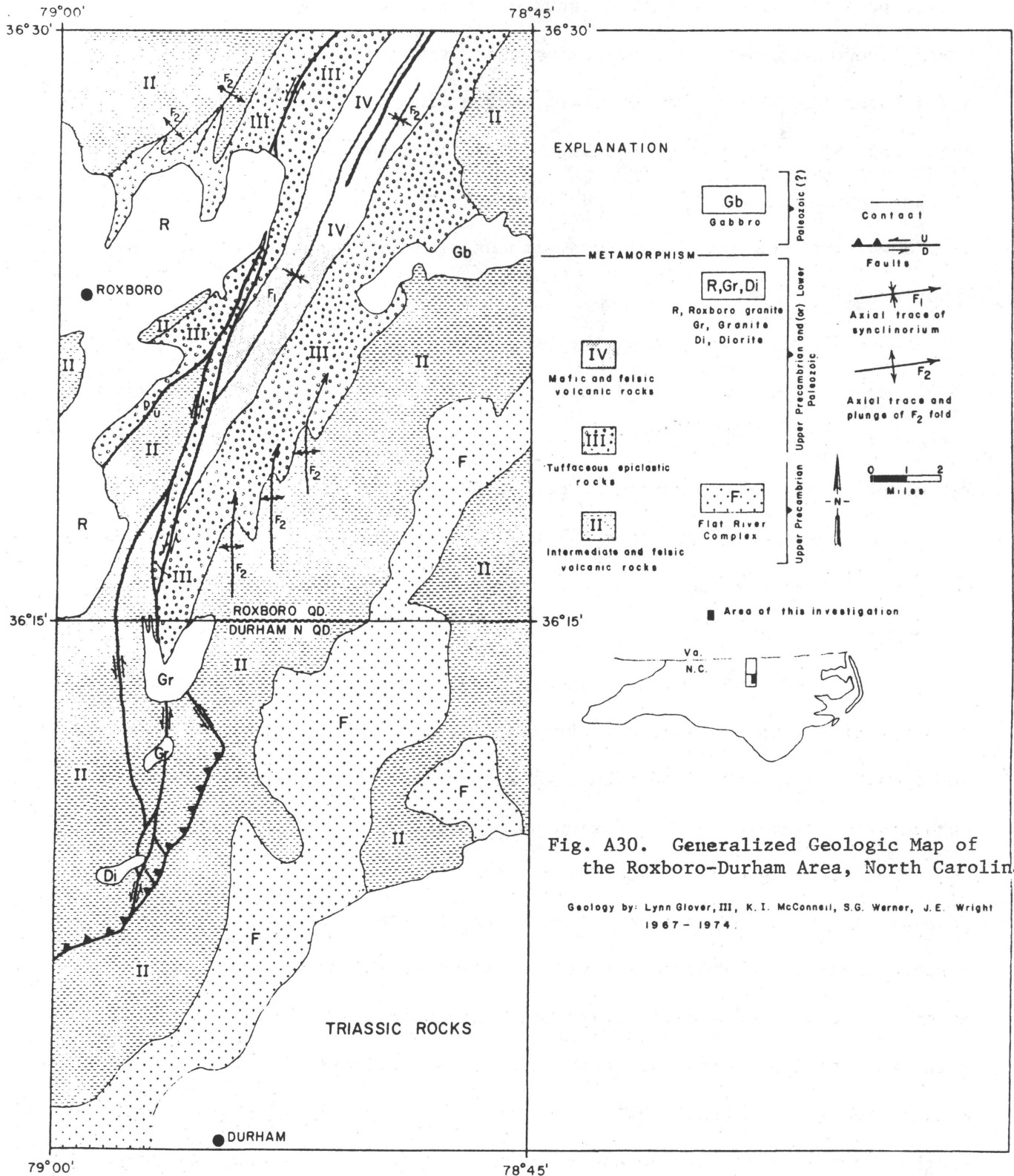
by Lynn Glover III

Geologic Framework

The Roxboro Metagranite is located at Roxboro, N.C. (Fig. A30) along the boundary between the Charlotte and Carolina Slate belts. The pluton has an irregular shape (Fig. A30), the maximum surface width being about 12 km. Publications by Glover and Sinha (1973), and Wilson (1975) are the principal published references to the geology of the area and much of the following is taken from these and unpublished data gathered subsequently.

There are two objectives in continuing work on the Roxboro in the context of this program. First, it represents a well-studied example (Glover and Sinha, 1973; Briggs, Gilbert and Glover, in press) of the oldest group of Piedmont granites, and secondly, the steep metamorphic gradient superimposed on it offers the possibility of determining the controls and extent of U and Th redistribution during metamorphism, although this may be complicated by a recently discovered late static recrystallization.

Prior to emplacement of the Roxboro Metagranite, at least 7 to 10 km of dominantly marine pyroclastic rocks accumulated in the region. The base of this sequence has never been seen, probably because it is obscured by high grade metamorphism in the Charlotte and Raleigh belts, and the top is missing because of erosion. The volcanics range in age from at least 700 m.y. to younger than 520 m.y. and comprise a bimodal calcalkaline suite. Basalt dominates the mafic mode, and rhyodacite the felsic mode. Andesite is present but not common. A minor amount of non-volcanic epiclastic debris is intercalated in the volcanic sequence, and its sialic character indicates erosion



from nearby (and underlying) continental crust. The large ratio of felsic to mafic modes, roughly 2/3, strongly indicates eruption through continental crust, possibly along an ancient subduction zone whose polarity is unknown. Comparison with modern volcanic suite chemistry (Miyashiro, 1974) suggests a thickness of about 30 km. of crust at the time of eruption 740 to 520 m.y. ago. Low initial Sr ratios (Fullagar, 1971) and the hot dry nature of some of the magma (Briggs, Gilbert and Glover, in press) suggest rapid ascent from deep crust and mantle sources without significant contamination by upper crustal rocks.

About 600 m.y. ago during the Virgilina deformation (Glover and Sinha, 1973), these rocks were folded into large NE trending structures and shortly thereafter were faulted in a compressional framework on a regional scale. Metamorphism may have occurred at depth, but at the crustal level now observed in these low grade rocks absence of relict metamorphic assemblages or early strain fabrics indicates that they were not raised above the zeolite facies.

At 575 ± 20 m.y. ago, the Roxboro granite was emplaced in the folded and faulted volcanic sequence (petrography and petrology discussed below), and probably erupted to contribute to a thick post-Virgilina volcanic sequence now removed in this region by erosion.

The first regional metamorphism evident at the crustal level now exposed probably occurred about 350 m.y. ago. At this time a steep regional metamorphic gradient was formed across the region establishing the principal architecture of the Carolina Slate belt (greenschist facies) - Charlotte belt (amphibolite facies) boundary which runs northeasterly through the Roxboro Metagranite (Fig. A30). The Carolina Slate belt lies along the southeastern side of this boundary and the Charlotte belt along the northwest. Both belts appear to involve the same volcanic sequence differing

Primarily in metamorphic and tectonic history.

Subsequent erosion, Triassic rifting and sedimentation has produced the surface distribution of rock units recorded on the geologic map in Fig. A30.

Petrography

The eastern low grade part of the Roxboro has yielded the most detailed and petrogenetically important data to date. Thus the part of the pluton east of long. 79°00' is herein summarized from Briggs, Gilbert and Glover (in press). Comments on the region west of 79°00' long. are presented at the end of this section briefly because the work is still in progress.

Granite forms the dominant facies of the Roxboro pluton, however alkali feldspar granite is probably common and granodiorite relatively rare. Averaged modal analyses are shown in Table A7. All premetamorphic facies contained plagioclase, quartz, K-spar, biotite and opaques. Additionally many samples have a well-preserved granophyric mesostasis. Plagioclase phenocrysts (some with relict zoning) range from subhedral to euhedral. Some relict euhedral quartz survived metamorphism although much is strained and/or recrystallized. Perthitic K-spar is mostly anhedral and commonly surrounds plagioclase and quartz phenocrysts. Biotite, magnetite and ilmenite are locally surrounded by rims of chlorite (on biotite) and titanite (on opaques).

Regional metamorphism resulted in relatively complete (but dominantly pseudomorphic) recrystallization of the igneous mineralogy to greenschist assemblages appropriate to the metamorphic mineral zones shown on Fig. A30. A very lightly developed foliation, parallel to that in the host rock, is nearly pervasive through the pluton. Random growth of chlorite and stilpnomelane on oriented metamorphic biotite and random stilpnomelane on perthite suggest a second low temperature thermal event after the main regional

Table A7. Averaged Modal Analyses From the Roxboro Metagranite East of 79° Long.
From Briggs, Gilbert and Glover, in press.

	CHLORITE ZONE			BIOTITE ZONE		
	Metagranite	Alkali- Feldspar Metagranite	Southern Portion	Metagranite	Alkali- Feldspar Metagranite	Metagranodiorite
Albite	34.8	25.00	28.6	33.6	37.2	34.7
Microcline	29.3	37.75	3.0	25.4	31.5	11.3
Quartz	27.1	33.75	30.9	30.1	26.9	26.4
Biotite	0.3	m	-	1.9	0.4	4.3
Stilpnomelane	2.3	1.50	-	1.5	1.4	0.6
Muscovite	2.4	m	13.5	1.7	0.5	7.0
Chlorite	m	-	5.9	0.5	m	m
Amphibole	-	-	0.1	-	0.4	-
Epidote	2.3	1.00	15.9	4.7	0.7	14.8
Allanite	m	-	m	m	m	-
Sphene	m	m	1.1	0.2	0.4	0.3
Garnet	0.2	-	-	-	-	-
Apatite (?)	-	-	0.1	m	-	-
Fluorite	m	m	-	m	0.2	-
Calcite	-	-	0.1	-	-	-
Zircon	m	m	m	m	m	m
Opaques	1.2	1.00	0.5	0.3	0.4	0.3
Total	99.9	100.00	99.7	99.9	100.00	99.7
# of Samples	2	1	3	36	6	2

m denotes minor amounts

metamorphism. All K-rich feldspar is nearly microcline and shows no compositional progression across the area. Thus either partial retrogression followed the main regional event or a separate low grade thermal event followed regional greenschist metamorphism.

In the western half of the Roxboro, west of 79° long., outcrops are less abundant and all are more deeply weathered. Reconnaissance petrography suggests a rather constant bulk composition similar to that in the eastern half. Euhedral plagioclase shows relict zoning by abundant epidote group minerals generated in calcic cores during metamorphism. Biotite is all of metamorphic derivation and granophyric textures are rare because of metamorphic recrystallization or a different igneous cooling history. Sparse but locally pervasive chloritization of metamorphic biotite and rare randomly oriented sprays of stilpnomelane suggest continuation of the late static low grade recrystallization after regional metamorphism as discussed above. Regional metamorphic grade of the country rock surrounding the western half of the Roxboro pluton is all of lower amphibolite facies.

Petrology

An extensive treatment of the petrology of the Roxboro Metagranite is beyond the scope of the present report, but is available for examination in preprint form. The following conclusions are quoted from Briggs, Gilbert and Glover (in press).

"The pluton located at Roxboro, North Carolina is predominantly a light gray to medium gray, microphaneritic metagranite. Phenocrysts of plagioclase, quartz, and perthite are accompanied by porphyroblasts of epidote. Relict igneous textural relationships suggest two possible fractional crystallization models, in both of which the order of crystallization was plagioclase, quartz, and then K-rich feldspar.

A crude approximation of the composition of the original plagioclase phenocrysts is An_{25} to An_{40} . Based on the composition of locally present granophyre, the pluton was emplaced under almost "dry" conditions with a P_{Total} of about 350 bars and a temperature in the vicinity of $950^{\circ}C$. The shallow depth of emplacement suggests that the Roxboro Metagranite represents the root of a volcanic sequence that once unconformably overlay the presently exposed sequence. During the middle Paleozoic, this granitic intrusive was metamorphosed at a minimum pressure of about 3 kbar and a temperature of approximately $400^{\circ}C$. A foliation, as shown by stringers of mainly biotite and epidote, was produced by the deformational phase accompanying regional metamorphism. All K-rich feldspar is now nearly pure microcline ($\sim Or_{97}$), and all plagioclase is now nearly pure low albite (An_{1-3}). Such feldspar compositions accompanied by late growth of ferristilpnomelane indicate a reequilibration under lower grade conditions than those realized during the peak of the major regional metamorphic event."

Drilling

Currently two drill holes have been completed (Rox 1 and Rox 2 to depths of 844' and 702' respectively) in the Roxboro and a third (Rox 3) is in progress. Sample intervals will be chosen for study when the temperature and gamma ray logging is completed. The hole sites were chosen to sample the full range of metamorphic grade superimposed on the granite.

Heat Production

Heat production values are plotted on the map in Fig. A31 and tabulated in Table A8. These values are lowest in the thin southern extension of the pluton where metamorphic strain fabrics are most pronounced. Although this is only chlorite zone metamorphism, metasomatic effects may be intense here because the deformation enhanced permeability during metamorphism. In these samples K-spar has been almost entirely replaced by muscovite in contrast to the rest of the pluton.

Elsewhere the variation in heat production across the pluton does not seem to vary in any systematic manner, averaging about 4.4 in both the low and high grade parts. However, Th/U ratios are greater in the western part suggesting possible greater post emplacement depletion of U there.

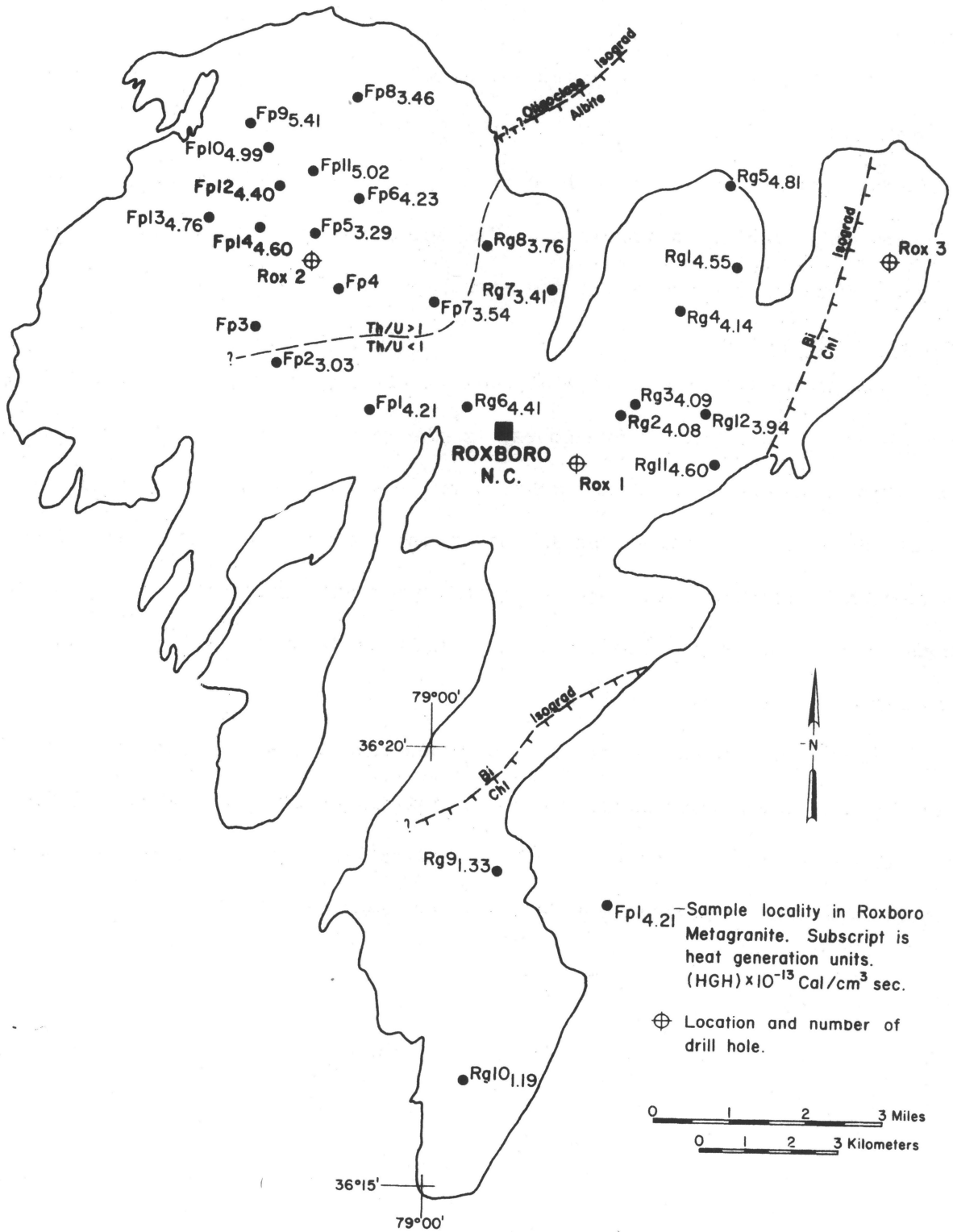


Fig. A31. Outline map of the Roxboro metagranite showing location of samples and heat production values.

Table A8. Heat generation values for surface samples from the Roxboro Metragranite

Location	Sample No.	Density, gm/cm ³	Uranium (U), ppm	Thorium (Th), ppm	Potassium (K), %	K ₂ O, %	Heat generation, A x 10 ⁻¹³ cal/cm ³ -sec	Comments
Roxboro, NC	RG-1	2.67*	2.77	11.88	3.62	4.34	4.55	Med.-coarse grained
	RG-2	2.67*	2.96	9.41	2.90	3.48	4.08	"
	RG-3	2.67*	2.88	9.79	2.83	3.40	4.09	"
	RG-4	2.67*	3.05	9.57	2.78	3.33	4.14	"
	RG-5	2.67*	3.27	11.61	3.62	4.34	4.81	"
	RG-6	2.67*	3.21	10.34	2.96	3.56	4.41	"
	RG-7	2.67*	2.32	7.30	3.26	3.91	3.41	"
	RG-8	2.67*	2.76	8.63	2.62	3.14	3.76	"
	RG-9	2.67*	0.81	2.98	1.41	1.69	1.33	"
	RG-10	2.67*	0.83	2.58	1.04	1.25	1.19	"
	RG-11	2.67*	3.33	11.06	2.93	3.51	4.60	"
	RG-12	2.67*	2.90	8.75	2.92	3.50	3.94	"
	FP-1	2.67*	2.95	10.05	3.02	3.62	4.21	"
	FP-2	2.67*	1.96	7.05	2.76	3.31	3.03	"
	FP-5	2.67*	1.91	8.18	3.18	3.82	3.29	"
	FP-6	2.67*	2.64	11.17	3.09	3.71	4.23	"
	FP-7	2.67*	2.18	8.93	3.21	3.86	3.59	"

*Indicates an assumed density.

Table A8 (continued).

Location	Sample No.	Density, gm/cm ³	Uranium (U), ppm	Thorium (Th), ppm	Potassium (K), %	K ₂ O, %	Heat generation, A x 10 ⁻¹³ cal/cm ³ -sec	Comments
	FP-8	2.67*	1.87	9.50	3.07	3.69	3.46	Med.-coarse grained
	FP-9	2.67*	3.70	13.68	3.53	4.23	5.41	"
	FP-10	2.67*	3.25	12.88	3.51	4.21	4.99	"
	FP-11	2.67*	3.20	13.18	3.55	4.26	5.02	"
	FP-12	2.67*	2.67	11.80	3.30	3.96	4.40	"
	FP-13	2.67*	2.98	13.15	3.06	3.68	4.76	"
	FP-14	2.67*	2.86	12.34	3.26	3.91	4.60	"
	S7-1	2.66	2.07	3.69	1.79	2.15	2.30	Felsic volcanic country rocks
	S7-2	2.70	3.94	7.38	2.87	3.45	4.39	"
	S7-3	2.72	2.36	5.95	2.61	3.13	3.12	"
	S7-5	2.72	3.24	6.95	2.45	2.94	3.81	"
	S7-6	2.67	3.28	7.14	2.15	2.58	3.73	"

*Indicates an assumed density.

REFERENCES

- Andersen, G. D. and P. D. Fullagar, 1977, Geochronology of the Boy Scout-Jones Molybdenum prospect, southwestern Halifax County, North Carolina (abs.): Geol. Soc. America, Abs. with Prog. 9, 114.
- Bateman, P. C., L. D. Clark, N. K. Huber, J. G. Moore, and C. D. Rinehart, 1963, The Sierra Nevada Batholith - A synthesis of recent work across the central part: U. S. Geol. Survey Prof. Paper 414-D.
- Bates, R. G. and H. Bell, III, 1965, Geophysical investigations in the Concord Quadrangle, Cabarrus and Mecklenburg Counties, North Carolina: U. S. Geol. Survey Geophysical Investigations Map GP-522.
- Beg, M. A. and L. T. Larson, 1975, The Catawba pluton: An example of porphyry copper type mineralization in the southern Appalachian orogen (abs): Geol. Soc. America, Abs. with Prog. 7, 469.
- Bell, H., III, J. R. Butler, D. E. Howell, and W. H. Wheller, 1974, Geology of the Piedmont and Coastal Plain near Pageland, South Carolina, and Wadesboro, North Carolina: Carolina Geol. Soc. Field Trip Guidebook, Div. Geol., S. C. State Dev. Board, 23p.
- _____, and P. Popenoe, 1976, Gravity studies in the Carolina Slate Belt near the Haile and Brewer Mines, north-central South Carolina: Jour. Res. U. S. Geol. Survey 4, 667-682.
- Bowman, J. T., 1970, Compositional variation of granite in eastern Wake County, North Carolina: M.S. thesis, N. C. State University, Raleigh.
- Briggs, D. F., M. C. Gilbert, and L. Glover, III (in press), Petrology and regional significance of the Roxboro metagranite, North Carolina: Geol. Soc. America Bull.
- Broadhurst, S. D. and J. M. Parker, 3rd, 1959, Guidebook for Piedmont field trip, featuring metamorphic facies in the Raleigh area, North Carolina, of the Southeastern Section of the Geological Society of America: N. C. Div. Mineral Res., 24p.
- Butler, J. R. and P. C. Ragland, 1969, A petrochemical survey of plutonic intrusions in the Piedmont, southeastern Appalachians, U.S.A.: Contrib. Mineral. Petrol. 24, 164-190.
- Carmichael, I. S. E., F. J. Turner, and J. Verhoogen, 1973, Igneous Petrology: McGraw-Hill, 739p.
- Carpenter, P. A., 1970, Geology of the Wilton area, Granville Co., North Carolina: M.S. thesis, N. C. State University.

- Clark, K. F., 1972, Stockwork molybdenum deposits in the western Cordillera: Econ. Geol. 67, 731-758.
- Cook, R. B., Jr., 1972, Exploration for disseminated molybdenum-copper mineralization in the Conner Stock, Wilson and Nash Counties, North Carolina (abs.): Econ. Geol. 67, 1003-1004.
- Councill, R. J., 1954, The commercial granites of North Carolina: N. C. Div. Mineral Res. Bull. 67, 59p.
- de Boer, J., 1967, Paleomagnetic-tectonic study of Mesozoic dike swarms in the Appalachians: Jour. Geophys. Res. 72, 2237-2250.
- Dickey, J. B., 1963, The geology of the Barton Creek area, northern Wake County, North Carolina: M.S. thesis, N. C. State Univ., Raleigh, 55p.
- Dostal, J., 1975, Geochemistry and petrology of the Loon Lake Pluton, Ontario: Can. Jour. Earth Sci. 12, 1331-1345.
- _____, S. Capedri, and C. Dupuy, 1976, Uranium and potassium in calc-alkaline volcanic rocks from Sardinia: Lithos 9, 179-183.
- Dybek, I. J., 1962, Zur Geochemie und Lagerstättenkunde des Urans: Clausthaler Hefte zur Lagerstättenkunde und Geochemie der mineralischen Rohstoffe, Heft 1, 163p.
- Farquhar, C. R., 1952, Crystalline rocks of north central Wake County, North Carolina: M.S. thesis, N. C. State Univ., Raleigh, 33p.
- Fortson, C. W., Jr., 1958, Geology of the Crabtree Creek area northwest of Raleigh, N. C.: M.S. thesis, N. C. State Univ., Raleigh, 101p.
- FrondeL, C., 1958, Systematic mineralogy of uranium and thorium: U. S. Geol. Survey Bull. 1064, 400p.
- Fullagar, P. D., 1971, Age and origin of plutonic intrusions in the Piedmont of the southeastern Appalachians: Geol. Soc. America Bull. 82, 2845-2862.
- Glover, D. P., 1963, A gravity study of the northeastern Piedmont batholith of North Carolina: M.S. thesis, Univ. of North Carolina, Chapel Hill, 41p.
- Glover, L. III and A. K. Sinha, 1973, The Virgilina deformation, a Late Precambrian to early Cambrian(?) orogenic event in the central Piedmont of Virginia and North Carolina: Am. Jour. Sci. 273-A, 234-251.
- Griffin, W. L. and M. T. Styles, 1976, A projection for analysis of mineral assemblages in calc-pelitic metamorphic rocks: Norsk Geol. Tidsskrift 56, 203-209.

- Harshman, E. N. and K. G. Bell, 1970, Urannite-bearing contact metamorphic deposits, Heaths Peak, Carbon Co., Wyoming: *Econ. Geol.* 65, 849-855.
- Harvey, B. W., 1974, The microscopic petrography and ore microscopy of the Boy Scout-Jones Molybdenum Prospect, Halifax Co., North Carolina: M.S. thesis, N. C. State Univ., Raleigh.
- Heier, K. S., W. Compston, and I. McDougall, 1965, Thorium and uranium concentrations and the isotopic composition of strontium in the differentiated Tasmanian dolerites: *Geochim. Cosmochim. Acta* 29, 643-659.
- _____, and J. J. W. Rogers, 1963, Radiometric determination of thorium, uranium, and potassium in basalts and in two magmatic differentiation series: *Geochim. Cosmochim. Acta* 27, 137-154.
- Hills, F. A. and J. R. Butler, 1968, Rubidium-strontium dates for some rhyolites from the Carolina slate belt of the North Carolina Piedmont (abs.): *Geol. Soc. America Spec. Pap.* 121, 445.
- Hunt, J. A. and D. M. Kerrick, 1977, The stability of titanite: Experimental redetermination and geologic implications: *Geochim. Cosmochim. Acta* 41, 279-288.
- Johannes, W. and P. M. Orville, 1974, Experimental determination of an isobaric invariant point and associated reactions involving anorthite in the system CaO-K₂O-Al₂O₃-SiO₂-CO₂-H₂O: Written communication, 1974, NATO Advanced Study Institute on Volatiles in Metamorphism.
- Julian, E. L., 1972, The Castalia Adamellite in Franklin and Nash counties, North Carolina, and the petrogenesis of some associated aplites and pegmatites: M.S. thesis, N. C. State Univ., Raleigh, 61p.
- Kulp, J. L. and F. D. Eckelmann, 1961, Potassium-argon ages of micas from the southern Appalachians: *Annals of the New York Acad. Sci.* 91, 408-416.
- Larsen, E. S., Jr. and G. Phair, 1954, The distribution of uranium and thorium in igneous rocks; *in*, H. Faul, ed., *Nuclear Geology*, p. 75-89: New York, John Wiley and Sons.
- Lowell, J. D. and J. M. Guilbert, 1970, Lateral and vertical alteration - mineralization zoning in porphyry ore deposits: *Econ. Geol.* 65, 373-408.
- Mann, J. I. and Zablocki, F. S., 1961, Gravity features of the Deep River-Wadesboro Triassic basin of North Carolina: *Southeastern Geol.* 2, 191-215.
- McSween, H. Y., Jr., 1972, An investigation of the Dutchman's Creek gabbro, Fairfield County, South Carolina: *Geologic Notes, Div. Geol., S. C. State Dev. Board* 16, 19-42.

- Miyashiro, A., 1974, Volcanic rock series in island arcs and active continental margins: *Am. Jour. Sci.* 274, 321-355.
- Parker, J. M., III, 1968, Structure of easternmost North Carolina Piedmont: *Southeastern Geol.* 9, 117-131.
- _____, 1977a (in press), Geology and Mineral Resources of Wake County, North Carolina: Div. Earth Resource, N. C. Dept. Nat. and Econ. Resources.
- _____, 1977b, Structure of Raleigh belt of eastern Piedmont in Wake County, North Carolina (abs.): *Geol. Soc. America, Abs. with Prog.* 9, 173.
- Privett, D. R., 1973, Paragenesis of unusual hydrothermal zeolite assemblage in a diorite-granite contact zone, Woodleaf, Rowan County, North Carolina: *Southeastern Geol.* 15, 105-118.
- Randazzo, A. F., 1972, Petrography and stratigraphy of the Carolina Slate Belt, Union County, North Carolina: N. C. Dept. of Natural and Economic Resources, Spec. Publ. 4, 38p.
- _____, and R. E. Copeland, 1976, The geology of the northern portion of the Wadesboro Triassic basin, North Carolina: *Southeastern Geol.*, 17, 115-138.
- Reinemund, J. A., 1955, Geology of the Deep River Coal Field, North Carolina: U. S. Geol. Surv. Prof. Paper 246, 159p.
- Robertson, A. F., F. K. McIntosh, and T. J. Ballard, 1947, Boy Scout-Jones and Moss-Richardson Molybdenum deposits, Halifax County, N. C.: Bureau of Mines Report of Investigations 4156, 9p.
- Schrader, E. L., W. J. Furbish, and J. Leanderson, 1977, The geochemistry and weathering history of a molybdenite occurrence at Hollister, North Carolina (abs.): *Geol. Soc. America, Abs. with Prog.* 9, 181-182.
- Shiver, R. S., 1974, The geology of the Heath Springs quadrangle, Heath Springs, S. C.: M.S. thesis, N. C. State Univ., Raleigh, 39p.
- St. Jean, J., Jr., 1964, New Cambrian trilobite from the Piedmont of North Carolina (abs.): *Geol. Soc. America Spec. Paper* 82, 307-308.
- Stevenson, J. S., 1951, Uranium mineralization in British Columbia: *Econ. Geol.* 46, 353-366.
- Sundelius, H. W., 1970, The Carolina slate belt; in, G. W. Fisher *et al.*, eds., *Studies of Appalachian Geology: Central and Southern*: John Wiley and Sons, Inc., 351-367.
- Talwani, M. and J. R. Heirtzler, 1964, Computation of magnetic anomalies caused by two dimensional structures of arbitrary shape: *Computers in the Mineral Industries, Part 1, Stanford Univ. Publ., Geol. Sci.* 9, 464-480.

- Tilling, R. I., D. Gottfried, and F. C. W. Dodge, 1970, Radiogenic heat production of contrasting magma series: Bearing on interpretation of heat flow: *Geol. Soc. America Bull.* 81, 1447-1462.
- U. S. Geological Survey Open-file Report, 1970, Aeromagnetic map of the Camden-Kershaw area, northcentral South Carolina.
- U. S. Geological Survey, 1973a, Aeromagnetic map of the northern parts of the Durham North and Creedmore quadrangles, north-central North Carolina, scale 1:62,500: GP-883.
- _____, 1973b, Aeromagnetic map of the Henderson quadrangle and parts of the Louisburg and Boydton quadrangles, north-central North Carolina, scale 1:62,500: GP-884.
- _____, 1973c, Aeromagnetic map of the Norlina quadrangle and parts of the Castalia and South Hill quadrangles, north-central North Carolina, scale 1:62,500: GP-885.
- _____, 1974, Aeromagnetic map of parts of the Greensboro and Raleigh 1° by 2° quadrangles, North Carolina, scale 1:250,000: Open-file Report 74-29.
- _____, 1976, Aeromagnetic map of parts of Georgia, South Carolina, and North Carolina, by the Coastal Plains Commission and the U. S. Geol. Surv., scale 1:250,000: Open-file Report 76-181.
- Uzkut, I., 1974, Zur Geochemie des molybdäns: Clausthaler Hefte zur Lagerstättenkunde und Geochemie der mineralischen Rohstoffe: Hefte 12, 226p.
- Waskom, J. D., 1970, Geology and geophysics of the Lilesville Granite Batholith, North Carolina: Ph.D. thesis, Univ. North Carolina, Chapel Hill, 78p.
- Watson, T. L., 1904, Granites of North Carolina: *Jour. Geol.* 12, 373-407.
- _____, 1910, Granites of the southeastern Atlantic States: U. S. Geol. Surv. Bull. 426, 282p.
- _____, and F. B. Laney, 1906, Building and ornamental stones of North Carolina: N. C. Geol. and Econ. Surv. Bull. 2.
- White, A. M., A. A. Stromquist, T. W. Stern, and H. Westley, 1963, Ordovician age for some rocks of the Carolina slate belt in North Carolina: U. S. Geol. Surv. Prof. Paper 475-C, C107-C109.
- Whitten, E. H. T., 1975, Appropriate units for expressing chemical composition of igneous rocks: *Geol. Soc. America Mem.* 142, 283-308.

Wilson, W. F., 1975, Geology of the Winstead quadrangle, North Carolina: Mineral Resources Section, N. C. Div. of Resource Planning and Evaluation, Raleigh.

_____, P. A. Carpenter, and J. M. Parker, III, 1975, Geologic map of Region J, North Carolina: N. C. Div. of Mineral Res.

Worthington, J. E. and N. R. Lutz, 1975, Porphyry copper-molybdenum mineralization at the Newell Prospect, Cabarrus County, North Carolina: Southeastern Geol. 17, 1-14.

Yund, R. A. and G. Kullerud, 1966, Thermal stability of assemblages in the Cu-Fe-S system: J. Petrol. 7, 454-488.

B. Geochemistry

A. K. Sinha, Principal Investigator
Barbara A. Merz, Research Associate

Rolesville Batholith

Barbara Merz and A. K. Sinha

Sixteen samples from the Rolesville batholith were analyzed by X-ray fluorescence and the results are given in Table B-1. Of the 16 samples, two are from the Castalia pluton, one from the fine-grained Louisberg pluton, and the rest from the Rolesville main pluton. These bodies and the sample sites appear on the map, Fig. A-22, in the petrology section of this report.

Strekeisen (1976) has proposed a rock classification scheme which uses plots of normative Or-Ab-An, one for samples with <17% normative Qz and one for those with >17%. C.I.P.W. norms were calculated and all the samples except B6-7 have >17% Qz and fall in the syenogranite-monzogranite fields of the appropriate diagram B6-7, with 11.3% normative Qz defined as an alkaline monzonite.

A Ca-Na-K diagram was used to characterize the samples as alkaline or calc-alkaline since there was insufficient compositional range for the Peacock index to be used. The data fell between the trends defined by calc-alkaline and alkaline rock suites except for B6-7 which, in agreement with its definition as an alkaline monzonite, fell on an alkaline trend. Thus the samples may be called slightly calc-alkaline, in contrast with the Liberty Hill and Winnsboro samples (report VPI&SU 5103-2) which plotted on the calcic side of the calc-alkaline trend.

Use of a Qz-Ab-Or diagram indicates a pressure during formation of 4 to 10 kb whether the magma is considered to be wet or dry. The

Table B-1. Chemical compositions of Rolesville samples.

	B6-7	F6-116-3	F6-99	F6-129-1	F6-116-1	B6-3-1	F6-78	F6-89
SiO ₂	63.26	69.11	69.16	70.10	70.45	70.58	70.77	70.99
Al ₂ O ₃	18.34	16.51	16.21	15.92	16.03	16.01	15.33	16.17
CaO	2.99	2.01	1.95	1.96	1.86	1.83	1.55	1.77
MgO	1.12	0.82	0.84	0.81	0.72	0.75	0.72	0.70
K ₂ O	3.34	4.43	4.34	3.91	3.98	4.26	5.22	4.35
FeO	2.89	2.08	2.16	2.10	1.98	1.90	2.37	1.58
Na ₂ O	5.15	4.45	4.44	4.51	4.66	4.47	3.97	4.55
MnO	0.03	0.04	0.05	0.04	0.05	0.03	0.05	0.04
TiO ₂	0.52	0.35	0.35	0.35	0.30	0.28	0.40	0.27
P ₂ O ₅	0.22	0.15	0.16	0.14	0.13	0.12	0.19	0.11
TOTAL	97.86	99.95	99.66	99.84	100.16	100.23	100.57	100.53

Table B-1 (continued).

	B6-24	F6-129-1	S6-288	S6-153	F6-88-2	F6-88-1	F6-88-3	S6-203
SiO ₂	71.00	71.97	72.31	72.90	73.20	75.70	76.42	77.22
Al ₂ O ₃	14.99	15.58	15.71	15.62	14.66	14.61	15.07	14.47
CaO	2.22	1.73	1.55	1.53	1.45	1.14	1.19	0.96
MgO	1.04	0.66	0.60	0.47	0.76	0.43	0.15	0.18
K ₂ O	3.56	4.17	4.94	4.95	4.39	4.79	4.78	4.53
FeO	2.08	1.67	1.62	1.57	1.90	1.20	0.59	0.70
Na ₂ O	4.03	4.39	3.94	4.01	4.00	4.00	4.22	4.56
MnO	0.05	0.04	0.03	0.04	0.05	0.03	0.02	0.05
TiO ₂	0.27	0.26	0.24	0.16	0.29	0.13	0.02	0.04
P ₂ O ₅	0.10	0.11	0.10	0.07	0.15	0.03	0.02	0.01
TOTAL	99.34	100.58	101.04	101.32	100.85	102.06	102.48	102.72

data plots in the primary orthoclase field of the phase diagram for saturated conditions at 4 kb as given by Steiner et al. (1975) but in the primary quartz field of the 10 kb saturated phase diagram of Luth et al. (1964). Similarly, under dry conditions the data plots in the primary feldspar field for 4 kb and the primary quartz field for 10 kb (Luth, 1969). Thus knowledge of the first phase to crystallize could narrow the possible pressure range. Petrographic evidence (see petrology report) suggests that a feldspar was probably the first phase to crystallize, so a pressure of about 4 to 6 kb is suggested. No chemical distinctions could be made between the Castalia, Louisberg and Rolesville main samples. The two Castalia samples usually plotted on opposite edges of the trends defined by the other samples and the one Louisberg sample amongst the Rolesville samples.

According to many authors, e.g., Tilling and Gottfried (1969), alkaline rock suites have higher U and Th contents than calc-alkaline of the same degree of differentiation. This means that for a given SiO_2 content, using SiO_2 as an indicator of differentiation, an alkaline rock should have more U and Th than a calc-alkaline one. Rolesville batholith appears to be more alkaline than Liberty Hill or Winnsboro, and the U and Th of the three bodies are compared on Figs. B-1 and B-2. U and Th contents were obtained by the geophysics

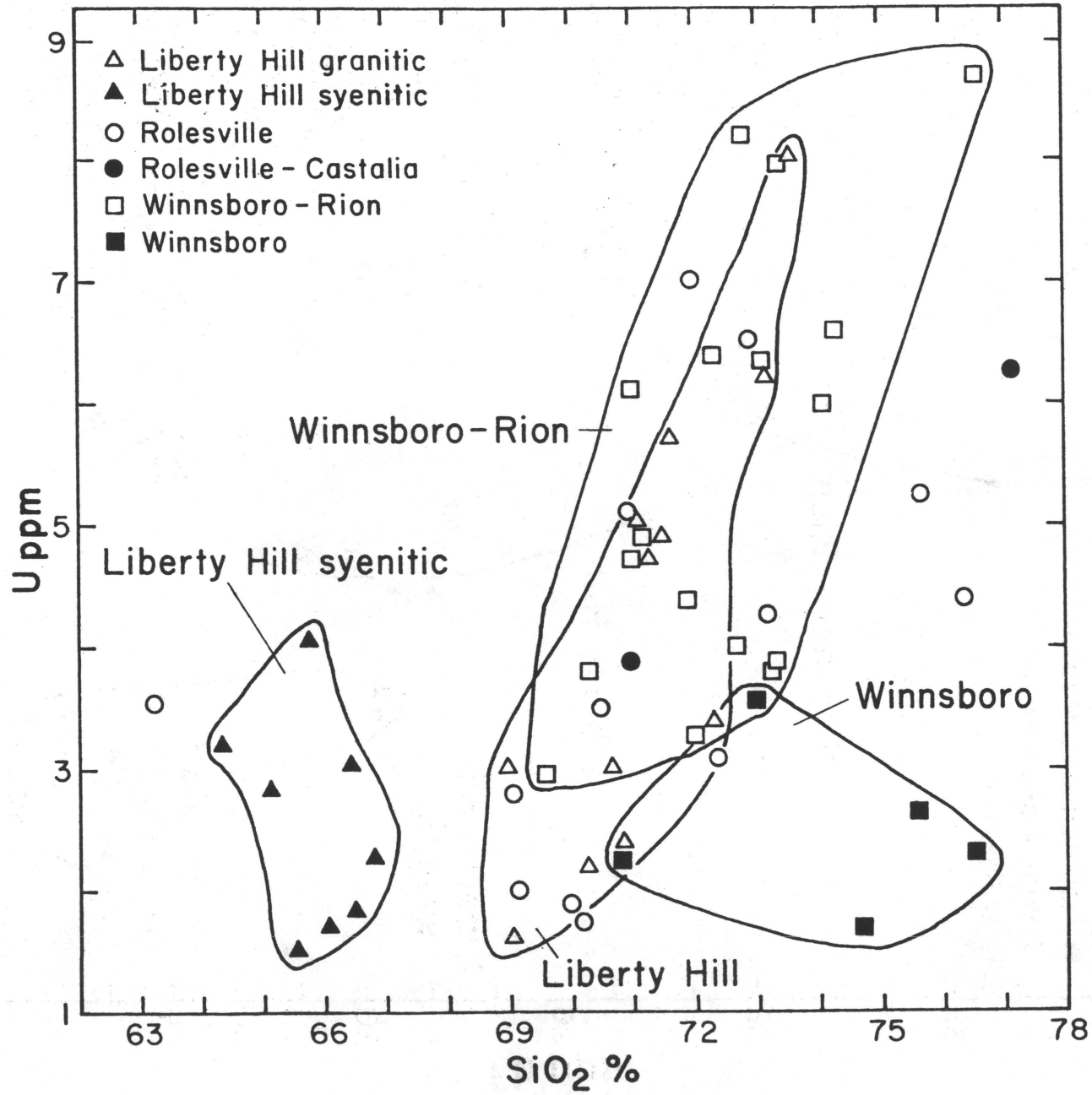


Figure B-1

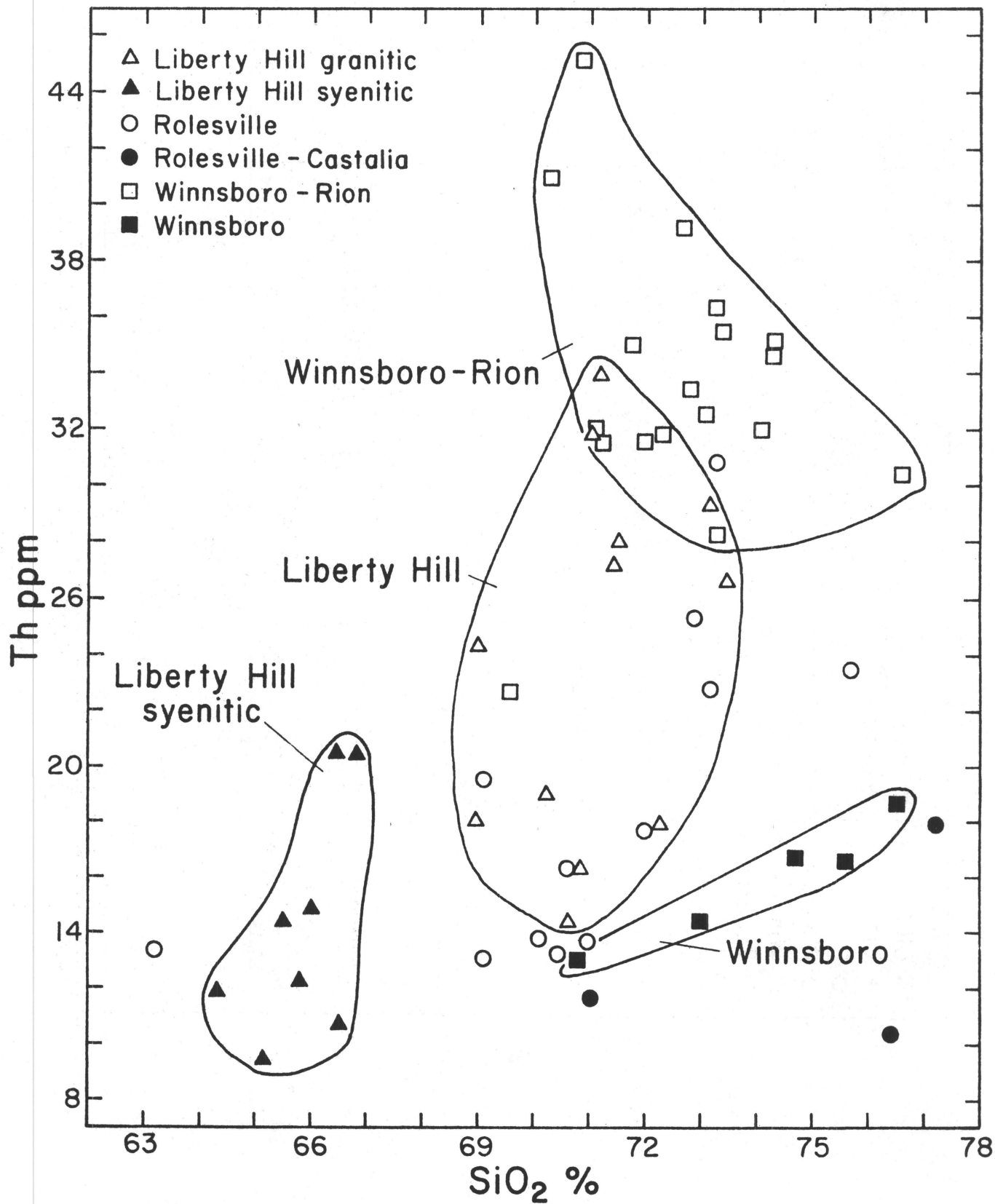


Figure B-2

group (see geophysics section, this report). Contrary to what would be expected, the U and Th contents of Rolesville samples are no higher for a given SiO_2 value than those of the Liberty Hill granites or the Rion pluton of the Winnsboro complex. Winnsboro granite can be seen to be relatively low in both U and Th. This could be an indication of U and Th loss from both the Rolesville batholith and the Winnsboro granite. As discussed in the section on Liberty Hill core data, some U loss has occurred even at depth in Liberty Hill, so loss from all surface samples can be expected.

Liberty Hill Bore Holes

Three cores have been obtained from Liberty Hill pluton. These holes, known as Kershaw 1, 2 and 3 are shown as Ker 1, 2 and 3 on Fig. A-3 in the petrology section of this report. The holes are about 50 m, 105 m, and 400 m deep, respectively.

The Liberty Hill surface samples have been divided into coarse-grained syenitic and fine- to coarse-grained granitic groups on the basis of normative compositions (report VPI&SU-5103-2). Ker 1 and Ker 3 have been drilled into fine-grained granite and Ker 2 into coarse-grained granite.

Three meter lengths of core were used as samples, the core being chipped and homogenized before splitting into portions for heat production determination for geochemical analysis. The geochemical data is given in Table B-2. Fig. B-3 shows SiO_2 , FeO, U and Th variation with depth with the ranges of elemental abundances in the surface samples given for comparison. The variations of MgO, MnO, P_2O_5 and TiO_2 with depth are similar in form to that of FeO. Na_2O and CaO contents have the same ranges as the surface samples except for the Ker 3 sample from 204 m depth which is highly altered and has low Na_2O and high CaO. The K_2O and Al_2O_3 ranges are the same as those of the surface samples. It can be seen from the Ker 2 and Ker 3 data that no regular changes in composition with depth occur.

C.I.P.W. norms were calculated and, comparing the normative and chemical compositions of the core samples with the granitic and syenitic surface samples, the cores could be classified as follows. The one

Table B-2. Chemical compositions of Kershaw core samples.

Depth,m	Ker 1 41-44	Ker 2 0.5-3.3	Ker 2 16-18	Ker 2 36-39	Ker 2 59-62	Ker 2 102-105	Ker 3 22-25	Ker 3 55-58	Ker 3 87-90	Ker 3 117-120
SiO ₂	73.82	66.79	65.92	66.09	65.95	66.80	71.73	70.01	63.00	68.48
Al ₂ O ₃	14.37	15.98	16.18	16.08	15.94	16.14	15.41	15.51	16.50	15.87
CaO	1.38	2.46	2.58	2.53	2.68	2.38	1.50	1.69	3.11	2.10
MgO	0.49	0.92	0.96	0.96	1.04	0.92	0.48	0.53	1.17	0.78
K ₂ O	5.27	5.06	4.87	5.01	4.82	5.32	5.49	5.48	4.63	5.36
FeO	1.91	3.24	3.32	3.32	3.47	3.07	2.05	2.62	4.37	2.69
Na ₂ O	3.72	4.07	4.20	4.02	4.02	4.01	3.80	3.81	4.26	3.91
MnO	0.05	0.06	0.07	0.06	0.07	0.06	0.04	0.05	0.08	0.06
TiO ₂	0.29	0.59	0.60	0.60	0.66	0.56	0.29	0.41	0.77	0.45
P ₂ O ₅	0.08	0.20	0.21	0.21	0.23	0.19	0.12	0.17	0.28	0.16
TOTAL	101.38	99.37	98.91	98.88	98.88	99.45	100.91	100.28	98.17	99.86

Table B-2 (continued).

Depth,m	Ker 3 162-165	Ker 3 204-207	Ker 3 241-244	Ker 3 282-285	Ker 3 338-341	Ker 3 354-357	Ker 3 369-372	Ker 3 384-387	Ker 3 397-401
SiO ₂	64.42	64.16	70.49	74.62	69.41	68.46	69.32	65.79	65.61
Al ₂ O ₃	16.46	15.05	15.05	15.11	15.42	15.73	15.32	16.07	15.90
CaO	2.83	5.41	1.90	1.14	1.97	2.05	2.06	2.49	2.58
MgO	1.09	0.66	0.70	0.25	0.76	0.75	0.78	0.93	0.98
K ₂ O	4.90	5.18	5.29	5.25	5.39	5.45	5.20	5.26	5.02
FeO	3.86	2.92	2.59	1.13	2.72	2.78	2.84	3.58	3.65
Na ₂ O	4.18	2.00	3.68	4.14	3.83	3.90	3.84	4.00	3.95
MnO	0.08	0.07	0.06	0.04	0.05	0.05	0.05	0.07	0.07
TiO ₂	0.67	0.52	0.45	0.11	0.48	0.49	0.51	0.65	0.70
P ₂ O ₅	0.24	0.18	0.15	0.03	0.16	0.17	0.18	0.23	0.25
TOTAL	98.73	96.15	100.36	101.82	100.19	99.83	100.10	99.07	98.71

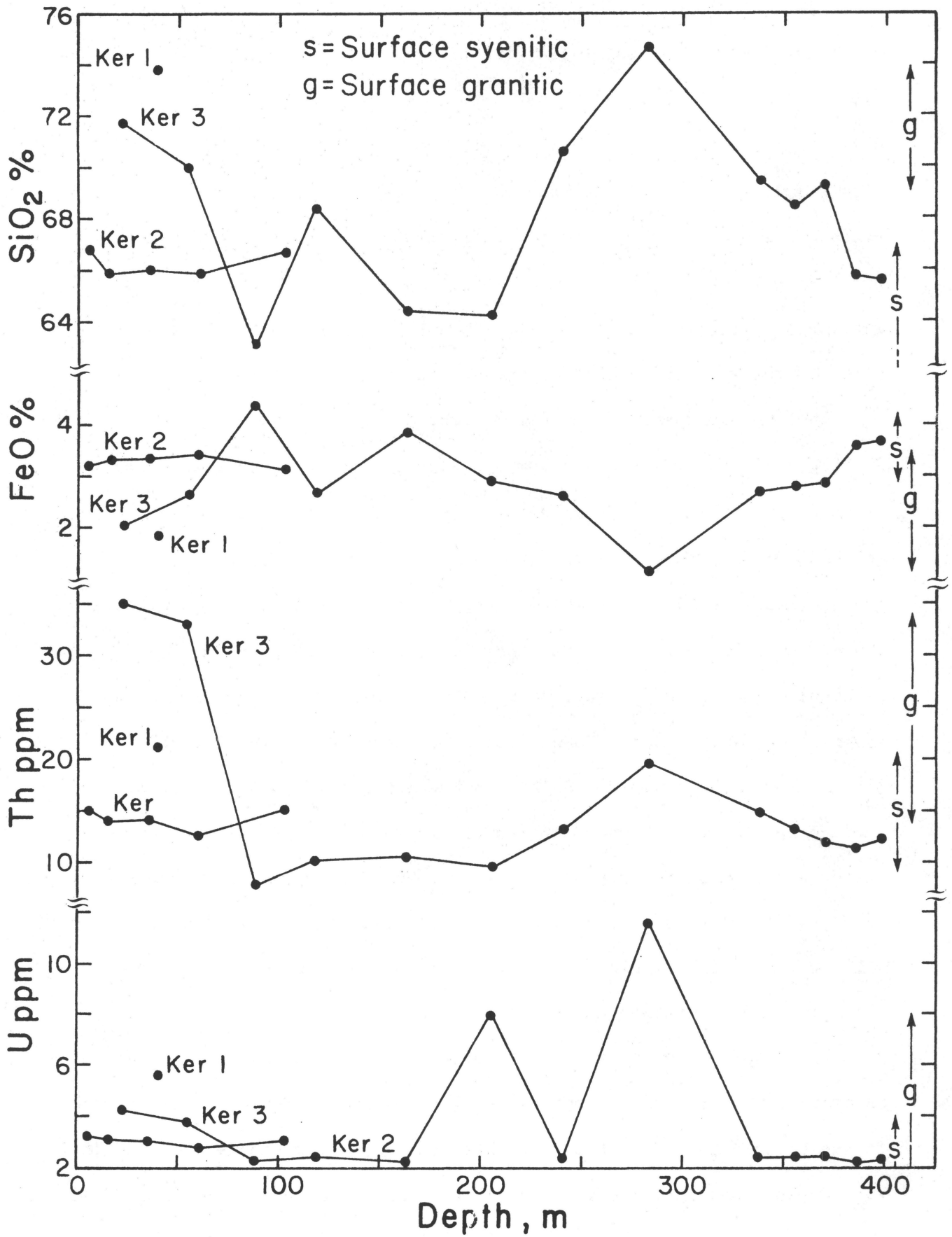


Figure B-3

sample from Ker 1 is comparable with the granitic surface samples and plots with them on AFM and Qz-Ab-An-Or diagrams. Ker 2 appears to be drilled in the area characterized by coarse-grained granites, but all five samples from this hole compare more closely with the syenitic surface samples. The SiO_2 contents of the Ker 2 samples, for example, range from about 65-67% while the surface syenitic samples have 64-67% and the granitic surface samples 69 to 73% SiO_2 . Ker 2 is located quite close to the area where surface syenitic samples were found.

The top two samples from Ker 3, from depth intervals 22-25 m and 55-58 m, are fine grained and compare closely with the fine- and coarse-grained granitic surface samples, falling in the same areas on AFM and Qz-Ab-An-Or diagrams. However, the next four deeper samples are coarse grained and resemble the syenitic samples more closely than the granitic. The sixth sample down, as mentioned above, from depth interval 204-207 m is highly altered and in many respects its chemistry is anomalous. The seventh and ninth samples down, from depth intervals 241-244 m and 338-341 m, are coarse grained and fall in between the syenitic and granitic surface samples on AFM and Qz-Ab-An-Or diagrams. The sample in between these two, from depth interval 282-285 m, is fine grained and granitic in character. It is very distinct from the two closest samples, plotting well away from the syenitic surface samples. The four deepest samples are again coarse grained and syenitic in character.

The U and Th contents of both surface and core samples have been determined by γ -ray spectrometry (see geophysics section of this report). It can be seen from Fig. B-3 that there is no regular change in U and Th with depth. Any increase in U and Th with depth, which might be expected

to arise due to the removal of U and Th by surface weathering, could be masked by the inhomogeneity of the core material.

In general, both U and Th increase in concentration with increasing differentiation and this shows up as increases in U and Th with increasing SiO_2 and, for example, decreasing TiO_2 , P_2O_5 and normative orthoclase. Since K_2O in these samples does not increase with degree of differentiation, K_2O vs U and Th plots do not define strong trends. Fig. B-4 shows TiO_2 plotted versus U. TiO_2 was chosen for this plot since it is considered to be one of the less mobile elements. As well as the overall negative correlation between the two elements, it can be seen that the surface samples fall into clear groups, one of syenitic and the other of coarse- and fine-grained granites. The core samples, numbered in order of increasing depth, can again be seen to be mainly syenitic in character with the exception of the Ker 1 sample, the top two Ker 3 samples and the eighth Ker 3 sample which again are granitic in character.

The Th/U ratios of the Liberty Hill samples, together with those from the Winnsboro pluton and Rolesville batholith, are plotted versus SiO_2 on Fig. B-5. Increase in Th/U with increasing SiO_2 has been attributed by several authors, for example, Rogers and Ragland (1961), to loss of U during the later stages of differentiation due to oxidation and removal in a fluid phase. However, the Th/U ratio might decrease with increasing SiO_2 content if the granites were formed by partial melting. Nagasawa and Wakita (1968) have suggested that Th is enriched over U in the first melt phase during partial melting.

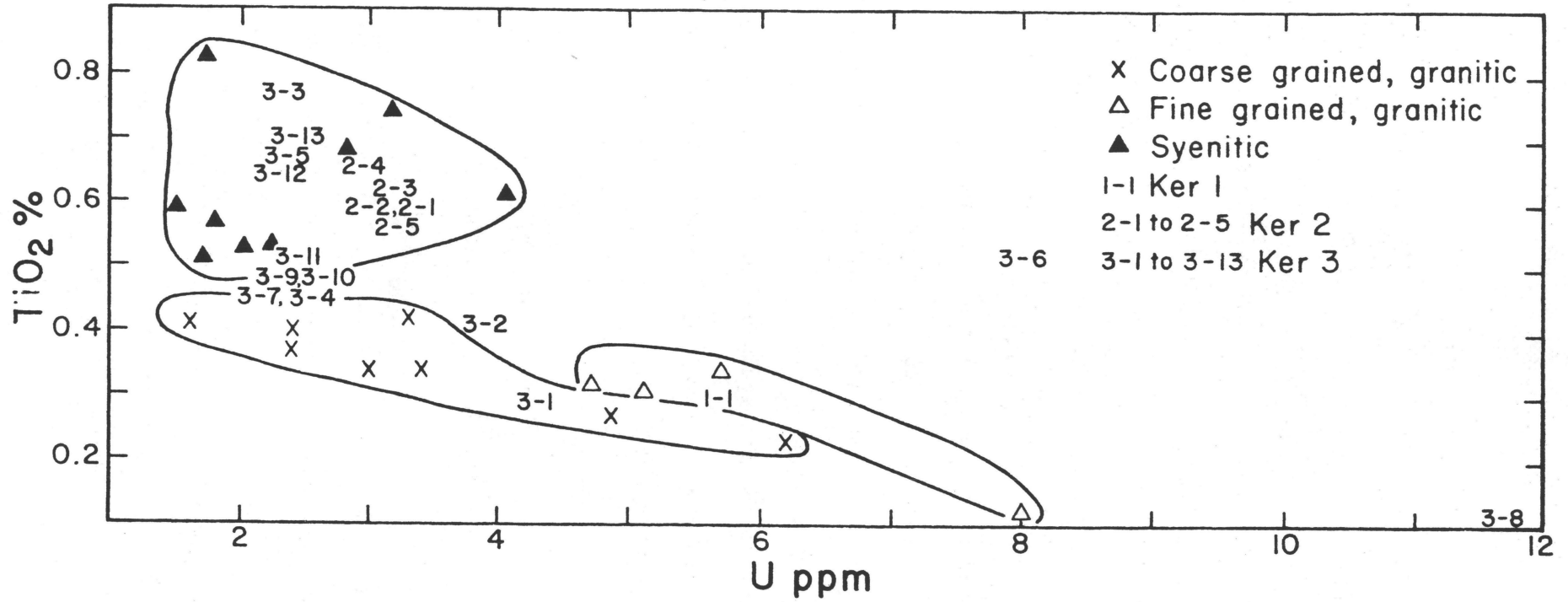


Figure B-4

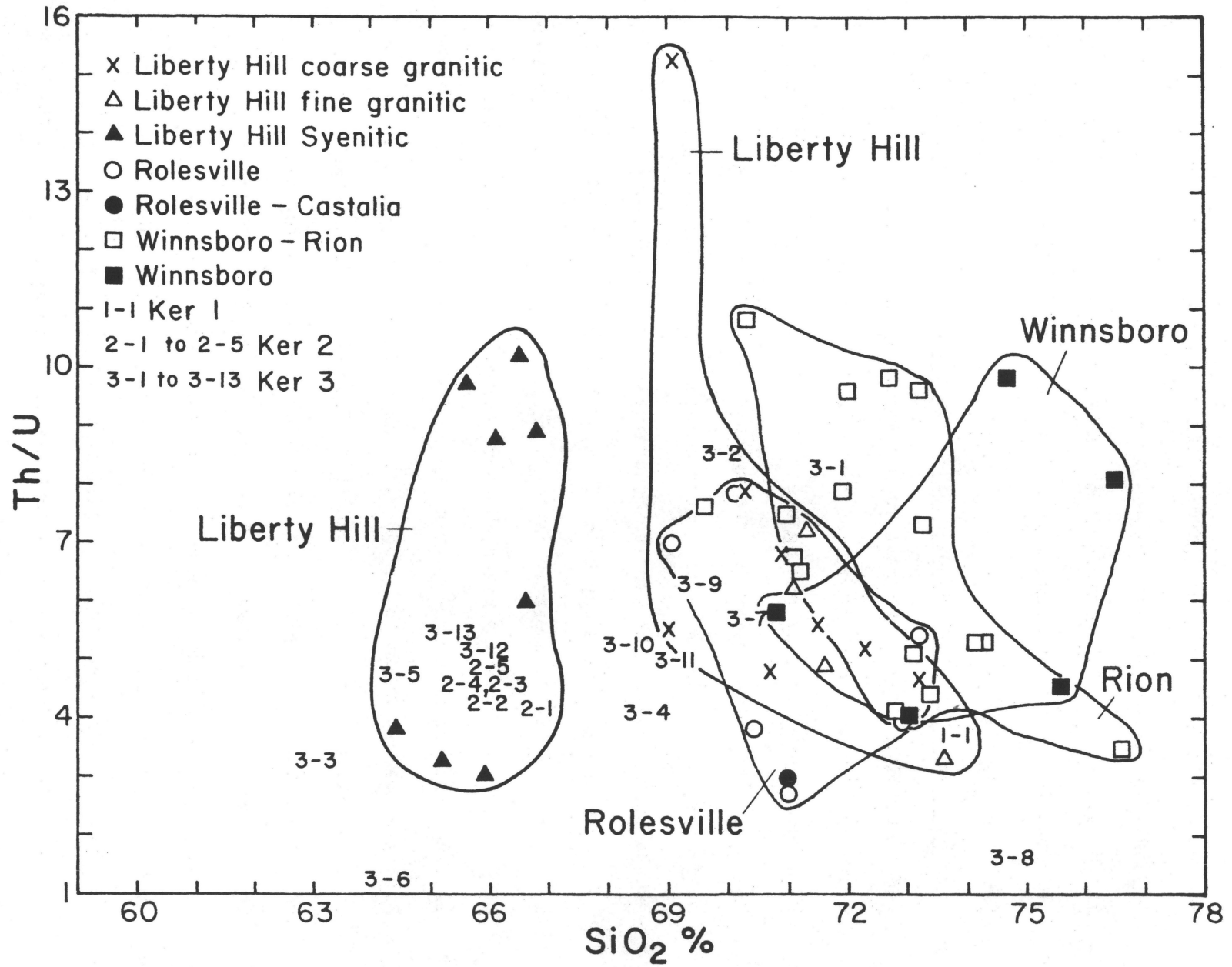


Figure B-5

Hence, a small melt fraction would have higher Th/U than a larger one. Our data, Fig. B-5, does not give strong support to either hypothesis but, as will be demonstrated below, loss of differing proportions of the original U and Th contents of the samples has probably occurred, so measured Th/U ratios no longer reflect those at the time of formation of the granites.

Uranium, Thorium, Lead Disequilibrium Study. If loss of U or Th has occurred in the recent past from a sample of known age, then the U and Th contents before the loss can be calculated by use of U, Th, Pb systematics. This is making use of the U, Th, Pb dating method in reverse, the unknown being not the age of the rock body but the "true" present-day U and Th contents. Such a method has been applied by Rosholt and Bartel (1969) to the Granite Mountains granite in Wyoming.

Four samples, from depths of 22 m, 241 m, 282 m and 397 m in Ker 3, were analyzed for Pb isotopic ratios and concentrations by mass spectrometry. Feldspar separated from another portion of the 397 m sample was also analyzed to determine initial Pb ratios. The age of the Liberty Hill granite was taken to be 300 m.y., as determined by Fullagar (1971) by the Rb-Sr method. It was found that from 0% to 55% of the U has been lost from the samples, the proportion lost decreasing with increasing depth. Th loss was from about 50% to 80%. Of the two syenitic samples, from 241 m and 397 m, the deeper has lost a lower proportion of its Th than the upper and similarly for the two granitic samples, from 22 m and 282 m. Considering all four samples together, however, the one from 394 m has lost a higher proportion of its Th than the sample from 282 m. Although these results are of a preliminary

nature, they illustrate two important points. Firstly, loss of substantial amounts of both U and Th has occurred, and this loss has not been only from the surface samples. In general, the proportion of U and Th lost appears to decrease with increasing depth, but about half of the Th has been lost at depths as great as 400 m. Secondly, higher proportions of Th than of U have been lost from all four samples. U is usually considered to be more easily removed than Th since it can be oxidized to a water soluble cation whereas Th cannot. Rosholt and Bartel (1969) found that there had been little or no loss of Th from the Granite Mountains granite while substantial amounts of U had been lost. In studying a weathering profile on a granite, Pliler and Adams (1962) found that 25% of the Th content and 60% of U were lost during the first stages of weathering. However, in laboratory acid leaching experiments on the same granite, Pliler and Adams found that 90% of the Th and only 67% of U were readily leacheable. This is in agreement with the findings of Tilton et al. (1955) who concluded from laboratory leaching experiments on a granite that "a substantial fraction of the uranium and even larger fractions of thorium...were found to exist in chemically unstable environments in the rock." It seems then that Th is potentially removable from granites and that the relative proportions of U and Th removed could be strongly influenced by prevailing conditions, such as pH.

References

- Fullagar, P. D., 1971, Age and origin of plutonic intrusions in the Piedmont of the southern Appalachians: *Geol. Soc. America Bull.* 82, p. 2845-2862.
- Luth, W. C., 1969, The systems $\text{NaAlSi}_3\text{O}_8\text{-SiO}_2$ and $\text{KAlSi}_3\text{O}_8\text{-SiO}_2$ to 20 kb and the relationships between H_2O content, P_{water} and P_{total} in granitic magma: *Am. Jour. Sci.* 267-A, p. 325-341.
- _____, R. H. Jahns, and O. F. Tuttle, 1964, The granite system at pressures of 4 to 10 kilobars: *Jour. Geophys. Res.* 69, p. 759-773.
- Nagasawa, H. and H. Wakita, 1968, Partition of uranium and thorium between augite and host lavas: *Geochim. Cosmochim. Acta* 32, p. 917.
- Pliler, R. and J. A. S. Adams, 1962, The distribution of thorium and uranium in a Pennsylvania weathering profile: *Geochim. Cosmochim. Acta* 26, p. 1137-1146.
- Rogers, J. J. W. and P. C. Ragland, 1961, Variation of thorium and uranium in selected granitic rocks: *Geochim. Cosmochim. Acta* 25, p. 99-109.
- Rosholt, J. N. and A. J. Bartel, 1969, Uranium, thorium and lead systematics in Granite Mountains, Wyoming: *Earth Planet. Sci. Letters* 7, p. 141-147.
- Steiner, J. C., R. H. Jahns, and W. C. Luth, 1975, Crystallization of alkali feldspar and quartz in the Haplogranite system $\text{NaAlSi}_3\text{O}_8\text{-KAlSi}_3\text{O}_8\text{-SiO}_2\text{-H}_2\text{O}$ at 4 kb: *Geol. Soc. America Bull.* 86, p. 83-98.
- Streckeisen, A., 1976, Classification of the common igneous rocks by means of their chemical composition; a provisional attempt: *N. Jb. Miner. Mh.* H. 1, p. 1-15.
- Tilling, R. I. and D. Gottfried, 1969, Distribution of thorium, uranium and potassium in the igneous rocks of the Boulder batholith region, Montana, and its bearing on radiogenic heat production and heat flow: *U. S. Geol. Survey Prof. Paper* 614-E, p. E1-E29.
- Tilton, G. R., C. Patterson, H. Brown, M. Inghram, R. Hayden, D. Hess, and E. Larsen, 1955, Isotopic composition and distribution of lead, uranium and thorium in a Precambrian granite. *Geol. Soc. Am. Bull.* 66, p. 1131-1148.

C. Geophysics

J. K. Costain, Principal Investigator

C. S. Rohrer, Research Specialist

J. A. Dunbar, Graduate Research Assistant

Geothermal Gradients and Heat Generation

C. S. Rohrer and J. K. Costain

An equilibrium temperature log was obtained from DDH KER-3 drilled into the Liberty Hill-Kershaw pluton in Lancaster County, S. C. Drilling was completed on November 1, 1976. In order to evaluate the transient thermal effects of drilling on the geothermal gradient, temperature logs were obtained over a period of several months. Temperature profiles and gradients are shown in Fig. C-1. Geothermal gradients are tabulated in Table C-1. Transient thermal effects of drilling are evident several months after the cessation of drilling; however, the gradient of $14.6^{\circ}\text{C}/\text{Km}$ obtained on March 3, 1977 (Fig. C-2) is essentially an equilibrium gradient, and a reliable heat flow determination will be obtained from this hole after thermal conductivity determinations have been completed.

Preliminary temperature logs have been obtained from DDH WIN-1 in the Winnsboro pluton in Fairfield County, S. C. and from DDH ROX-1 in Person County, N. C. These holes have not yet reached thermal equilibrium, and reliable gradients for heat flow determinations will not be available for several weeks.

Wells logged for temperature in the Coastal Plain during the present report period are listed in Table C-2 and shown in Fig. C-3. Locations of wells are shown in Figs. C-5, C-6, and C-7. A map of the mean annual surface air temperature was prepared from meteorological data (U. S. Dept. of Commerce, 1973) for the State of Virginia (Fig. C-8). Similar maps for North Carolina and South Carolina are in

Table C-1. Geothermal gradients in KER-3 and WIN-1.

	Nov. 19, 1976	Dec. 19, 1976	Jan. 26, 1977	% change from Nov. 19
KER-3	14.6°C/Km	14.8°C/Km	14.9°C/Km	+2.05
WIN-1	--	--	18.4°C/Km	

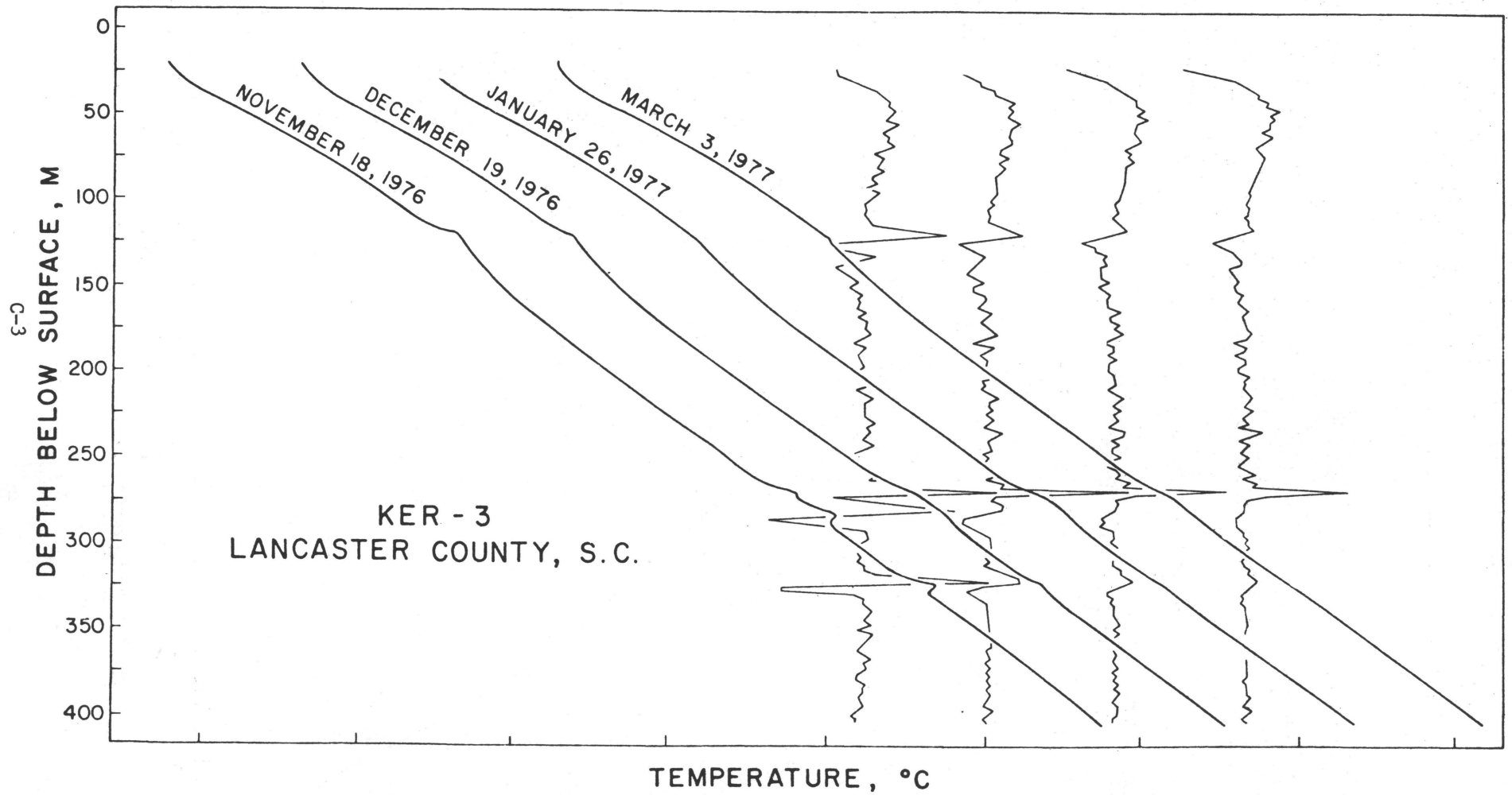


Fig. C-1. Comparison of temperature and gradient logs over a four-month period for KER-3.

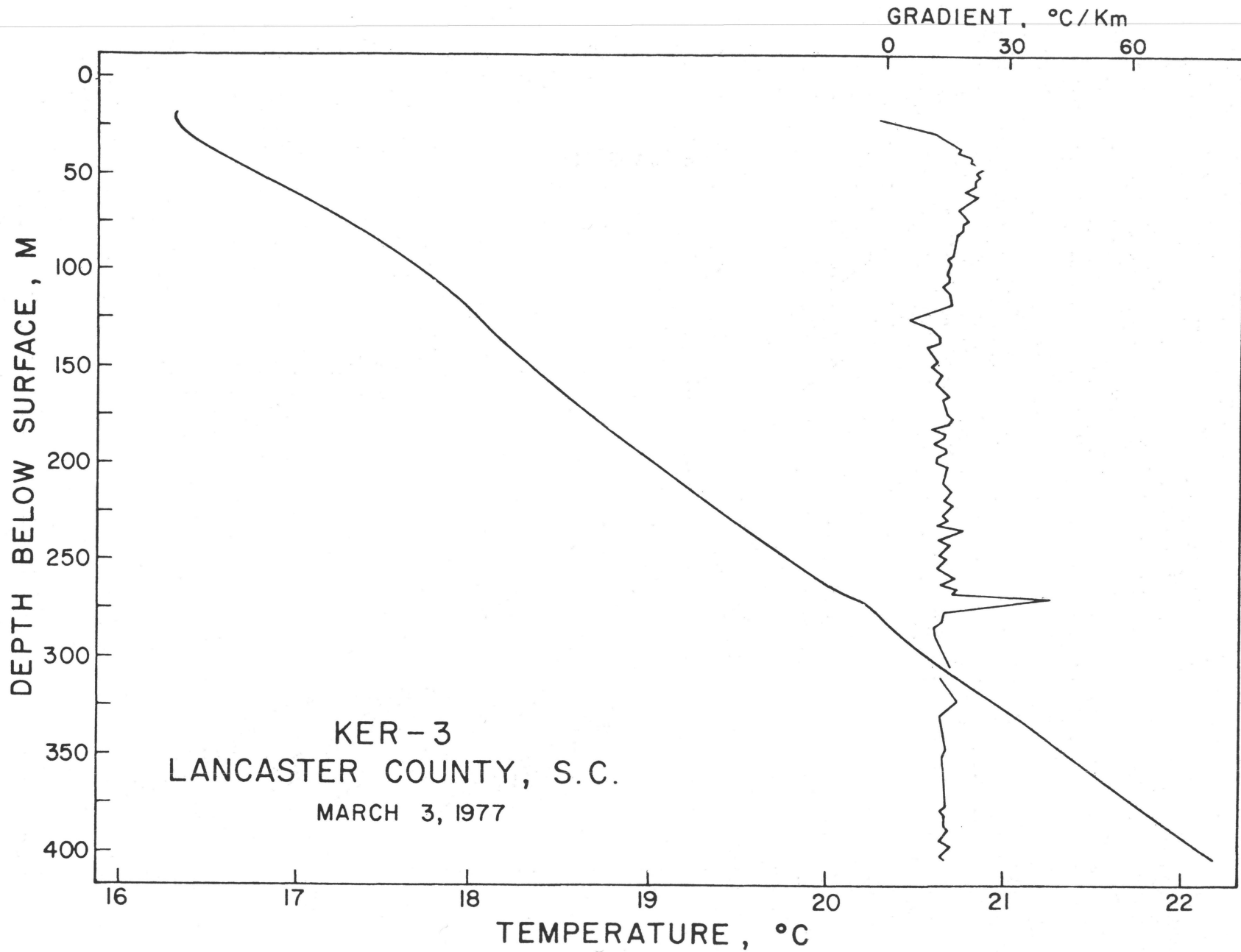


Fig. C-2. Temperature and gradient logs for KER-3, March 3, 1977.

Table C-2. Data pertaining to wells logged during present report period.

Well No.	Latitude	Longitude	State	Bottomhole temp., °C	Well depth, meters	Average surface temp., °C	Average gradient, °C/Km
161-4	36°46'35"	76°32'32"	VA	19.8	148	15.5	29.4
161-42	36°34'08"	76°35'00"	VA	22.1	251	15.5	26.3
161-47	36°35'11"	76°49'29"	VA	23.3	283	15.5	27.5
161-76	36°36'00"	76°54'30"	VA	19.6	306	15.5	13.5
TWSE77-3	36°47'00"	76°24'30"	VA	24.7	277	15.5	33.2
61C2	36°52'21"	76°12'13"	VA	25.1	296	15.5	32.4
61C3	36°52'21"	76°12'13"	VA	24.8	294	15.5	31.7
GEO-88	33°15'01"	79°15'14"	SC	31.5	389	18.4	33.7
KER-3	34°32'20"	80°44'51"	SC	22.2	405	16.3	14.6
WIN-1	34°18'48"	81°08'42"	SC	26.7	574	16.6	17.6
ROX-1	36°23'12"	78°58'00"	NC	17.0	257	15.1	7.4

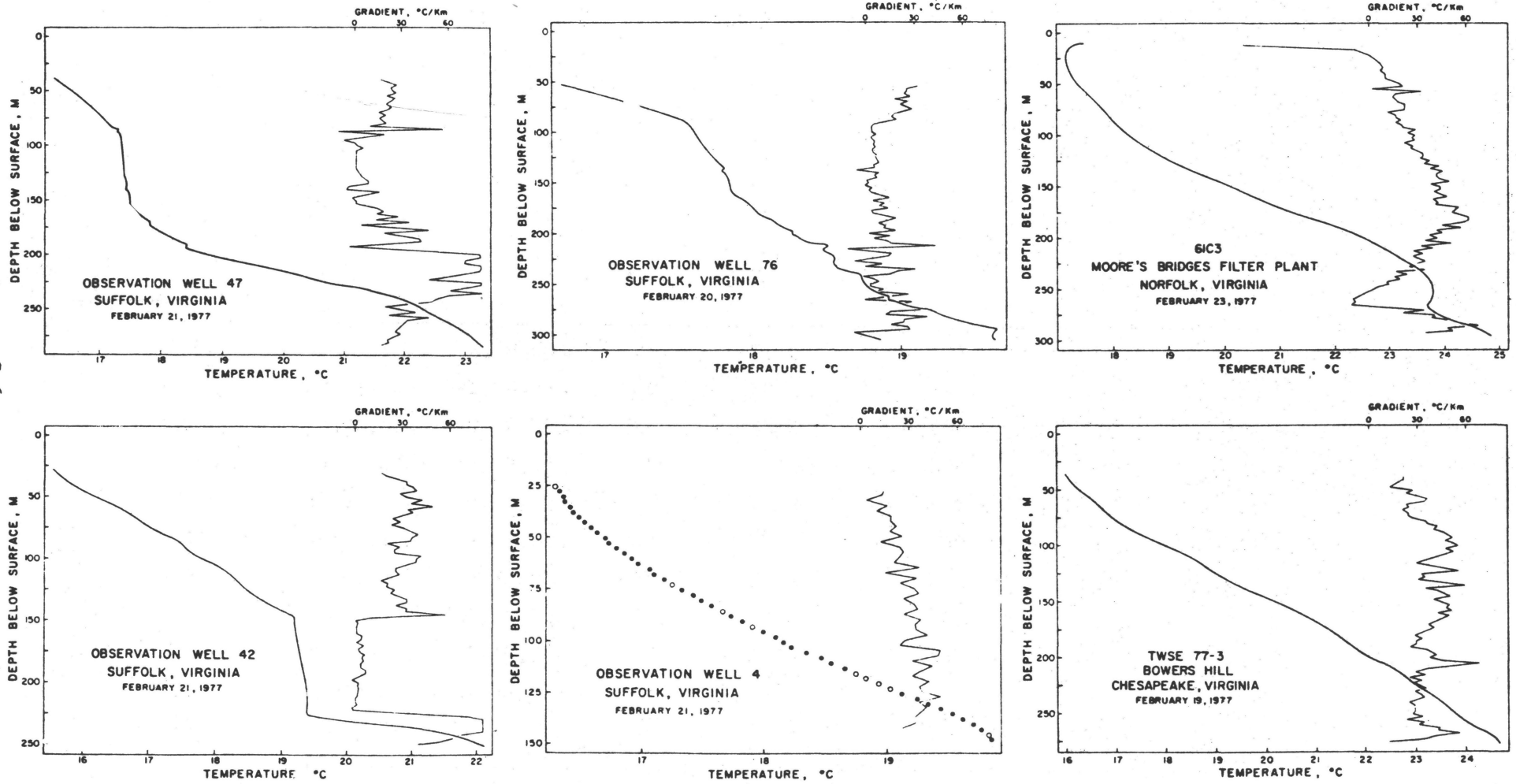


Fig. C-3. Temperature and gradient logs for wells logged during present report period.

C-7

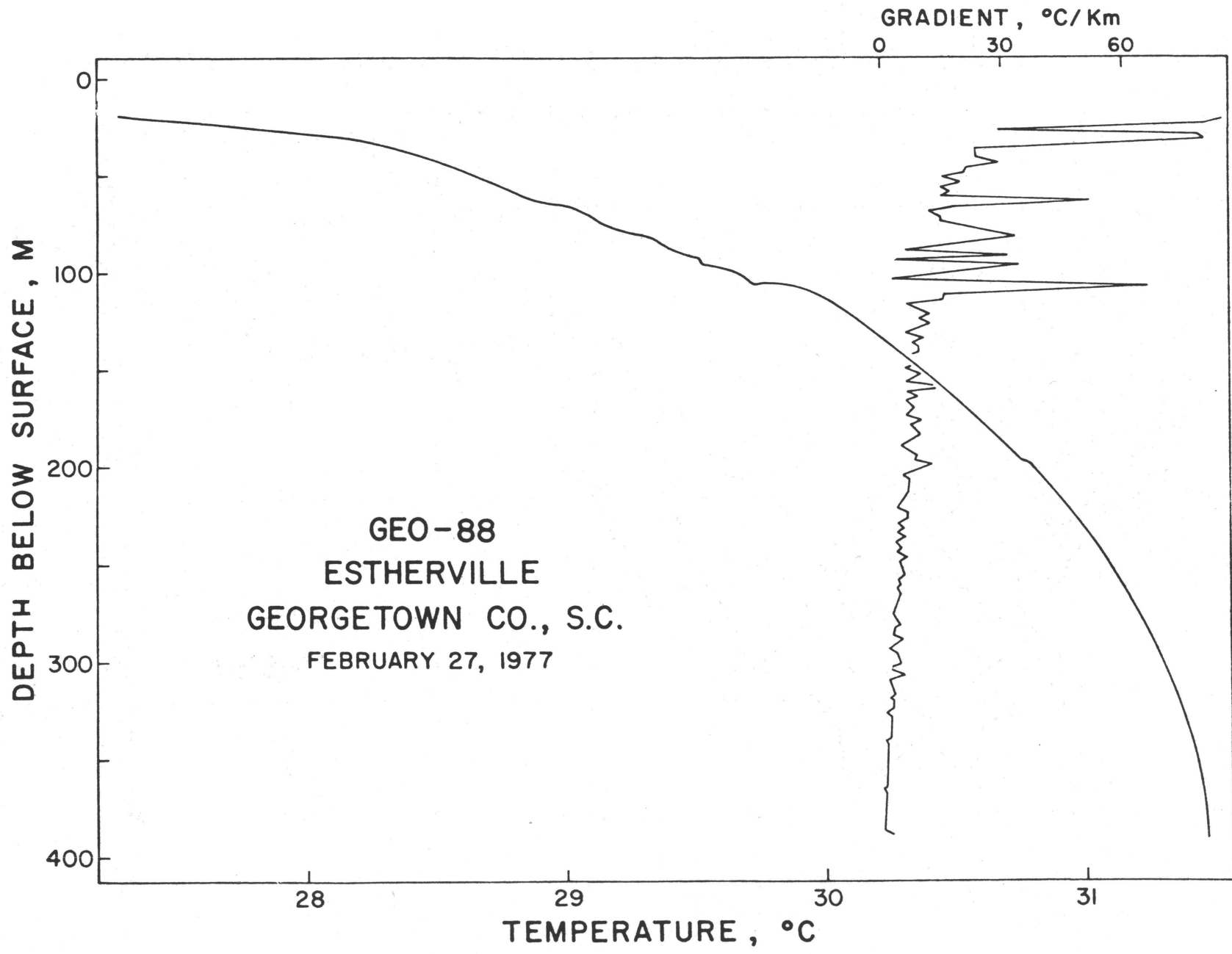


Fig. C-4. Temperature and gradient log for GEO-88 (an uncemented well), February 27, 1977.

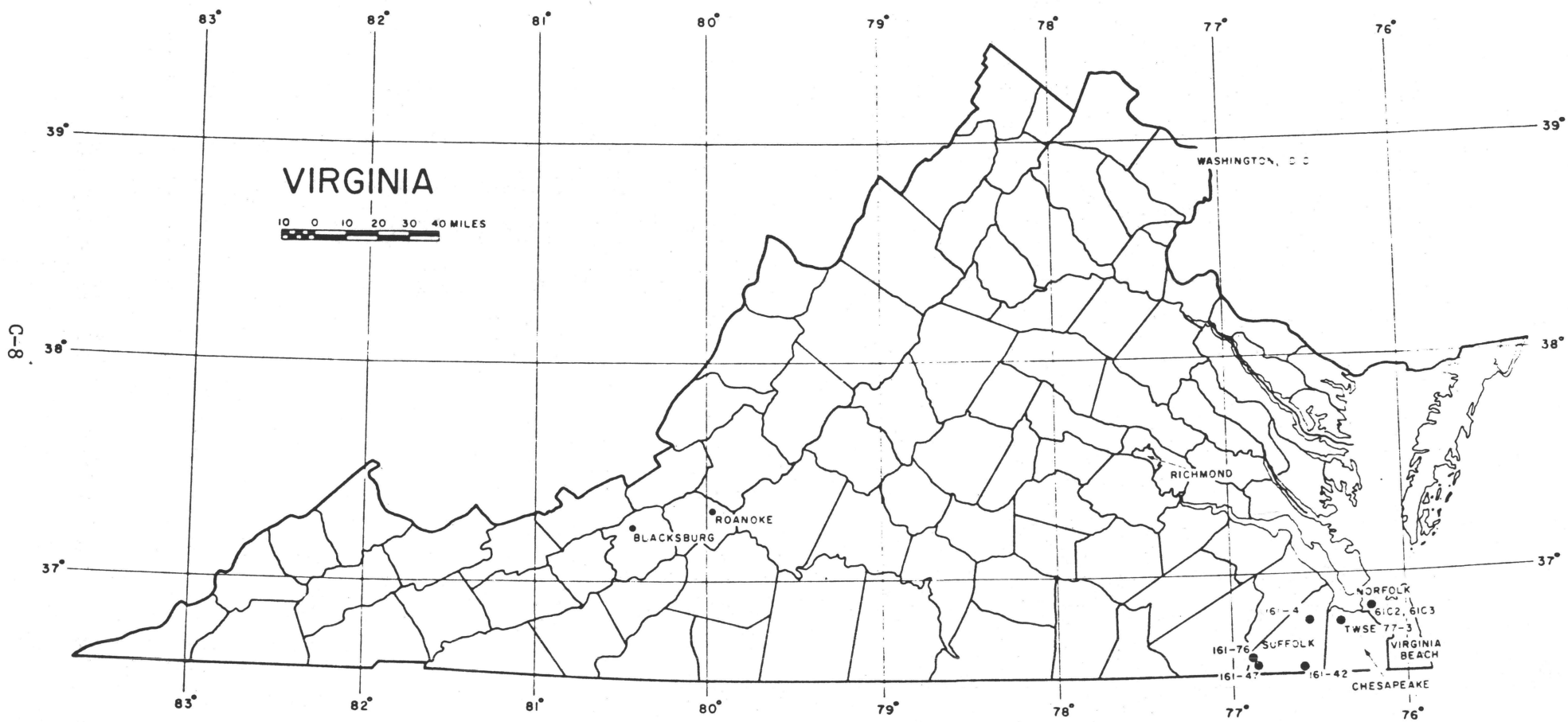


Fig. C-5. Wells logged in Virginia during present report period.

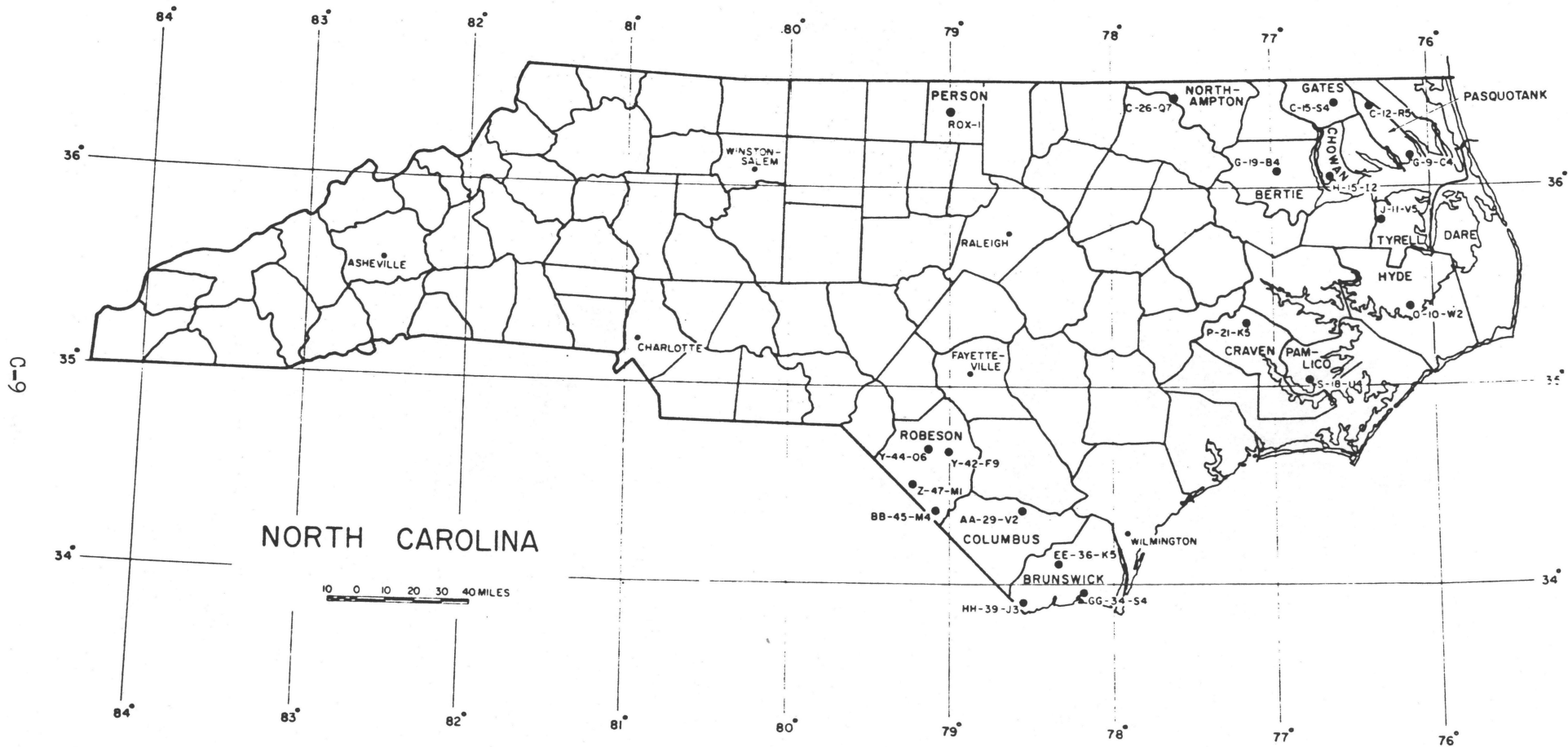


Fig. C-6. Wells logged in North Carolina up to and including this report period.



Fig. C-7. Wells logged in South Carolina up to and including this report period.

C-11

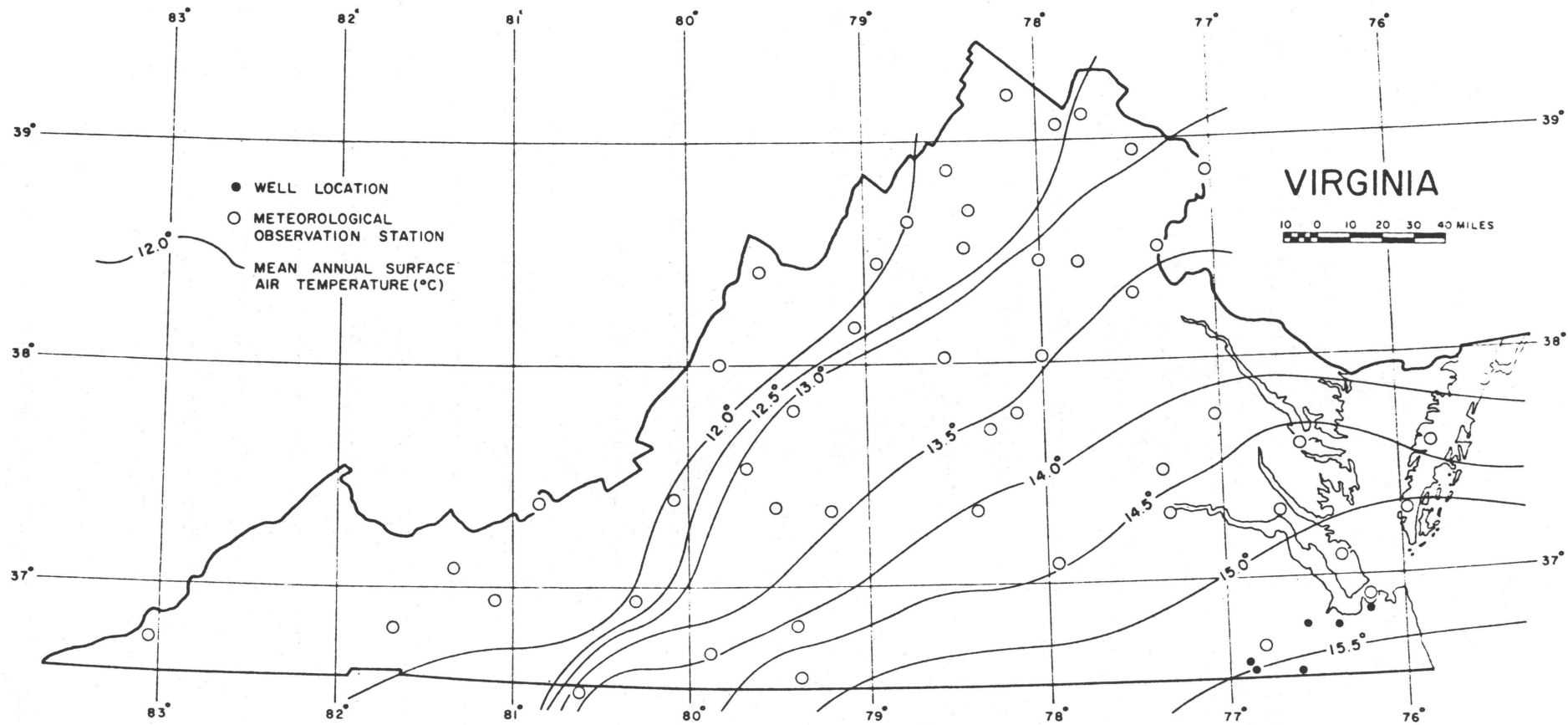


Fig. C-8. Contour map of mean annual surface air temperature.

Progress Report VPI&SU-5103-2. From maps of mean annual surface air temperature and from bottomhole temperatures in wells, average thermal gradients in Coastal Plain sediments were determined. The geothermal gradients are listed in Table C-2. It is apparent from Figs. C-3 and C-4 that the temperature gradients in most of the wells penetrating Coastal Plain sediments are disturbed by groundwater circulation between confined and semi-confined aquifers. For this reason, we need additional data from cemented wells.

Heat generation in surface samples and in drill core was determined at VPI & SU using gamma-ray spectroscopy. Sample weights of 600 grams of crushed rock were used. Values of heat production obtained during this report period are given in Tables C-3, C-4, C-5, and A-8 and are discussed here and elsewhere in this report.

Assuming a linear relationship between heat flow and surface heat production in buried igneous rocks of the form

$$q = q_0 + DA$$

where $q_0 = 0.8 \times 10^{-6}$ cal/cm²-sec and $D = 7.5 \times 10^5$ cm (Report VPI&SU-5103-2), we can expect thermal gradients of approximately 40°C/Km in an overlying sedimentary insulator with a thermal conductivity of 4.5 mcal/cm-sec-°C (VPI&SU-5103-1, p. 9). Higher gradients will be obtained for lower values of thermal conductivity or higher values of heat generation. The heat flow near Charleston, S. C. as determined by the U. S. Geological Survey (USGS Open File Report 76-148) from the Clubhouse Crossroads Core Hole No. 1 drilled into Coastal Plain sediments is 1.2 HFU (1 HFU = 10^{-6} cal/cm²-sec). The average value of thermal conductivity within the sedimentary section was found to be

Table C-3. Heat generation values for surface samples from the Liberty Hill pluton, SC.

Location	Sample No.	Density, gm/cm ³	Uranium (U), ppm	Thorium (Th), ppm	Potassium (K), %	K ₂ O, %	Heat generation, A x 10 ⁻¹³ cal/cm ³ -sec
<u>Coarse-grained rocks</u>							
Liberty Hill pluton, S. C.	S6-47	2.63	3.3	18.04	4.39	5.27	6.0
	S6-54 **	2.64	3.0	14.5	4.5	5.40	5.2
	S6-56 **	2.66	1.8	10.8	4.3	5.16	3.9
	S6-58	2.58	3.43	17.82	4.31	5.17	5.91
	S6-65 **	2.65	2.4	18.9	4.8	5.76	5.74
	S6-69 **	2.66	1.5	14.6	4.4	5.28	4.4
	S6-71 **	2.61	6.2	29.2	4.3	5.16	9.6
	S6-74	2.63	4.88	27.17	4.41	5.29	8.49
	S6-86 **	2.65	1.6	24.4	4.5	5.40	6.1
	S6-88	2.67	2.02	20.62	4.33	5.20	5.73
	S6-89*	2.65	1.7	15.0	4.2	5.04	4.6
	S6-90	2.64	2.26	20.17	4.16	4.99	5.7
	S6-108	2.66	1.72	8.89	5.45	6.54	3.8
	S6-110**	2.64	2.4	16.3	4.5	5.40	5.2
	S6-135	2.66	4.06	12.32	4.03	4.84	5.49
F6-24	2.69	2.83	9.54	3.63	4.36	4.22	
F6-25	2.68 (2.65)***	3.17	11.99	4.0	4.80	4.92	
<u>Fine-grained rocks</u>							
Liberty Hill pluton, S. C.	S6-57	2.63	5.13	31.89	4.25	5.10	9.40
	S6-99**	2.61	2.6	23.0	4.6	5.52	6.5
	S6-100	2.64	5.70	23.02	4.19	5.03	9.12

Table C-3 (continued).

Location	Sample No.	Density, gm/cm ³	Uranium (U), ppm	Thorium (Th), ppm	Potassium (K), %	K ₂ O, %	Heat generation, A × 10 ⁻¹³ cal/cm -sec
<u>Fine-grained rocks (cont.)</u>							
	S6-101*	2.61	8.0	26.5	3.9	4.68	10.1
	S6-111*	2.64 (2.63)***	4.7	34.0	4.2	5.04	9.5
<u>Aplite</u>							
Liberty Hill pluton, S. C.	S6-51	2.59	6.45	33.81	4.90	5.88	10.5

* Denotes analysis by U. S. Geological Survey, Denver, Colorado.

** Denotes analysis by University of Wyoming, Laramie, Wyoming.

***Average value for group.

Table C-4. Heat generation values for surface samples from the Winnsboro, SC pluton.

Location	Sample No.	Density, gm/cm ³	Uranium (U), ppm	Thorium (Th), ppm	Potassium (K), %	K ₂ O, %	Heat generation, A x 10 ⁻¹³ cal/cm ³ -sec
Winnsboro pluton, S. C.	S6-2	2.61	2.79	12.67	4.16	4.99	4.71
	S6-16	2.60	2.65	16.64	4.68	5.62	5.38
	S6-24	2.61	4.90	17.99	4.16	4.99	6.86
	S6-25	2.58	1.51	12.12	4.36	5.23	3.85
	S6-26	2.62	2.32	18.71	4.44	5.33	5.50
	S6-27	2.67	2.24	13.01	3.93	4.72	4.48
	S6-29	2.65	3.56	14.44	4.33	5.17	5.59
	S6-43**	2.57	2.0	17.2	4.3	5.16	4.91
	F6-23	2.63	2.76	10.94	4.25	5.10	4.45
	F6-30	2.62	2.04	21.25	4.62	5.54	5.80
	F6-66	2.62	2.20	7.92	4.01	4.81	3.54
	S6-14**	2.61 (2.62)***	1.7	16.7	4.1	4.92	4.7
Winnsboro pluton, S. C.	S6-18**	2.71	4.0	15.5	3.0	3.60	5.9
	S6-20	2.69	4.88	13.90	3.21	3.85	6.1
	S6-22	2.70 (2.70)***	4.42	16.27	3.3	3.96	6.31
<u>K-feldspar rich</u>							
Winnsboro pluton, S. C.	S6-23**	2.63	2.0	17.2	4.3	5.16	5.0
	S6-23-2	2.63	1.12	20.55	4.77	5.72	5.18
	F6-39	2.62 (2.63)***	3.64	21.22	4.87	5.84	6.87

C-15

Table C-4 (continued).

Location	Sample No.	Density, gm/cm ³	Uranium (U), ppm	Thorium (Th), ppm	Potassium (K), %	K ₂ O, %	Heat generation, A × 10 ⁻¹³ cal/cm ³ -sec
<u>Rion pluton</u>							
Winnsboro, S. C.	S6-10**	2.62	6.6	34.6	4.3	5.16	10.7
	S6-13	2.62	8.7	30.5	3.75	4.50	11.18
	S6-33	2.61	7.97	35.5	4.35	5.22	11.65
	S6-34*	2.64	3.8	41.0	4.4	5.28	10.2
	S6-36	2.64	4.71	32.13	4.35	5.22	9.24
	S6-42	2.63	8.21	33.47	4.29	5.15	11.53
	F6-3	2.65	4.89	31.62	4.40	5.28	9.31
	F6-4	2.65	2.97	22.67	3.91	4.69	6.51
	F6-10**	2.60	3.8	36.4	4.7	5.64	9.4
	F6-13	2.61	3.87	28.35	4.11	4.93	7.94
	F6-19**	2.62	4.0	39.2	4.5	5.40	9.91
	F6-21	2.60	3.28	31.66	4.35	5.22	8.15
	F6-22*	2.60	4.4	35.0	4.2	5.04	9.4
	F6-40	2.62	6.38	32.56	4.30	5.16	10.24
	F6-45	2.62	6.01	32.07	4.09	4.91	9.88
	F6-52	2.64	6.38	31.93	4.37	5.24	10.22
	F6-59	2.62	6.09	33.08	4.27	5.12	10.15
	F6-60	2.62	7.77	32.84	4.20	5.04	11.11
F6-18	2.64	6.14	45.85	4.43	5.32	12.42	
		(2.62)***					

Table C-5. Heat generation values for surface samples from Rolesville, N.C.

Location	Sample No.	Density, gm/cm ³	Uranium (U), ppm	Thorium (Th), ppm	Potassium (K), %	K ₂ O, %	Heat generation, A x 10 ⁻¹³ cal/cm ³ -sec	Comments
Rolesville, N.C.	B6-4-1	2.64	4.92	44.07	4.36	5.23	11.36	Granite dike from country rock
	B6-6	2.65	5.78	15.66	3.44	4.13	6.96	Med - crs. grained granite of Rolesville main phase
	B6-24	2.64	3.91	11.69	2.86	3.43	4.99	Castalia pluton med-c. gr.
	B6-41-4	2.63	1.54	24.14	4.54	5.44	5.98	Med-c. grained granite of Rolesville main phase
	F6-88-2	2.64	4.24	22.81	3.43	4.12	7.18	"
	F6-89	2.63	5.14	13.76	3.50	4.20	6.21	"
	F6-101	2.63	4.14	7.50	3.26	3.92	4.50	Pencil gneiss from country rock
	F6-116-1	2.64	3.47	13.26	3.08	3.69	5.03	Med-c. grained granite of Rolesville main phase
	F6-116-3	2.65	2.78	19.50	3.64	4.37	5.81	"
	F6-127	2.64	5.79	21.40	3.09	3.71	7.81	"
	F6-129-1	2.66	1.77	13.89	3.13	3.76	4.14	"
	F6-129-2	2.64	6.99	19.73	3.33	4.00	8.42	Coarse grained
	F6-148	2.58	2.90	20.14	3.68	4.41	5.84	"
	S6-153	2.63	6.49	25.36	4.00	4.80	9.07	Fine grained
	S6-179	2.62	2.86	11.71	3.35	4.02	4.43	Castalia pluton med-c. gr.
	S6-203	2.63	6.26	17.88	3.57	4.28	7.59	Castalia pluton med. gr.

Table C-5, continued.

Location	Sample No.	Density, gm/cm ³	Uranium (U), ppm	Thorium (Th), ppm	Potassium (K), %	K ₂ O, %	Heat generation, A x 10 ⁻¹³ cal/cm ³ -sec	Comments
	S6-255	2.62	2.77	13.26	3.43	4.41	4.64	Coarse grained
	S6-288	2.62	3.07	30.81	3.77	4.53	7.82	Louisburg pluton fine-gr. granite
	F6-130	2.64	3.30	21.04	3.72	4.46	6.38	Med-c. grained granite of Rolesville main phase
	B6-3-1	2.64	1.87	16.30	3.42	4.11	4.64	"
	B6-7	2.66	3.56	13.61	2.63	3.16	5.08	Med/coarse granodiorite
	F6-78	2.64	3.40	24.18	4.18	5.02	7.07	Med-c. grained granite of Rolesville main phase
	F6-88-1	2.62	5.24	23.57	3.84	4.61	7.95	"
	F6-88-3	2.60	4.41	10.43	3.82	4.59	5.22	Med-grained leuco-granite
	F6-99	2.64	1.99	13.09	3.40	4.08	4.17	Med-c. grained granite of Rolesville main phase

4.2 TCU (1 TCU = 10^{-3} cal/cm-sec-°C). The hole bottomed in basalt of unknown thickness of thermal conductivity 4.5 TCU. Thus, the higher values of heat generation given in Tables C-3, C-4, C-5 and A-8 and observed values of thermal conductivity of Coastal Plain sediments near Charleston, S. C. support the possibility of locating favorable geothermal targets in Coastal Plain sediments. Optimum targets are at locations of thick accumulations of sediments of relatively low thermal conductivity overlying rocks of relatively high heat generation.

Gravity anomalies over granitic intrusive rocks are generally negative. We have logged almost all of the existing holes in the Coastal Plain that are greater than about 100 meters in depth. The existing holes are relatively few (about 100) and do not adequately sample thermal gradients over negative gravity anomalies.

Fig. C-9 shows areas of relatively high geothermal gradients in Coastal Plain sediments in the eastern United States. This figure was prepared from data from Progress Reports VPI&SU-5103-1 and -2 and from the AAPG Geothermal Gradient Map of North America (1976). The areas of relatively high geothermal gradient approximately coincide with negative Bouguer gravity anomalies, thus supporting the possibility that the higher gradients are due to buried heat sources.

Additional data have been obtained since the preparation of Fig. C-9. We have obtained temperature data from all existing wells in the vicinity of the Portsmouth-Norfolk-Virginia Beach negative gravity anomalies (Fig. C-10). The gradients are listed in Table C-2. No existing wells are located in the center of the gravity lows, and none of the wells are cemented. Gradients on the flank of the large

negative anomaly appear to be higher than normal with one exception (161-4; 29.4°C/Km). The large negative anomaly west of Norfolk is undoubtedly caused by buried granitic rocks; the negative anomalies to the east and south where the sediments are thicker may also be due, in part, to buried plutonic rocks.

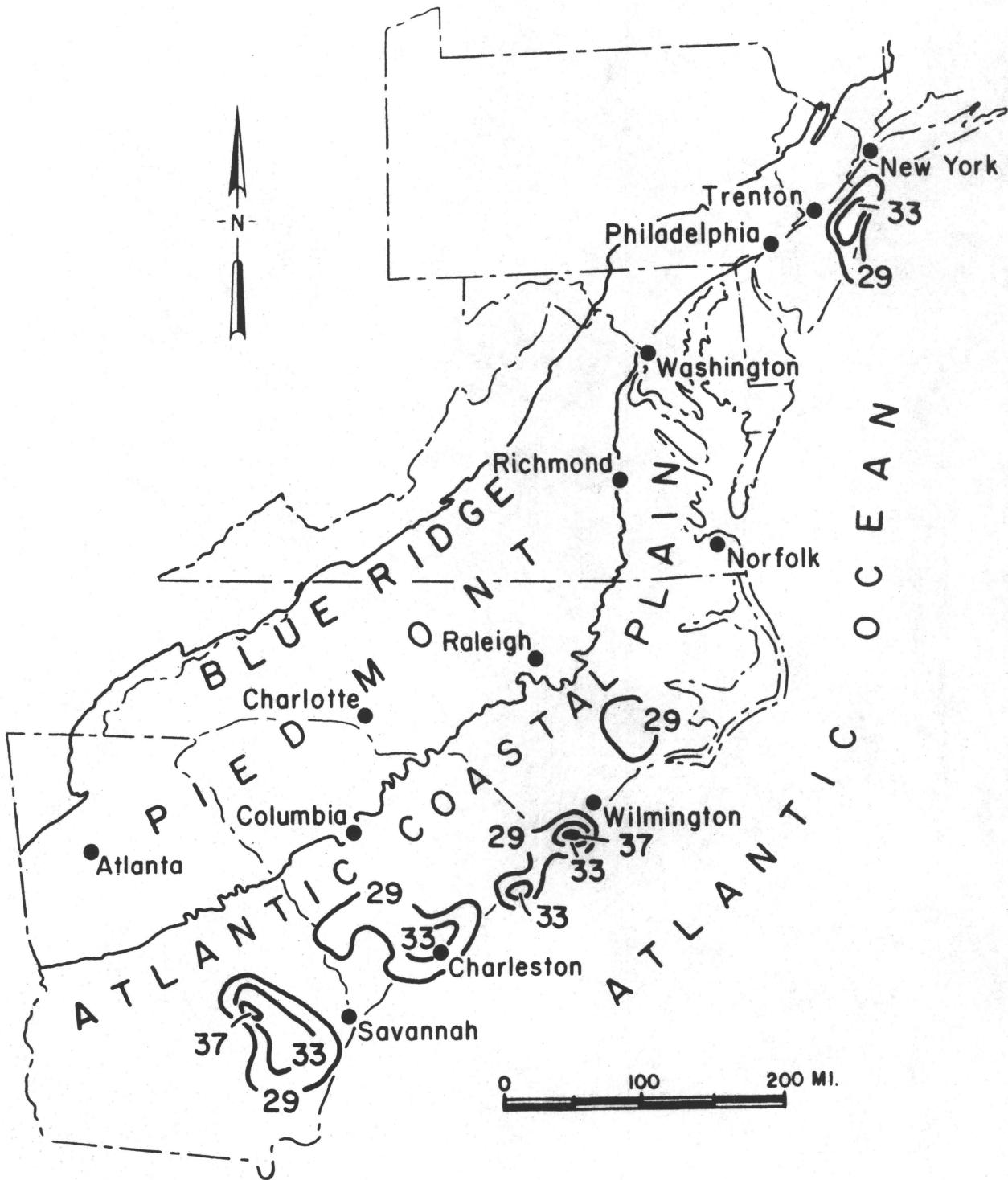
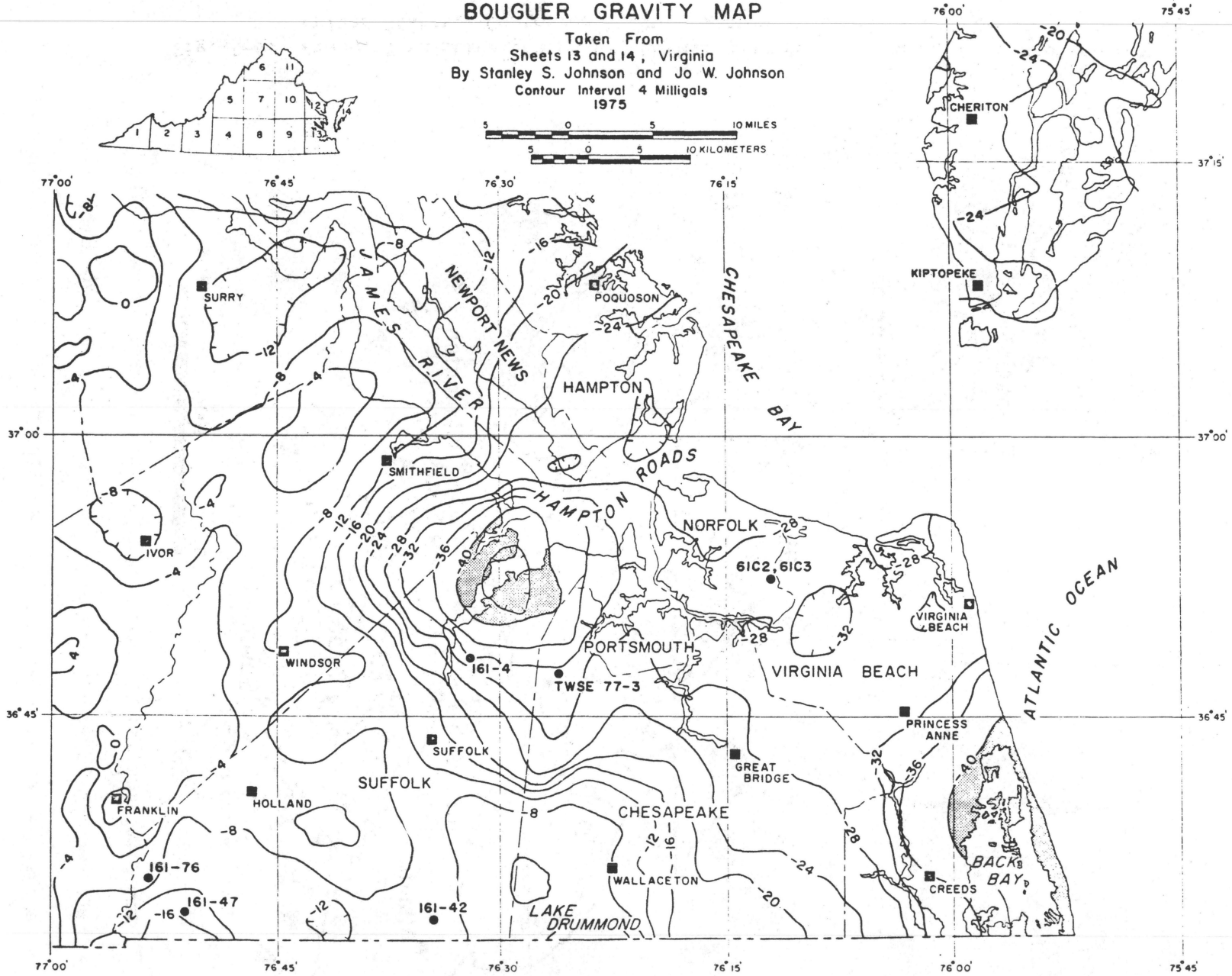
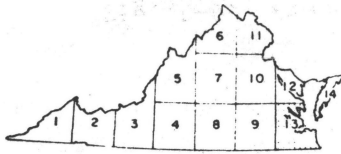
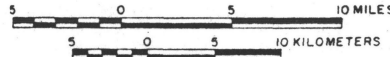


Fig. C-9. Areas of relatively high geothermal gradient in Coastal Plain sediments in eastern United States. Contoured °C/km. Contour interval = 4°C/km.

BOUGUER GRAVITY MAP

Taken From
Sheets 13 and 14, Virginia
By Stanley S. Johnson and Jo W. Johnson
Contour Interval 4 Milligals
1975



C-22

Fig. C-10. Bouguer gravity map showing gravity lows in Norfolk, Va. area.

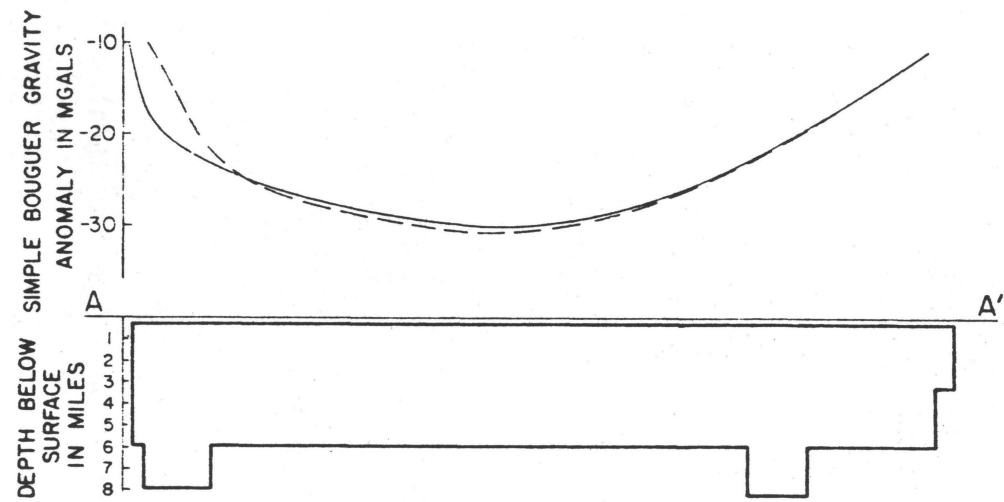
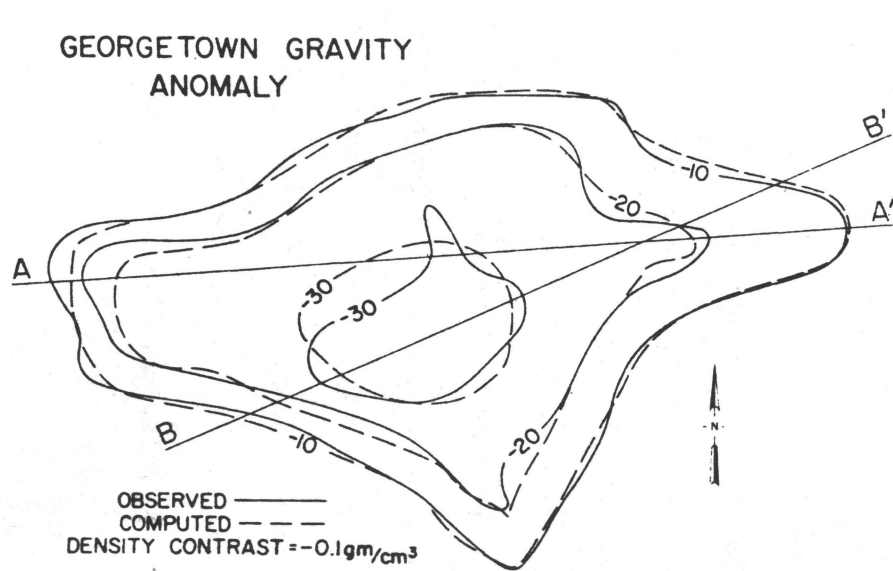
Modeling of Coastal Plain Gravity Anomalies

J. A. Dunbar and J. K. Costain

Simple Bouguer gravity data of the southeastern United States show a number of negative gravity anomalies in the Piedmont and Coastal Plain. The association of anomalies with the larger granitic intrusions is quite distinct in the Piedmont (Bell and Popenoe, 1976) where these rocks are exposed and where the gravity coverage is adequate. In the region of the Coastal Plain we have modeled two of these, one near Georgetown, S. C. and one near Norfolk, Va.

Preliminary gravity models of the Georgetown and Norfolk areas have been developed using the three-dimensional method of Talwani (1965). A single density contrast was assumed in each case. Density contrasts used in the models ranged from -0.1 to -0.2 gm/cm³. Contrasts between granitic rocks intrusive into metamorphic basement cannot reasonably be assumed to exceed 0.2 gm/cm³. Contrasts between sediments in Triassic basins and basement rocks should be less than 0.1 gm/cm³ because of the indurated and impermeable nature of the Triassic sediments as known elsewhere in the southeastern United States.

The gravity model of the Georgetown low is shown in Fig. C-11. No regional gravity field was assumed. For the density contrast assumed (-0.1 gm/cm³), approximately tabular mass extending to a depth of almost six miles. In several locations a better fit to the observed field is obtained by extending the model somewhat deeper. The results are compatible with an igneous intrusive complex. The model does not suggest a buried Triassic basin because of the relatively large density



C-24

MODEL PLATES TOP VIEW

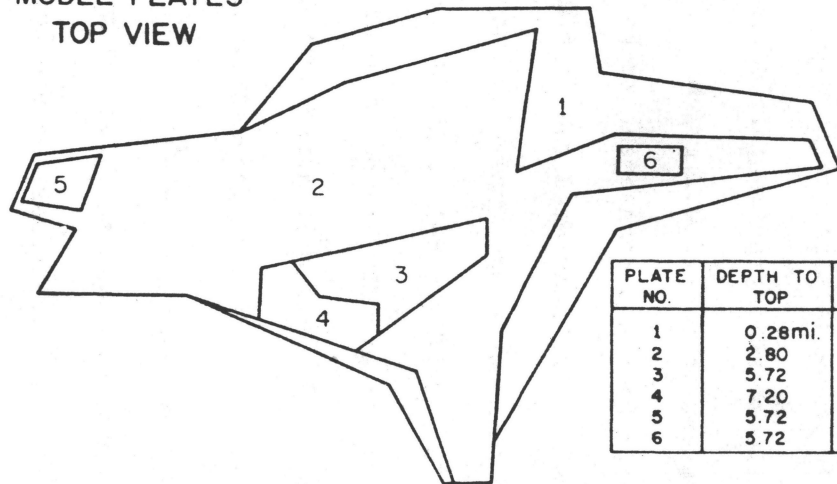


PLATE NO.	DEPTH TO TOP	DEPTH TO BOTTOM
1	0.28 mi.	2.80 mi.
2	2.80	5.72
3	5.72	7.20
4	7.20	9.60
5	5.72	7.60
6	5.72	7.60

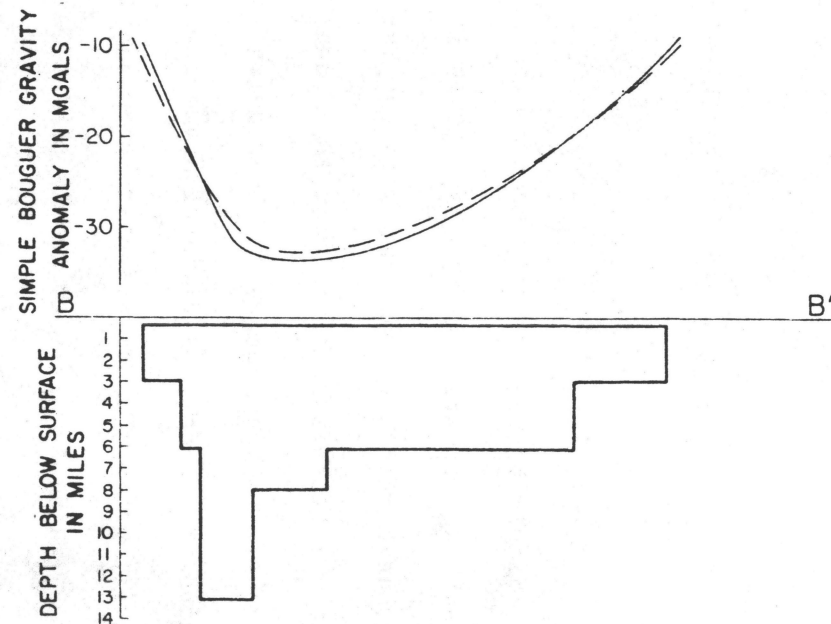


Fig. C-11. Georgetown, S.C. gravity anomaly model.

contrast assumed. A smaller density contrast would extend the base of the model to greater depths.

Preliminary gravity models of the Norfolk, Va. lows based on density contrasts of -0.15 and -0.2 gm/cm^3 are shown in Figs. C-12 and C-14, respectively. The vertical dimensions of each are shown in Tables C-6 and C-7. After subtracting a regional gravity field from the Bouguer gravity anomaly, a granitic intrusion approximately conical in shape and extending to a depth of greater than six miles is strongly suggested. Further modeling will evaluate the negative gravity anomalies south of Virginia Beach.

NORFOLK GRAVITY ANOMALY

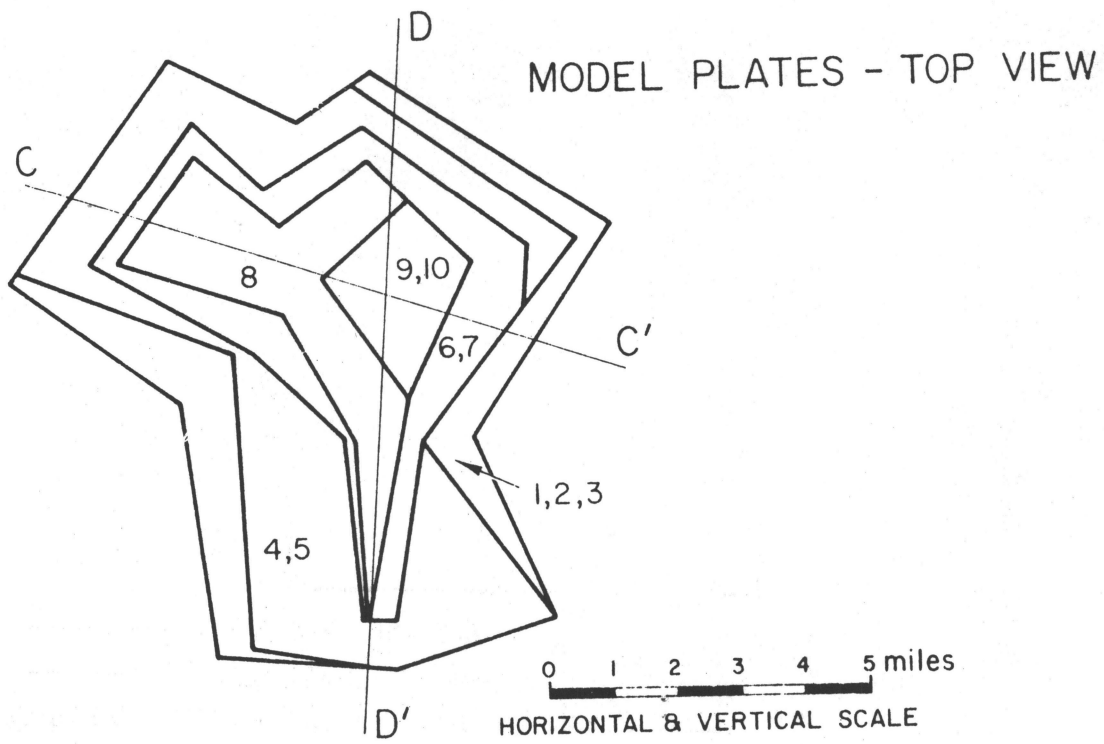
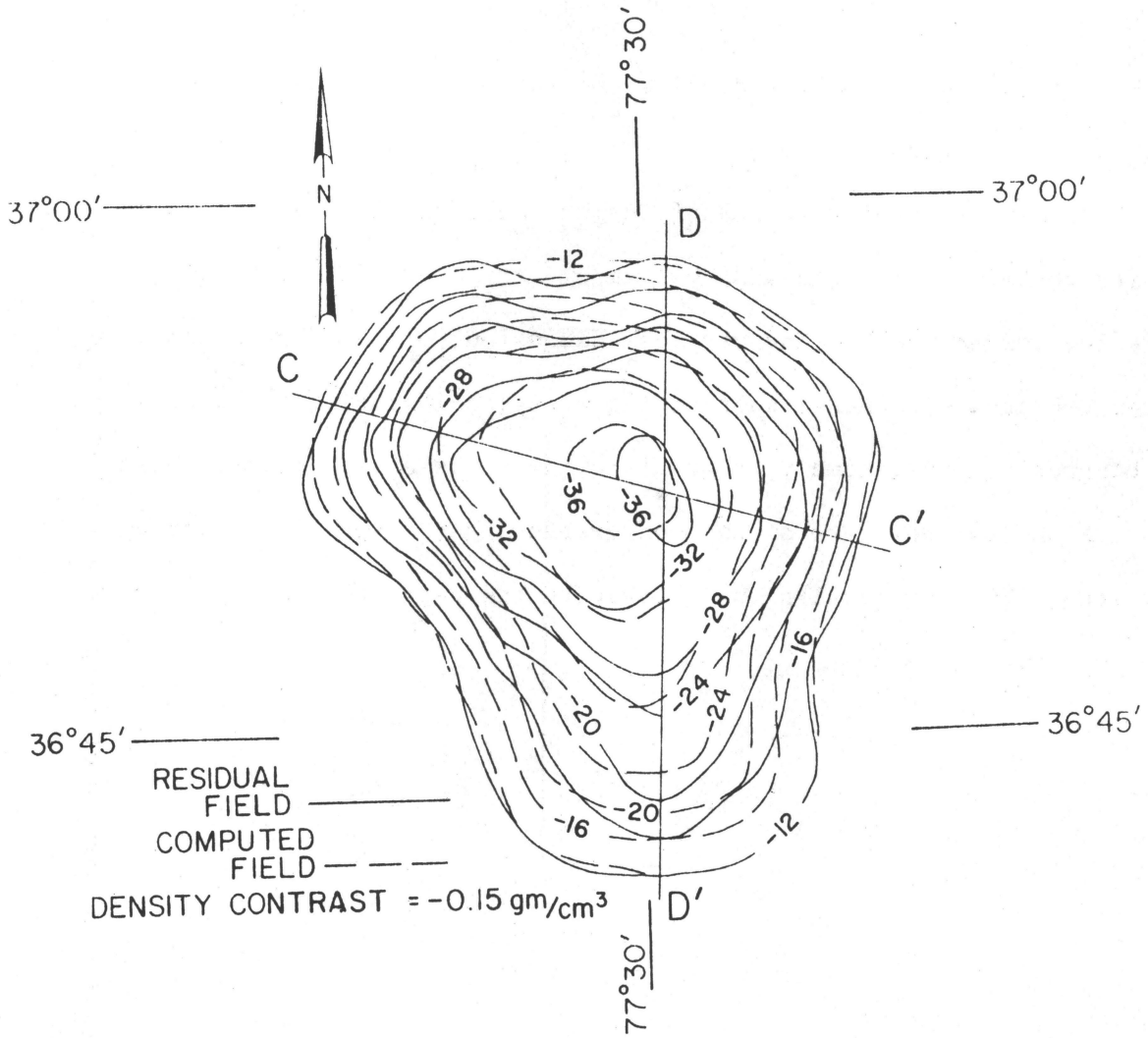


Fig. C-12. Norfolk gravity anomaly model using a density contrast of -0.15 gm/cm^3 .

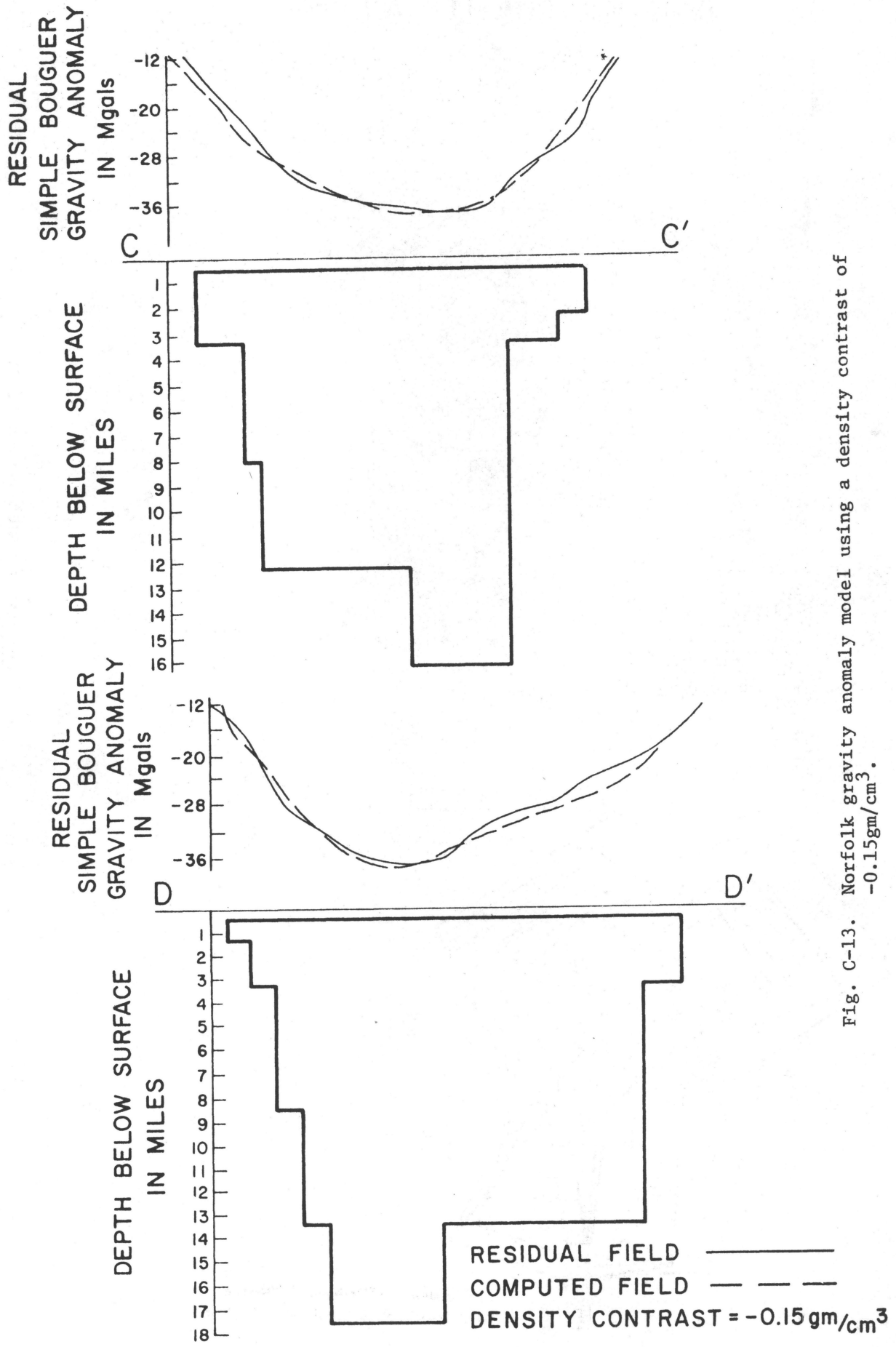


Fig. C-13. Norfolk gravity anomaly model using a density contrast of -0.15 gm/cm^3 .

NORFOLK GRAVITY ANOMALY

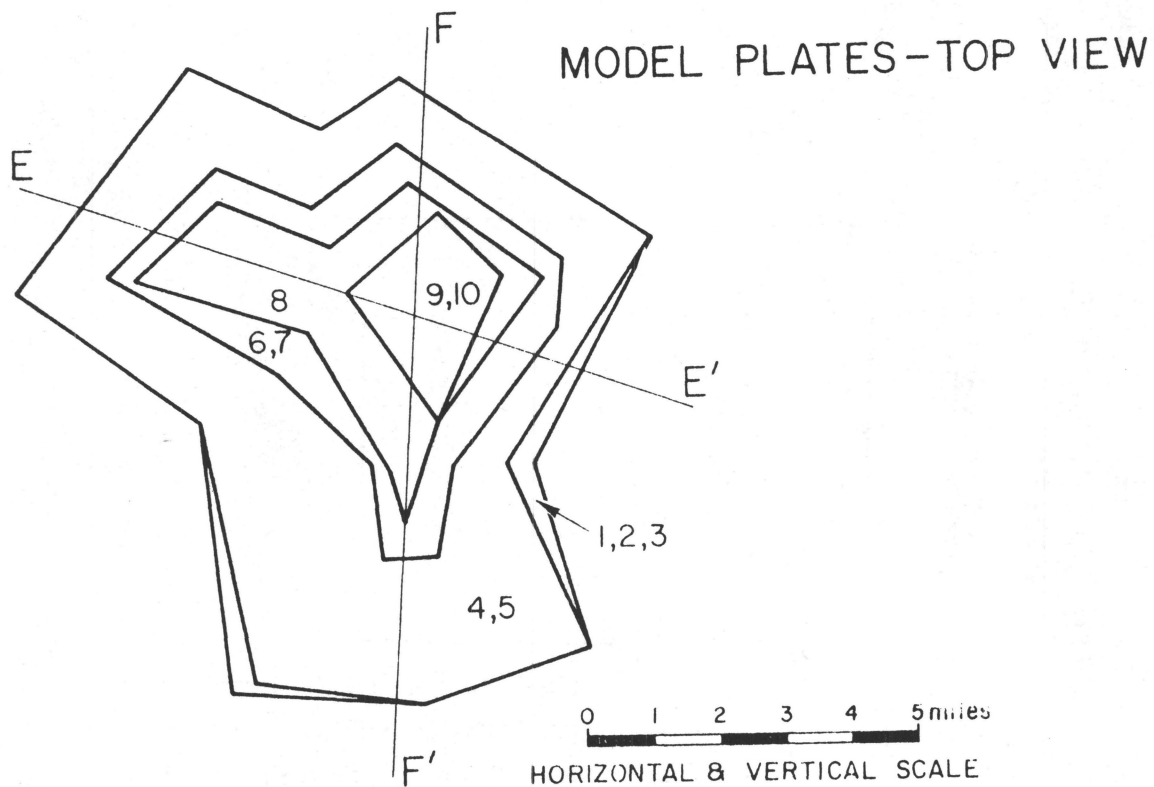
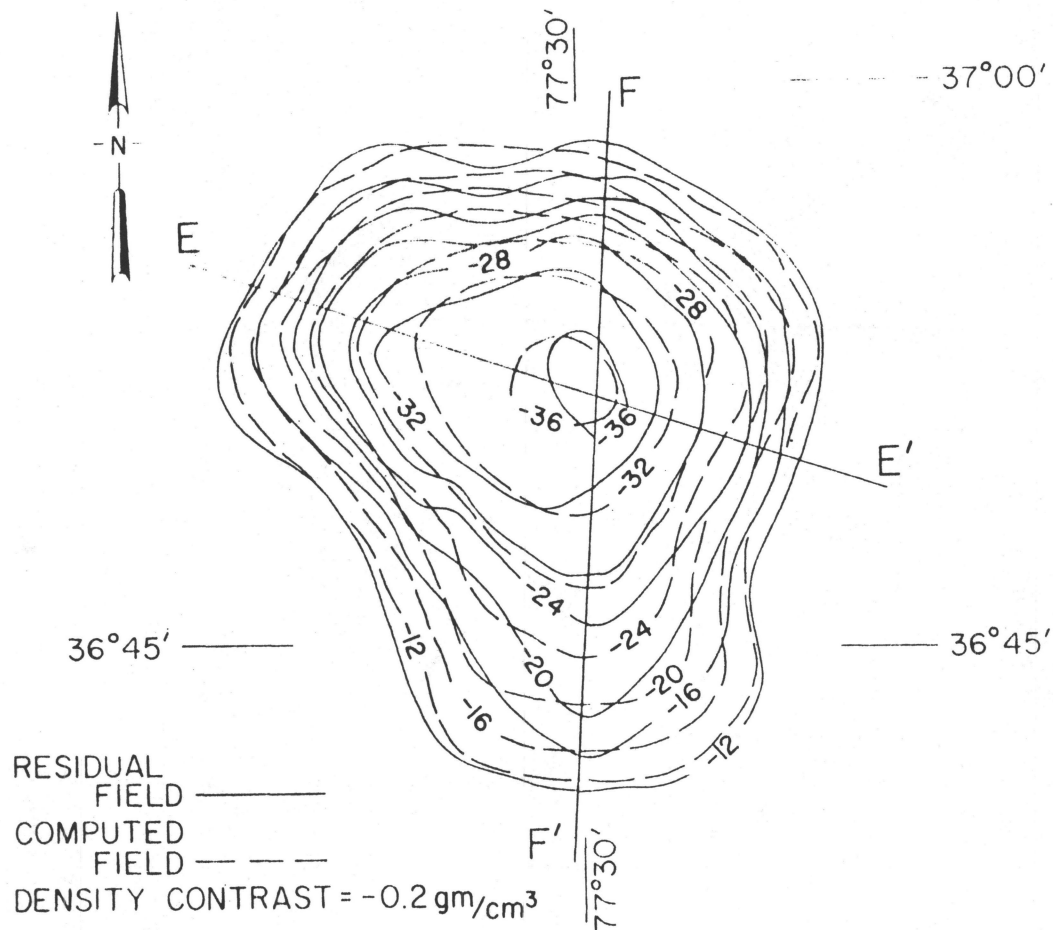


Fig. C-14. Norfolk gravity anomaly model using a density contrast of -0.2 gm/cm^3 .

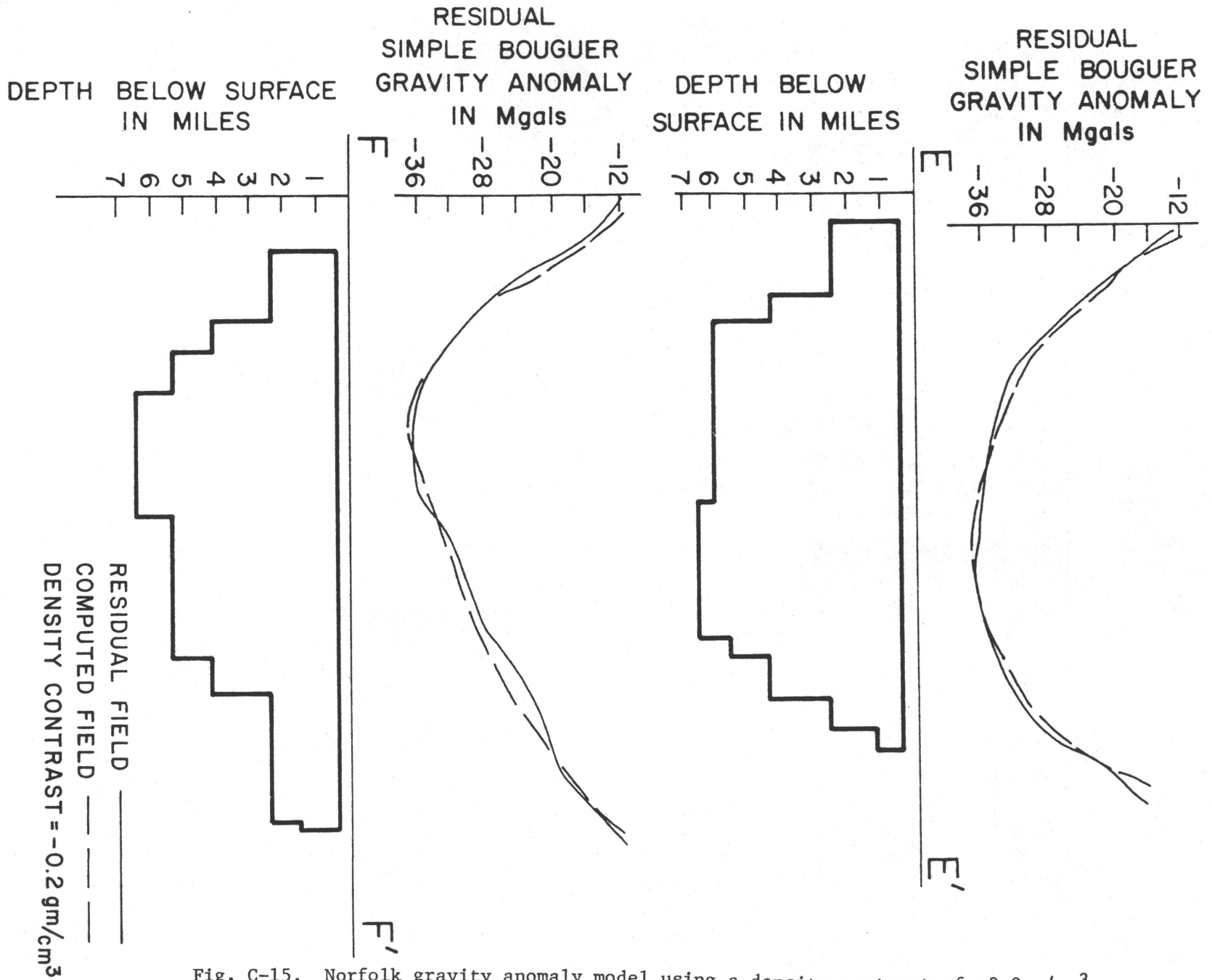


Fig. C-15. Norfolk gravity anomaly model using a density contrast of -0.2 gm/cm^3 .

Table C-6. Vertical dimensions of the Norfolk model.
 Density contrast = -0.15 gm/cm^3 .

Plate No.	Depth to Top (miles)	Depth to Bottom (miles)
1	0.38	0.40
2	0.40	0.60
3	0.60	1.20
4	1.20	2.00
5	2.00	3.00
6	3.00	4.00
7	4.00	8.00
8	8.00	12.00
9	12.00	15.98
10	15.98	10.00

Table C-7. Vertical dimensions of the Norfolk model.
 Density contrast = -0.2 gm/cm^3 .

Plate No.	Depth to Top (miles)	Depth to Bottom (miles)
1	0.38	0.40
2	0.40	0.60
3	0.60	1.00
4	1.00	1.60
5	1.60	2.40
6	2.40	3.40
7	3.40	4.20
8	4.20	5.30
9	5.30	6.28
10	6.28	6.30